P2

AT5/17045

THE EFFECTS OF ELEVATED TEMPERATURES ON THE STRUCTURAL PROPERTIES OF FIBER COMPOSITE MATERIALS SUITABLE FOR USE IN SPACE SHUTTLE AND OTHER SPACE VEHICLES

FINAL REPORT

October, 1972

By:

Maurice A. Wright
Associate Professor of Metallurgical Engineering

The University of Tennessee Space Institute
Tullahoma, Tennessee 37388

Submitted to:

The George C. Marshall Space Flight Center
National Aeronautics and Space Administration
Huntsville, Alabama 35812

TABLE OF CONTENTS

LIST OF FIGURES

LIST OF TABLES

FOREWORD

This final report summarizes the work carried out at The University of Tennessee Space Institute for The George C. Marshall Space Flight Center under The Cooperative Agreement Modifications Nos. 2 and 4 for the period July 1, 1971 through October 15, 1972, with Felix P. LaIacona of the Materials Division as the technical monitor.

The director and the principal investigator of the work reported herein was Dr. M. A. Wright, Associate Professor of Metallurgical Engineering. Mr. J. Wills was responsible for obtaining the data and performing the statistical calculations on the individual fibers and fiber bundles. Mr. H. T. Kulkarni was responsible for obtaining some of the mechanical properties from the composite specimens. He also was responsible for analyzing the stress distribution in shear specimens by modifying the computer program originally sent to us by Mr. Fritz Hatt of the Virginia Polytechnic Institute. Mr. R. Harney and Mr. R. Hall also made significant contributions to the program by constructing the thermal cycling apparatus under the general supervision of Mr. J. Goodman.

Some of the results of this program have been reported or are in the process of publication in the technical literature [1, 2, 3].

SUMMARY

Various mechanical properties of boron reinforced 6061, 1100, or 2024 aluminum alloys were measured in the as received condition and after thermal cycling. It was observed that cycling these materials through temperatures that varied between room temperature and either 315°C, 365°C, or 425°C could seriously degrade the properties. Observations of the surfaces of some specimens indicated that small perturbations appeared after very few cycles. These widened and deepened as the test proceeded until they developed into macroscopically visible surface cracks. The appearance of these cracks coincided with the maximum degradation of the mechanical properties.

The extent of the observed effects depended on alloy type and the maximum cyclic temperature used. Increasing the maximum temperature produced an increase in the damage. The longitudinal, transverse, and shear properties of the reinforced 2024 material were the most affected. A smaller degradation was produced in the 6061 material; however, some of the properties of the reinforced 1100 material were improved slightly.

The results are discussed in terms of upper and lower strength bounds calculated from the strengths of individual

fibers extracted from the as-received or thermally cycled specimens.

INTRODUCTION AND DISCUSSION

Substantial interest is currently being shown in the application of metal based composite materials to components suitable for use in aerospace structures and propulsion systems. Key to the design of components using composites is the fatigue resistance and behavior of these materials, particularly with respect to thermal fatigue.

It is generally accepted that the fatigue resistance of a composite to cyclically applied loads is largely controlled by the properties of the matrix. Specifically, for short lifetimes, a simple relationship has been shown to exist between the plastic strain, e_p, generated in the matrix and the number of cycles required to fracture a composite specimen [4]. Recent work at the University of Tennessee Space Institute has shown that the fatigue life of a composite is extensive when the matrix is strained only in the elastic range. However, a large decrease in the fatigue life is observed as soon as the strain in the matrix becomes plastic. Indeed, we have found that a plastic strain of 0.1% results in an order of magnitude decrease in the observed number of cycles to failure of a boron-aluminum composite. Fortunately, gross plastic flow in a commercially useful composite does not

usually occur since the plastic strain induced in the matrix by an applied stress is designed to be small.

In addition to the excellent room temperature properties, composite materials exhibit a very attractive high temperature capability. Thus, they are prime candidates for use in areas where frictional heating or high temperature combustion occurs. In this environment, it is extremely difficult to avoid the generation of thermal stresses, since composites are fabricated from constituents which exhibit markedly different thermal characteristics. If the composite is well bonded, neither the matrix nor the reinforcement is able to change dimensions freely on heating. And, since each constituent must expand or contract an equal amount, constraints will be generated in the system. If the interfacial bond is strong, the stresses in the respective phases can be very large. The results of a very simple analysis indicate that very large plastic strains will be generated in the matrix of an aluminum-based material containing 50 v/o boron fibers when subjected to a temperature variation of about 200°C. Other more sophisticated analyses also indicate that appreciable plastic strains will be generated in the matrix [5].

The realization that temperature changes could result in the generation of large internal stresses has led to a number of experimental investigations of the effect. P. Shahinian [6] studied the effect of thermal cycling on the properties of boron reinforced 2024 and 6061 aluminum alloys,

and a 6061 aluminum alloy reinforced with silicon carbide coated boron. He observed that cycling between 110°C and 500°C caused a roughening of the surfaces of these materials by a slip process. Accumulation of the slip displacements gave a gross surface deformation which was clearly evident after 500 cycles and this damage increased in severity with further cycling. After 1000 or more cycles, the deformation became more severe and many of the valleys contained holes or cracks which exposed the filaments. He noted a significant decrease in the tensile strength of the materials studied. Thus, the work confirmed the results of Anthony and Chang [7] who observed a 20% reduction in tensile strength of a composite of aluminum-27 v/o boron after cycling 1000 times between room temperature and 800°F.

Volk, et. al., [8], noted a similarly large degradation in the strength of carbon reinforced nickel specimens. Also, they noted an effect which they termed "a ratcheting process," in which the matrix redistributed itself along the fiber length.

More recently Kreider, et. al., [9], have studied the thermal cycling behavior of borsic-reinforced 6061 aluminum alloy. They noted a decrease in density, which they attributed to void formation and a decrease in the flexural strength of 13 percent. They believe however, that the actual degradation in the mechanical properties was small considering the severity of the test. Pepper, et. al., [10] noted a similarly small effect when an aluminum-silicon alloy reinforced with

graphite fibers was thermally cycled between -193°C and +500°C. It can be argued, therefore, that simple theory predicts, and experiments verify, that problems relating to thermal fatigue may be encountered when composite materials are subjected to cyclic temperature changes.

At this point it is worth recalling that the stresses generated in a composite are entirely dependent on the bond that exists between the matrix and the fibers. Obviously, if the bond between the fibers and the matrix is very weak, then the fibers would behave as a simple bundle. They would transfer no stress to the matrix, and thermal fatigue would not be a problem. It should be recalled that the fabrication of metal matrix composites is quite a complex operation; thus, it is probable that a large variation in the fiber-matrix bond strength exist in real materials. And, we believe, this variation is responsible for the differences in mechanical properties that are commonly observed between otherwise identical specimens. Obviously, conclusions recorded by different investigators could be severely influenced by inherent, unknown, and unwanted differences in the fabricated composites.

In this report, we have investigated the effect of cyclic temperature variations applied to the boron-reinforced aluminum alloys 1100, 2024, and 6061. We were aware that any effects produced by the various treatments would depend sensitively on the fiber-matrix bond strength. This influenced our decision to examine the strength characteristics of individual fibers

both before and after the thermal fatigue treatment. Using these results, the bundle theories of Coleman [11] and the cumulative damage theory of Rosen [12], we calculated the upper and lower strength bounds expected to be exhibited by composite specimens. We ignored the stress concentration effect associated with broken fibers and assumed that a perfect matrix-fiber bond would result in a composite specimen exhibiting a strength approaching the upper bound. Lower composite strength values were assumed to result from poorer quality bonds.

After the various thermal fatigue treatments, we again examined the strength characteristics of individual fibers, and from these results, we again calculated the upper and lower strength bounds.

The longitudinal and transverse modulus, major and minor Poisson's ratios, shear strength, transverse strength and density were also measured. Thus, when all the data was analyzed, we could deduce whether the property degradation, if any, produced by the thermal fatigue treatment resulted from changes in the matrix, the matrix-fiber bond, or the strength of the individual fibers.

The experimental techniques used in this investigation are described in Section 3. The results are presented in Section 4, and our discussions are included as Section 5. The conclusion makes up Section 6.

EXPERIMENTAL TECHNIQUES

i. Test Material

The test material was fabricated by the Amercom Corporation using a proprietary diffusion bonding technique. In general, the process consisted of applying a pressure of several thousand pounds per square inch to foil-filament arrays at a temperature of about 500°C. The organic binder which was used to maintain the integrity of the original material was burnt off during the diffusion bonding operation. After fabrication, the material was cooled in air by placing the composite panel on a large aluminum heat sink.

Three reinforced aluminum alloys, 1100, 2024, and 6061, were fabricated, each containing a nominal 50 v/o 0.01346 cm (0.0053 inch) diameter boron fibers. The dimensions of each panel shown schematically in Figure 1 were sufficient to allow the preparation of 20 longitudinal specimens, 12 transverse specimens and 8 shear specimens. These specimens were cut from each panel using electric discharge machining (EDM).

ii. Test Specimens

Aluminum tabs 3.81 cm(1.5 inches) long by 2.54 cm (1 inch) wide were bonded to the ends of the longitudinal and transverse specimens using Eastman 910 adhesive. The modulus of both types of specimens was obtained using a commercially available

Instron extensometer. Some selected specimens were more fully instrumented by bonding two longitudinal and two transverse strain gauges to the specimen gauge length. In this way, the respective modulus values and Poisson's ratios could be obtained. A double slotted shear specimen, as shown schematically in Figure 2, was fabricated by cutting slots into the specimen blank using the EDM process. Initially, the distance between the cut slots was 5.08 cm (2 inches); however, specimens of this type fabricated from 6061 and 2024 material failed in tension by cracks propagating from the machined slots. The net stress applied at the reduced cross section at fracture was lower than the strength of an unnotched test piece; thus, these materials were notch sensitive. The distance between the slots was reduced to 2.54 cm (1 inch) for most of the tests; however, in some cases the distance was reduced further to 1.905 cm (0.75 inches). The effect of decreasing the distance between the cut slots was investigated using a finite element analysis technique. The results shown in Appendix I indicated, for an orthotropic, homogeneus material at least, that shear strengths obtained from the different specimen geometries may be different. For the results reported here, the differences in apparent shear strengths resulting from differences in the spacing of the slots were small and therefore were neglected. As pointed out in the appendix, larger differences may become apparent if shear strengths from specimens of widely different geometries are compared.

Initially, the mechanical properties of each specimen were obtained by applying a load, at a crosshead speed of 0.0508 cm (0.02 inches) per minute, in an Instron tensile test machine using the gripping arrangement shown in Figure 3. In later tests however, the large Instron wedge type grips were used. A spirit level technique was used in all tests to insure that the fiber axis of each specimen corresponded closely to the load axis of the machine. In this way, apparent strength losses due to off-axis loading of the specimen were avoided.

The strain produced in each specimen was obtained directly by monitoring the output of a conventional extensometer attached to the specimen sides with spring-loaded clamps, or from the output of the strain gauges previously mentioned.

iii. Individual Fiber Tests

Individual boron fibers were extracted from specimens by dissolving away the matrix material in a sodium hydroxide solution. The fibers were washed in methyl-ethyl-ketone solution and were handled at all times with tweezers applied at their ends to prevent any defects from being introduced into the test gauge length.

Fiber tensile tests were performed using self-aligning pneumatic grips pressurized at about 4.92 kg/cm^2 (70 psi). Figure 4 shows the experimental test grip arrangements. Aluminum foil was used to line the grips in order to minimize crushing of the fibers and to distribute the applied load evenly. Tests were performed at a crosshead speed of 0.0508 cm (0.02 inches) per minute, which was the slowest testing speed available. The test gauge length was accurately set by using the gauge length adjusting dial on the machine. Tests were performed at gauge length of 5.08 cm (2 inches), 3.81 cm (1.5 inches), and 2.54 cm (1 inch), and the failure loads were recorded on the Instron chart.

iv. Fiber Bundle Tests

Fiber bundles were prepared by dissolving a predetermined amount of the aluminum matrix in sodium hydroxide to provide a gauge length of 7.62 cm (3 inches). The remaining matrix material was protected from the solution by a layer of silicone rubber. Tabs were glued to the ends of the specimens before each bundle was pulled to failure using a crosshead speed of 0.0508 cm (0.02 inches) per minutes. The fiber bundle tests were monitored acoustically to determine if, and how many, fiber breaks occurred before the bundle failed. Two 1.27 cm (0.5 inch) Druel and Kjaer microphones picked up the signal which was recorded on an Ampex 150 tape machine. The background noise was filtered out from the recording by rejecting all signals with a fre-

quency below 5 khz. The desired signal was then displayed visually on a BNK Model 2305 Level Recorder.

v. Density Tests

The specific gravity of composite specimens was determined by weighing the specimen in air and methyl-ethyl-ketone, a fluid which thoroughly wetted the specimen. A standard mechanical chemical balance was used for the weight measurements. The specific gravity of the specimens was determined from the expression:

$$P_c = \frac{AP_c}{A+H+F} \qquad \ldots 1$$

where:

A = Weight of specimen in air (gm),

H = Weight of hook in liquid (gm),

F = Weight of hook and sample in liquid (gm),

P_c = Density of liquid (methyl-ethyl-ketone) (gm. $cm.^{-3}$).

vi. Thermal Fatigue Apparatus--zero static load

A thermal fatigue apparatus was constructed which is shown in Figure 5. Essentially, the equipment consisted of a resistance heated furnace that moved in the vertical plane by the action of a reversible electric motor. The specimens were held at a fixed point; thus, they were alternately heated and cooled as the furnace moved over them. In order to increase the cooling rate, cold air was blown over the specimens

when they were outside the furnace. The temperature of the furnace was controlled by a proportional controller connected to an S.C.R. power supply. The temperature variations of the specimens were monitored from the output of a thermocouple attached to the center of one specimen. Each specimen was subjected to one heating and cooling cycle, similar in profile to that shown in Figure 6, every three minutes.

The specimen holder used for the major part of this program is shown in Figure 7. Six specimens were accommodated, two shear, two transverse, and two longitudinal. These were loosely held in the holder so that constraints were not produced, and bending, due to this effect at least, was avoided particularly at the higher cycling temperatures. Before each thermal cycling experiment, the specimen holder was accurately positioned along the axis of the furnace by adjusting its position until the temperature at each specimen position was identical.

vii. Thermal Fatigue Apparatus--positive static load

The above tests were carried out on specimens that were not subjected to any external load. However, a few additional tests were carried out on specimens that were statically loaded, also. The experimental apparatus in which this type of experiment was carried out was similar to that previously described, with the exception that the individual specimens were loaded by means of weights acting

through a beam arrangement. This apparatus is shown in Figure 8. A smaller test specimen was used in this apparatus since the maximum load that could be applied at each test position was 295.45 kg. (650 lbs.). For the proper use of this apparatus, it was extremely important that the specimen by mounted perfectly vertical and without twist. To insure this, a loading fixture was developed and is shown in Figure 9. The grips were accurately positioned in this fixture before the specimen was mounted. Then the fixture, complete with grips and specimen, was placed into the thermal fatigue apparatus. The alignment was checked with a spirit level, the load was applied, and finally the fixture was removed. The specimen and the load axis of the machine were therefore coincident and the specimen was not subjected to any torsional moments.

RESULTS

i. As-Received Composites

The nominal volume fraction, v/o, of fibers in each composite specimen was 0.50. However, in order to be quite sure that any observed variation in properties did not result from differences in reinforcement content, the number of fibers contained in selected specimens was counted. This was done by observing a suitable cross-section, usually the failure surface, through a low power binocular microscope. The majority of the specimens contained a mean of 44 v/o fibers, although values as low as 39 v/o and as high as 49 v/o were recorded. If the variation in the volume fraction contributed significantly to the mechanical property data, then an asterisk, *, is placed by the results reported herein. The volume fraction of fibers in the specimens from which the transverse properties were obtained was not recorded.

The mechanical properties of the aluminum alloys, 1100, 6061, and 2024 reinforced with nominally 50 v/o boron fibers is shown in Table I. It can be seen that the reinforced 6061 and 2024 materials are significantly stronger than the corresponding 1100 material. The reason for this is not known; however, the results of work to be described later indicate that the reinforcement extracted from a typical 1100 alloy specimen was significantly weaker than that extracted from the 6061 and 2024 materials. It would appear, therefore,

that either the reinforcement in the 1100 material had been damaged by the fabrication procedure or it was significantly weaker before it was incorporated into the matrix. According to the supplier, the boron fibers were taken from the same stock material. Thus, we believe that the lower strengths resulted from fabrication techniques; temperature, pressure, etc., that differed from alloy to alloy.

The modulus of the as-received, reinforced 6061 and 2024 material also appeared to be greater than that exhibited by the specimen cut from the reinforced 1100 alloy. However, the volume fraction of fibers present in this specimen was found to be 0.39 instead of the more normal 0.44. In effect therefore all of the longitudinal modulus values correspond to those calculated by substituting into the rule of mixtures the appropriate volume fraction of fibers, taking the modulus of the fibers to be about 4.2785×10^6 kg/cm^2 (60×10^3 ksi) and the modulus of the matrix as 703.1×10^3 kg/cm^2 (10×10^3 ksi).

As has been discussed by many authors, the transverse properties of a composite are largely controlled by the properties of the matrix and the matrix-fiber bond. The trend in the results indicated here supports these arguments. Most of the shear strength values reported here reflect the corresponding shear properties of the unreinforced alloys. And, the transverse moduli correspond very closely to those expected using the finite element analysis approach of Chen and Lin [13]. In the same paper, these two authors present an argument which suggests that, in the main, the transverse strength should also reflect the tensile strength of the matrix.

Values of the transverse strength lower than expected would indicate a weak interfacial bond strength. From the results presented here, we concluded that the interfacial bond strengths of these specimens was reasonably good. Some variation existed from specimen to specimen with the maximum difference being exhibited by the 2024 specimens.

Since the ratio between the minor and major Poisson's ratios was approximately that expected using orthotropic plate theory and the density of each specimen approached theoretical, it was concluded that the as-received material was of reasonable quality and representative of the present day state-of-the-art.

ii. Individual Fiber Tests--as-received specimen

Boron fibers were extracted from three specimens fabricated from reinforced 1100, 6061, and 2024 aluminum matrix material, respectively. The strength of 50 fibers of gauge lengths, 5.08 cm (2 inches), 3.81 cm (1.5 inches), and 2.54 cm (1 inch) were obtained for each alloy sample; thus, a total of 450 fibers were tested from as-received specimens. The failure stresses of the fibers extracted are shown in Tables II - X. Also, the diameters of 50 randomly selected fibers were measured with a micrometer, and the results are shown in Table XI. The mean diameter reading was determined to be 13.46×10^{-3} cm (5.3×10^{-3} inches). The data represented in Tables II - X are summarized in Table XII by computation of the mean and standard deviation of each batch of fibers; however, inspection of the individual failure stresses

indicated possible dubious outlying readings that were not representative. By application of Chauvent's rejection criterion, such outlying points were determined and rejected and the new means and standard deviations were computed. These values are shown in Table XIII, in terms of both load and ultimate tensile stress. It can be seen that the mean strengths of the fibers extracted from the 6061 and 2024 material were approximately 40.78 x 10^3 kg/cm^2 (580 ksi). This is appreciably greater than the mean strength of about 27.35 x 10^3 kg/cm^2 (389 ksi) exhibited by the fibers extracted from the 1100 alloy. The standard deviation in each case varied but the average was about 3.52 x 10^3 kg/cm^2 (50 ksi).

It should also be noted that the data obtained from all of the fibers showed a tendency for the mean strengths to increase with decreasing gauge lengths. This agrees with current theories on the strength of brittle solids and supports the data reported by other workers [14],[15].

Using a stress interval of 2.81 x 10^3 kg/cm^2 (40 ksi), the frequency data tabulated in Tables XIV - XXII and illustrated graphically in Figures 10 - 18 was obtained. These histograms indicated that the failure stress was best described by some statistical distribution function. Results obtained by the other investigators noted above have shown that brittle fibers tend to obey a Weibull distribution characterized by the equation discussed by Corten [16]:

$$G(\sigma) = 1 - \exp\left\{-\frac{L}{d}\left(\frac{\sigma - \sigma_*}{\sigma_o}\right)^{\omega}\right\} \qquad \ldots 2$$

where: σ^* = Lower limiting strength (assumed here equal to 0 kg/cm^2 (0 psi),

σ_o = Distribution scale factor,

ω = Distribution shape factor, (describes scatter of data),

L/d = Fiber length to diameter ratio.

Accordingly, the results obtained here were arranged in the form:

$$\ln\ln\left\{\frac{1}{1-G(\sigma)}\right\} = \omega\left\{\ln\sigma - \ln\sigma_o\right\} + \ln\frac{L}{d} \quad \ldots 3$$

and the inidividual values are indicated in Tables XIV through XXII. Graphical representations of this data are indicated in Figures 19 through 21. The linearity of these plots suggest that the trends of the fiber strengths obtained in this investigation are similar to these reported by others. The straight lines obtained in these figures were drawn using a least squares method fit. The parameters ω and σ_o were determined from each line, and are shown in Table XXIII. It can be observed that there was a variation in the parameters ω and σ_o with gauge length for each alloy type; however, this variation was less obvious when these parameters were combined in the form $\sigma_o(\omega e)^{-1/\omega}$; and, since the theoretical analysis indicated that ω and σ_o should be constant with gauge length, experimental variations were assumed to be due to random sampling and experimental error.

With these constants of the Weibull expression known, it was possible to calculate the mean values and the strengths expected from a bundle of fibers of any length, L. Specifically,

the mean strength, $\bar{\sigma}$(calc), of a number of fibers of length, L was calculated using:

$$\bar{\sigma}\,(\text{calc}) = \sigma_o \left(\frac{L}{d}\right)^{-1/\omega} \Gamma\left(1 + \frac{1}{\omega}\right) \qquad \ldots 4$$

where Γ is the gamma function,

the bundle strength, σ_B, was calculated using:

$$\sigma_B = \sigma_o \left(\frac{L}{d}\ \omega\ e\right)^{-1/\omega} \qquad \ldots 5$$

and, the ratio between the bundle strength and the mean strength, called the Bundle Efficiency factor, was:

$$\epsilon = \frac{\sigma_B}{\bar{\sigma}\,(\text{calc.})} \qquad \ldots 6$$

It can be observed from Table XXIII that the values of the mean strengths of the fibers calculated using expression 4 were very close to those calculated directly from the original data. In fact, statistical comparison indicated that the results were identical at the 95% significance level. The strengths of bundles of fibers, calculated using expression 5, are also included in the table. It is to be noted that the strengths of a bundle of these boron fibers is generally expected to be about 70% of the mean strength.

iii. General Observations of Thermally Fatigued Materials

In some initial tests carried out very early in the test program, specimens of 6061 aluminum, reinforced with nominally 50 v/o, 0.01016 cm (0.0040 inch) diameter, boron filaments, were thermally

cycled between room temperature and 315°C for 2500, 4000, and 6000 cycles respectively. The density of each specimen was determined in the as-received condition and after each period of cycling. The complete results shown in Table XXIV indicate that an insignificant drop in density was observed after 2000 thermal cycles. As the number of cycles increased however, the density began to fall until after 6000 cycles, it had dropped by 2%.

Observation of the surfaces of the specimens indicated that a marked surface roughening had been produced by the thermal fatigue process. The surface of a specimen cycled for 2500 cycles is shown in Figure 22; slight surface irregularities were observed at this early stage in the test. These surface perturbations lengthened and deepened as the thermal cycling treatment continued, until after 4000 cycles, they became quite prominent. After 6000 cycles, very deep cracks or notches were present as shown in Figure 23. Attempts to observe these cracks inside the volume of the material were not successful in these initial experiments; however, they were noted in subsequent tests, especially those involving the reinforced 2024 material. An example of this is shown in Figure 24. In this figure, extensive ratcheting of the internal matrix layers is plainly visible. Due to an experimental problem, a compressive load was applied to this particular specimen and it failed in bending. This resulted in the appearance of the split fibers. However, this type of fiber damage was not observed in any of the specimens subsequently failed, reinforced with 0.0135 cm (0.0053 inch) diameter fibers. These initial

results indicated that 6000 thermal cycles were necessary in order to achieve the maximum degradation in the composite mechanical properties. Thus, all of the remaining specimens were exposed to this number of cyclic temperature variations. It should be noted here, however, that damage to some specimens, especially those fabricated from the reinforced 2024 alloy, could be detected at an early stage.

The thermal fatigue experiments were conducted by subjecting specimens, reinforced with 0.0135 cm (0.0053 inch) diameter fibers, to 6000 thermal cycles in which the temperature was varied between room temperature and either 315°C, 365°C, or 425°C. The reinforced 1100 material was little affected by cycling to any of the maximum temperature limits. However, the magnitude of the damage in the reinforced 6061 and 2024 materials increased as the maximum cycling temperature used in the test was raised. This observation was a general one, since it was noted that the degree of damage varied from specimen to specimen, due presumably to the variations in the fiber-matrix bond strength previously discussed.

In contrast to the observations obtained using the 1100 material, a significant degree of surface damage was sustained by both the reinforced 6061 and 2024 materials, with a maximum degradation occuring in the reinforced 2024 material cycled to the higher temperature limits. In this material, cycled up to 365°C, the surface irregularities were very pronounced and appeared as visible cracks at an early stage in the fatigue lifetime. The width of these cracks increased progressively until in some cases, the first layer of boron fibers

was exposed. This is shown in Figure 25. A photo micrograph of a similar specimen taken with the scanning electron microscope is presented in Figure 26 and this also shows the extent of the surface damage. As will be discussed later, the mechanical properties of some of these materials was degraded by simply heating the specimens; however, the maximum degradation was undoubtedly associated with the appearance of these macroscopically cracked surface layers. And, this effect only occurred in those specimens that were subjected to cyclic temperature changes.

The maximum cyclic damage was sustained by specimens cycled using a maximum temperature of 425°C. Again, the surface appearance of the reinforced 1100 material was not changed significantly by the thermal fatigue treatment. However, both the reinforced 6061 and 2024 materials sustained appreciable surface damage, and the measured mechanical properties were relatively poor. The surface apppearance of the reinforced 6061 material was similar to that discussed for the 2024 material subjected to a maximum cyclic temperature of 365°C. However, additional damage was sustained by the 2024 material. In some specimens formed from this material, the ratcheting process shown in Figure 24 was so extensive that the matrix-fiber bond was extensively weakened, and the first aluminum layer disintegrated and fell away from the specimen. This is shown in Figure 27. Figure 28 was obtained from one of these specimens. It is quite

apparent that the surface layer had disintegrated and some of the fibers have bent away from the specimen surface. As expected, tensile properties of these specimens were extremely poor. Actual measurements indicated that the thermal fatigue treatment was sufficient to reduce the tensile strength by about an order of magnitude.

In general, specimens reinforced in the longitudinal direction did not distort when subjected to the cyclic temperature changes. In some cases, however, a slight twist developed particularly in the case of the one inch wide shear specimens as shown in Figure 29. Although many factors may be involved, intuitive reasoning led us to believe that this twisting effect was probably caused by a slight misalignment in the fibers present in the specimens. This would essentially produce a cross-plied, unbalanced composite. The coupled stress condition that would be developed on heating would cause the specimen to twist. Creep of the matrix would then result in the twist being present at room temperature.

The transverse properties of fatigued materials were also difficult to measure in some cases due to changes in the shape of the specimens. Some of these transverse specimens, particularly those subjected to the higher cyclic temperatures, were quite severely bent, when removed from the cycling apparatus, as shown in Figure 30. We were never able to isolate the cause of this problem. Although we intuitively suspect that the transient temperature gradient which undoubtedly existed along the length of each specimen as it was heated and cooled was responsible. Other temperature

gradients were present during testing. With the furnace stationary, measured values of the temperature difference that existed between the center and top of the specimens was found to be 2°C. The difference between the center position and the bottom of each specimen was slightly larger, being 5°C. Undoubtedly, conduction effects resulted in the temperature of the gripped portion of each specimen being different from the remaining section despite the presence of a layer of asbestos thermal insulation placed between the specimen and the aluminum grip material.

Bent transverse specimens were removed from the thermal fatigue apparatus and formed back to their original configuration by creep loading them at a constant temperature of 250°C. Great care had to be exercised during the performance of this operation otherwise the specimens would crack or break into two or more pieces.

Oxidation products were also observed to be formed on the boron fibers present in transverse specimens after thermal cycling. As shown in Figure 31, the oxidized cross section of the boron fibers exhibited a characteristic pattern that presumably reflects the growth conditions experienced during the fabrication of the fiber. Oxidation of the former tungsten core was also observed. In this case, the oxidation product extruded from the cross section to give the petal-like configuration shown in Figure 32.

iv. Mechanical Properties of Thermally Fatigued Materials

A summary of the mechanical properties of boron reinforced

1100 aluminum subjected to 6000 thermal cycles is shown in Table XXV. Although the largest cyclic temperature changes caused a small strength reduction, it is readily apparent that a dramatic change in the properties measured parallel to the fibers does not occur. Also, subjecting the specimen to a constant temperature of 425°C for nine hours did not degrade the tensile strength severely, although the modulus values appeared to go down. This degradation of the elastic modulus also tended to be exhibited in specimens thermally cycled to the same maximum temperature. The reason for this effect is not immediately obvious for other experiments carried out by the author [4] and others [17] have indicated that the elastic modulus is not affected by heating at elevated temperatures for short times. The unidirectional tensile strength of the 1100 reinforced material thermally cycled between room temperature and 425°C appeared to decrease slightly from the values exhibited by the material cycled between the lower temperature ranges.

The transverse strengths and the longitudinal shear strengths also appear to be degraded by the cyclic temperature variation to the highest maximum temperature used. The work of Chen and Lin, previously referred to, indicates that a decrease in the matrix-fiber bond strength would lower the transverse strength without affecting the transverse modulus significally. Presumably, the same effect would be responsible for the degradation in the shear strength.

Observations with the scanning electron microscope indicate that failure of these composite specimens in the

transverse direction results from the failure of the fiber-matrix bond. An example of transverse failure is shown in Figure 33. The surface of the boron fiber is clearly visible with little or no aluminum matrix material adhering to it. Failure of the matrix-matrix interface is also observed. In contrast to reported observations on specimens reinforced with 0.0107 cm (0.0042 inch) diameter fibers, there was no evidence of any fiber splitting.

The mechanical properties of boron reinforced 6061 aluminum alloy obtained after the various cyclic treatments are shown in Table XXVI. As mentioned previously, the as-received properties of this material were markedly superior to the reinforced 1100 material. The greater longitudinal strength values were attributed to the superior strengths exhibited by the reinforcements extracted from the 6061 material. The longitudinal and transverse modulus values were similar to those values exhibited by the reinforced 1100 material. In contrast, superior transverse strength and shear strengths were exhibited. This is expected however, for the results simply reflect the inherent strength differences in the matrix materials.

Subjecting the reinforced 6061 material to cyclic temperature variations using a maximum temperature of 315°C did not degrade the properties of this material significantly. However, degradation was initiated when the maximum cyclic temperature was raised to 365°C. The extent of the degradation varied from specimen to specimen. Some specimens exhibited negligible surface damage and a corresponding small decrease

in mechanical properties, while other specimens were easily damaged and a significant decrease in the mechanical properties occurred.

Undoubtedly, the maximum degradation occurred when the maximum cyclic temperature was raised to 425°C. In this case, it was noted that the longitudinal tensile strength dropped to a value similar to that exhibited by the 1100 material. The extent of the damage varied from specimen to specimen in a manner similar to the results obtained at the lower temperatures. However, it is to be noted that the transverse strength and shear strength values were reduced by treatment at this high temperature.

Specimens heated at a constant 425°C for a period of nine hours appeared to exhibit mechanical properties almost identical to some of the specimens that had been subjected to the thermal fatigue environment. It is therefore difficult to separate the effects caused by a simple exposure to the elevated temperature from the effects caused by the cyclic temperature variations. Optical examinations indicated that the surface rumpling type of damage was exhibited by the specimen subjected to the thermal fatigue environment only. However, only in one case was the surface layer ratcheted or cracked sufficiently to expose boron fibers. The strength of this composite was significantly lower than the other tested specimens, being 5610.6 kg/cm^2 (79.8 ksi)

The mechanical properties of the boron-reinforced 2024 aluminum alloy subjected to the thermal cycling treatments is shown in Table XXVII. The as-received properties are

similar to those exhibited by the reinforced 6061 material and superior to the reinforced 1100 material. Also, the transverse properties appear to be superior to the 6061 material reflecting the inherent superiority of the properties of the 2024 matrix. It should be reported here, however, that the transverse properties seemed to vary from specimen to specimen, an effect we believe to be associated with variations in the integrity of the matrix fiber bond. Presumably, this integrity varies according to the position that each specimen occupied in the fabricated panel.

The reinforced 2024 aluminum matrix materials were not affected by cycling between room temperature and 315°C, at least for the number of thermal cycles applied here. Increasing the maximum cyclic temperature to 365°C produced an effect similar to that observed in the reinforced 6061 material. The surfaces of both these materials exhibited marked rumpling, and some property variation was observed; however, a severe strength loss was only observed when macroscopically observable cracks were formed in the surface layers. Once surface cracks became visible, the strength of the material was quickly degraded. The observed effects varied markedly from specimen to specimen especially when the maximum cyclic temperature was maintained less than 365°C. For instance, it was noted that while the tensile strength of some specimens appeared to be little affected by the treatment, a significant drop in the strength of other specimens occurred. Small decreases in the transverse tensile strength were also noted.

Cyclic temperature changes using a maximum temperature of 425°C produced a dramatic strength degradation in all specimens of boron reinforced 2024 material. In some of the materials, the surface aluminum layers became separated from the composites specimen. In these specimens, the attachment of strain gauges became almost impossible, and the modulus values reported here for these specimens may therefore contain large errors. The transverse strength of these materials also appeared to be degraded; however, as mentioned previously all of the specimens were bent and had to be creep formed back to their original shape. After creep forming, each specimen was carefully examined using an optical microscope to confirm that the forming operation had not introduced cracks parallel to the fibers; however, their presence should not be discounted, and thus the creep forming operation may be responsible for the low transverse tensile strengths and modulus values reported. The values of the shear strengths observed again depended on the specimens. If severe ratcheting of the surface was exhibited, then a low shear strength was obtained.

The specimens reacted to the constant temperature of 425°C for nine hours in a manner similar to the reinforced 6061 material. The tensile strengths were reduced to values similar to that exhibited by both the thermally cycled reinforced 6061 and the as-received 1100 material. Thus, it appears that simply holding the specimens at an elevated temperature of 425°C for extended time can result in a small

degradation in the tensile strength; however, thermal cycling produces ratcheting of the matrix surface, which eventually causes macroscopically visible surface cracks to appear. A dramatic decrease in the strength of the composite then occurs.

v. Individual Fiber Tests--thermally fatigued specimens

The failure stresses of the fibers extracted from thermally cycled specimens are tabulated in Tables XXVIII through XXXVI. Subsequent computations identical in principle to those described previously using the results obtained from fibers extracted from as-received specimens are presented in Tables XXXVII through XLV. The histograms obtained from these fiber strengths are presented in Figures 34 through 42, and the Weibull distribution plots are shown in Figures 43 through 45. The observed linearity of the data suggests that the strengths of these fibers extracted from thermally fatigued specimens can be described by a Weibull-type distribution similar to that used to describe the strength of fibers extracted from as-received specimens. The mean strengths of the fibers again depend on gauge length, the smaller gauge length fibers being stronger. The mean strengths of the fibers extracted from the 6061 material were higher than the values obtained from the 1100 material. The mean strength values of the 6061 and 1100 reinforcement materials were 35.788×10^3 kg/cm^2 (509.02 ksi) and 29.797×10^3 kg/cm^2 (423.81 ksi) respectively, for the 3.81 cm (1.5 inch) fibers. In contrast, the mean strength of the fibers extracted from the 2024 material was extremely low, reflecting

the degradation in strength of the composite material subjected to the 425°C maximum cyclic temperature environment. In this case, the mean strengths of fibers of gauge length 3.81 cm (1.5 inches) had been reduced from the as-received value of 39.952 x 10^3 kg/cm^2 (568.25 ksi) to 14.468 x 10^3 kg/cm^2 (205.78 ksi)

The parameters σ_o and ω were determined using the methods described previously, and the results were averaged. The mean fiber strengths using these computed values exhibited good agreement with the mean fiber strengths computed using the raw data, as shown in Table XLVI.

vi. Strength of Fiber Bundles

Bundles of fibers were prepared from the three as-received reinforced alloys and from the three alloys after they had been subjected to the cyclic temperature variations using a maximum temperature of 425°C. The failure loads and the number of fibers in each bundle were noted. After these bundles had been pulled to failure, the failure stress was computed by dividing the failure load by the area of one fiber multiplied by the number of fibers in the bundle. The results are tabulated in Table XLVII from which it can be seen that the strengths were 15.596 x 10^3 kg/cm^2 (221.82 ksi), 16.581 x 10^3 kg/cm^2 (235.83 ksi), and 21.114 x 10^3 kg/cm^2 (300.30 ksi) for bundles of fibers prepared from as-received 6061, 1100, and 2024 materials, respectively.

Also, shown in Table XLVII, the strengths of similar bundles prepared from thermally cycled specimens were 15.935 x 10^3 kg/cm^2 (226.64 ksi), 18.973 x 10^3 kg/cm^2 (269.86 ksi), and 7.456 kg/cm^2 (106.05 ksi), respectively, for bundles

prepared from the 6061, 1100, and 2024 alloys.

It can be easily noted that cyclic temperature variations produce a degradation in the strength of bundles of fibers extracted from the 2024 material only. The strength of the fiber bundles formed from the 6061 material is not affected, and the strength of bundles obtained from the 1100 material appears to increase. In this respect, therefore, the bundle strengths reflect the results obtained from the composite specimens.

The number of broken fibers present in a bundle of fibers extracted from as-received material was obtained from the acoustic recording experiments described in the previous section. The total number of fiber breaks immediately prior to bundle failure was surprisingly small, as shown in Table XLVIII. Indeed, noise resulting from the breakage of only three fibers was recorded from bundles extracted from the 6061 material. And, only eighteen of nineteen fibers broke prior to fracture of the bundles formed from the remaining two alloys.

vii. Effect of Thermal Cycling on Loaded Specimens

A small number of thermal fatigue experiments were carried out on specimens also subjected to a tensile load. Unfortunately, shortage of specimens precluded an extensive study; thus, only a few observations could be obtained. Specifically, a major problem was encountered which could be traced to relatively low high temperature interlaminar shear properties of the composites. For instance, it was impossible to complete

a test at maximum cyclic temperatures of 365°C or 425°C, using the gripping arrangement shown in Figure 46, for the first aluminum layer sheared from the test piece and the specimen pulled out of the grip. This occurred after very few thermal cycles had been completed and, as shown in Figure 47, it resulted in transfer of the first aluminum layer to the grip material.

Tests using an applied stress of about 2460.8 kg/cm^2(35 ksi) maximum temperature limit of 315°C were completed; however, the surface observations were similar to those previously reported using unstressed specimens, and the failure loads were not affected by the treatment.

DISCUSSION

i. Failure Mode of Composites

a. Calculation of Lower Bounds

Using the statistical data obtained from the strength of the individual fibers as described in the previous section and the theory of Daniels and Coleman, [14], [11], the strength expected from a bundle of these fibers could be calculated. According to Coleman, values for the mean strength of the fibers, $\bar{\sigma}$(calc), and the strength of a bundle of such fibers, σ_B, can be computed from expressions 5 and 6 previously referred to. Values of $\bar{\sigma}$(calc) and σ_B were computed and have been shown in Tables XXIII and XLVI. We believe that the agreement between these mean values calculated using computed values of σ_o and ω are extremely close to those calculated

using the conventional methods. Thus, we believe that reasonably accurate values of the mean strengths and the bundle strength can be calculated not only for the fiber lengths investigated, but also for other fiber lengths of interest. In our case, the gauge length of each specimen was 7.62 cm (3 inches). Since it proved experimentally difficult to test fibers of this length, the strength of a bundle of 7.62 cm (3 inch long) fibers extracted from 6061, 2024, and 1100 aluminum was computed and found to be 28.090 x 10^3 kg/cm^2 (399.53 ksi), 26.950 x 10^3 kg/cm^2 (383.31 ksi), and 17.914 x 10^3 kg/cm^2 (254.80 ksi) respectively.

The values of the mean strengths of fibers extracted from composite specimens thermally cycled 6000 times between room temperature 425°C was also calculated using the values of σ_o and ω obtained from the applicable Weibull type plots. Again, the values of the mean strengths obtained in this manner were very close to those calculated using the usual expressions. We again concluded that accurate values of the mean strengths and the bundle strengths of fibers extracted from thermally fatigued materials could be calculated for differing lengths of fibers. In this case, the strength of a bundle of 7.62 cm (3 inch long) fibers extracted from thermally cycled 6061, 2024, and 1100 aluminum alloys was found to be 19.333 x 10^3 kg/cm^2 (274.98 ksi), 6.019 x 10^3 kg/cm^2 (85.61 ksi), and 19.930 x 10^3 kg/cm^2 (283.47 ksi) respectively. It is to be noted that while the expected bundle strength of the fibers extracted from the 1100 material was similar for both the as-received and thermally cycled fibers, the bundle strength expected from the 6061 material was decreased by a

small but significant amount; however, the bundle strength of the 2024 material was decreased dramatically.

The strengths of actual bundles of fibers prepared according to the technique described in the previous section is compared to the theoretically expected values in Table XLIX. It was noted during the actual testing of the bundles that some of the fibers were broken and some were misaligned slightly; thus, some of the experimental determinations of the bundle strength appeared to be lower than theoretically expected. However, in the main, reasonably close agreement was observed.

Either of the two bundle strength values, experimental or theoretical, can be used to predict a lower bound of strength for composite specimens. If the matrix material is assumed to carry no load and to transfer no stress between the fibers, then the lower bound of strength will be identical to the bundle strength as calculated or measured here. Variations in the reinforcement content in actual composites can be allowed for by multiplying the appropriate bundle strengths by the fiber volume fraction present in each specimen. Accordingly, the expected lower strength bounds were calculated and are included in Table XLIX. It should be mentioned here that with this model the matrix is assumed to contribute nothing to the strength of the material. In practice a small tensile load would be sustained by the matrix; however, it is doubtful whether this effect would contribute more than an additional 351.5 (5) to 703 kg/cm^2 (10 ksi)to these lower strength bounds.

b. Calculation of Upper Bounds

Observation of the actual strength exhibited by the reinforced aluminum alloys indicate that the strengths of composite specimens are much greater than the lower bounds calculated in the previous section. Thus, we must conclude that the matrix reinforces the fibrous material in a synergistic manner. In other words, the presence of the matrix allows the composite to carry more stress than would be expected using a simple load sharing argument. In effect, therefore, the matrix exhibits an efficiency factor greater than one.

According to Rosen, [12] , the matrix in a composite can function to localize the effect of fiber breaks. Specifically, the load formally carried by the broken fiber is transferred to adjacent fibers through the matrix over a length equal to the transfer length, δ . If the elastic deformations occurring in the metal matrix are neglected and if the shear yield strength of the matrix is assumed equal to the shear strength, then, δ can be calculated by inserting the appropriate values into the expression:

$$\delta \quad \frac{\sigma d}{2\tau} \qquad \ldots 7$$

where σ is the stress in the fibers at failure of the composite, i.e., σ_B, d is the fiber diameter, and τ is the shear strength of the matrix. Proceeding with the theory of Rosen, a composite is considered to be made up of many bundles of fibers of length, δ, arranged in series. Failure of one of these bundles results in total failure of the composite. Since the actual value of δ is small, the strength of a bundle of fibers can be calculated by substituting the

appropriate length values into equation 5. Unfortunately, the ineffective length, δ, and the bundle strength, σ_B, are interdependent, that is, from equation 7:

$$\sigma_B = \frac{2\tau\delta}{d}$$

and, from equation 5,

$$\sigma_B = \sigma_o \left\{ \frac{(L-\delta)}{d} \omega e \right\}^{-1/\omega}$$

Since both equations must be satisfied, the ineffective length and the bundle strength have to be computed iteratively until the values obtained satisfy the above two equations. The flow chart of this computation is illustrated in Figure 49. Initially, the ineffective length was calculated using the strength of a bundle of 7.62 cm (3 inch long) fibers, (i.e., the lower strength bound) and the iteration proceeded until the upper strength bound was obtained. The parameters σ_o and ω were determined from the data reported previously, and the matrix shear strength values used were those determined in this program using the double shear specimens. The ineffective lengths so calculated are shown in Table L for both the as-received and cycled fibers. It can be seen that ineffective lengths of 0.254 cm (0.100 inch), 0.320 cm (0.126 inch), and 0.188 cm (0.074 inch) were computed for the as-received fibers extracted from 6061, 1100, and 2024 materials, respectively. These lengths increase to 0.351 cm (0.138 inch), 0.681 cm (0.268 inch), and 0.828 cm (0.326 inch) for the fibers extracted from similar matrix material that has undergone 6000 thermal cycles. This increase is directly related to the decreased properties obtained from thermally fatigued composite shear specimens; in effect, the

matrix fiber bond strength was reduced. The upper strength bounds were finally calculated by substituting the length, δ, into the expression that describes the bundle strength, and substituting this value into the rule of mixtures, as discussed previously. The upper strength bounds for the as-received specimens were then calculated to be 18.18×10^3 kg/cm^2 (258.54 ksi), 12.57×10^3 kg/cm^2 (178.77 ksi), and 18.981×10^3 kg/cm^2 (269.97 ksi) for the 6061, 1100, and 2024 aluminum alloy matrix materials, respectively. Similarly, the respective upper bounds for the cycled specimens were 17.211×10^3 kg/cm^2 (244.79 ksi), 16.898×10^3 kg/cm^2 (240.34 ksi), and 10.979×10^3 kg/cm^2 (156.15 ksi). These results are shown together with the lower bound results in the **Table LI.**

Inspection of the data indicates that the upper strength bounds were remarkably similar for both the as-received and thermally cycled specimens of reinforced 6061 aluminum. And, although the upper strength bound increased, the lower bounds for the 1100 matrix material were similarly unaffected. Thermal cycling reduced the theoretical lower strength bounds of the reinforced 6061 material from the as-received 12.501×10^3 kg/cm^2 (177.8) to the thermal cycled 8.79×10^3 kg/cm^2 (125.0 ksi) values. The prime cause of this was the reduction in the bundle efficiency factor, ϵ, which resulted from the increased scatter in the strengths of the fibers extracted from the thermally cycled material. The small increase in the ineffective length and the small decrease in the strengths of individual fibers also contributed. By far, the large degradation was observed in the strengths of fibers extracted from the 2024 material. A large decrease in the mean strength

of the extracted fibers was observed, and the ineffective length exhibited by this material was increased from a value of 0.188 cm (0.074 inch) to the value of 0.828 cm (0.326 inch), due mostly to the decrease in the effective shear strength of the 2024 matrix material caused by the ratcheting process. All of these effects contributed to the decrease of about 7.734×10^3 kg/cm^2 (110 ksi) in the upper strength bounds and a decrease of 9.843×10^3 kg/cm^2 (140 ksi) in the lower strength bounds.

c. Calculation of the Number of Broken Fibers

We have assumed in this discussion that the failure of composite specimens occurs through the failure of individual fibers at certain points in the cross section. Total failure of each specimen occurs by the accumulation of fiber breaks. Work by Hedgepeth et.al., [18],[19], has indicated, however, that the load formerly carried by a broken fiber will produce a load concentration in adjacent fibers. Only fiber elements of length, δ, adjacent to the broken element will be subjected to the increase in stress, however. Thus, providing the characteristics of the fiber strength distributions and the stress concentration factors associated with the breaks are known, the probability of failure of adjacent fibers can be calculated. Further calculation can then indicate the probability of total composite failure resulting from an initial crack in a single fiber.

If, in a composite system, there are "n" fibers and "mn" elements where:

$$m = \frac{L}{\delta}$$

then, the number of elements that can be expected to fail under a stress, σ, will be:

$$E_1(\sigma) = mng(\sigma) \qquad \ldots 8$$

In this work, m and n are known and $g(\sigma)$ can be obtained from the strengths of individual fibers; thus, $E_1(\sigma)$ can be easily calculated.

As pointed out by Rosen and Zweben [20] , the probability that an adjacent element has broken due to the load concentration K_1 caused by a single broken fiber, must equal the probability that its strength lies between σ and $K_1(\sigma)$, this probability is:

$$g(K_1 \sigma) - g(\sigma) \qquad \ldots 9$$

This probability can be easily calculated using the results obtained from the strengths of individual fibers and the stress concentration factors for a three-dimensional composite calculated by Hedgepeth and Van Dyke. In addition, the probability that any or all of the adjacent fibers will break can be calculated using the probability theory shown in the paper by Rosen and Zweben. Effectively, therefore, it is possible to calculate the expected number of multiple fibers breaks $E_2(\sigma)$, $E_3(\sigma)$, etc., that exist in a composite immediately prior to failure. By substituting the data shown elsewhere in this report into expression 8, the number of broken fibers present in a specimen immediately prior to fracture was calculated. The results shown in Table LII indicated that a bundle of 7.62 cm (3 inch long) fibers prepared from the as-received or thermally fatigued materials would be expected to fail after a very small number of individual fibers had broken. In this table, the function $g(\sigma)$ was calculated using the Weibull expression for bundles of length equal to three inches. The theoretical values were obtained by using the theoretically expected bundle strengths. In contrast, the values shown in the experimental observations were

obtained using the actual strengths of bundles determined from experiment. For the most part, the agreement between the two sets of data is remarkably good. In all cases, failure of the bundle of fibers is expected after failure of very few individual fibers, i.e., about 10. As described in a previous section, the number of broken fibers at failure of a bundle was monitored acoustically by reporting the noise associated with fiber breakage. The small number of broken fibers obtained in this manner, previously shown in Table XLVIII, confirms the theoretical conclusion that failure of a bundle of fibers should occur after very few individual fibers had broken.

Using the methods of calculation described above, the number of broken fibers existing in a composite immediately prior to failure was calculated. In order to generate the data, the values of the ineffective length at the observed failure strength of each composite were calculated. Cumulative frequency functions $g(\sigma)$ were then calculated by inserting the appropriate ineffective length, δ, into the Weibull equation.

The number of fiber breaks in as-received and thermally cycled composite specimens immediately prior to failure is shown in Tables LIII and LIV. It is strikingly apparent when this data is compared to the data generated for 7.62 cm (3 inch) long bundles that the presence of the matrix has resulted in a substantial increase in the total number of fiber breaks expected immediately prior to failure of a specimen. Interestingly enough, however, the total number of broken

fibers per layer is about the same, irrespective of whether the layer length is equal to 7.62 cm (3 inches) or is equal to the ineffective length, δ . Additional calculation indicates that the probability of two broken fibers existing side by side in the same layer is finite, although the number of these multiple breaks per layer is small. Also, there is a small number of triple fiber breaks expected at failure of the as-received material. Here again, the number per layer is expected to be small. The effect of cyclic temperature variations is to increase the total number of broken fibers prior to failure of a 7.62 cm (3inch) long bundle. The biggest increase being expected in the bundle extracted from the 2024 material. The presence of a matrix of 1100 or 6061 aluminum only increases the total number of breaks that can be tolerated in a thermally fatigued specimen by a factor of four. However, failure of a specimen of thermally cycled 2024 material occurs after 35 fibers have broken irrespective of whether or not the reinforcement is surrounded by matrix.

Cumulative frequency curves calculated for as-received and thermally cycled reinforcement material for lengths equal to 7.62 cm (3 inches) and the ineffective length, δ , are shown in Figures 49 through 54. It is immediately obvious that the presence of the matrix results in a movement of the cumulative frequency curve to higher stress values. More important perhaps is the observation that failure of both the bundles and of the composites occurs at a stress where the probability of failure of the individual fibers is extremely small. In fact, failure of both the bundle and the as-

received composite materials occur at about the same point on the respective cumulative frequency curves, i.e., $G(\sigma) < 0.1$. Of more interest perhaps, the failure strengths of most of the composites occur at a stress at which the probability of failure of 7.62 cm (3 inch) long fibers is about 0.5. This means that composite strength values calculated by substituting mean fiber strength data obtained for long fibers into the well-known rule of mixtures will yield an expected composite strength of the correct order of magnitude. Nevertheless, the basis of this simple, widely used calculation is incorrect.

In the above discussion, we have assumed that the upper bound of composite strength is given by the stress necessary to break a certain number of fibers. Failure of the specimens is then assumed to occur in cumulative manner. As pointed out by Zweben [21] however, the transfer of stress from a broken fiber may result in fracture of adjacent fibers and the propagation of a macroscopic crack. Failure of a composite may then occur at a stress lower than the expected upper bound. In the present work, some initial double slotted specimen failed prematurely in tension. In each case, a crack propagated from the root of the EDM cut slots in a direction perpendicular to the fiber axis. Two specimens of 6061 material failed in this manner at an applied gross tensile stress of 3.59 $\times 10^3$ kg/cm^2 (51 ksi). Using the theory of Hedgepeth and Van Dyke, the elastic load concentration in the fiber immediately adjacent to the 1.27 cm (0.5 inch) long internal slot was calculated to be 6.7. Since the average stress in the fibers at failure

of a composite containing 44 v/o reinforcement was approximately 8.16 x 10^3 kg/cm^2 (116 ksi), then the stress in the fiber immediately adjacent to the machined slot was about 52.94 x 10^3 kg/cm^2 (753 ksi). In comparison, the strength of parallel-sided tensile specimens of reinforced 6061 material was about 15.47 x 10^3 kg/cm^2 (220 ksi). The mean stress in the fibers at this strength level was, therefore, 35.15 x 10^3 kg/cm^2 (500 ksi). And, as discussed above, approximately three adjacent fibers had failed immediately prior to composite failure. From Hedgepeth, et.al., the elastic stress concentration factor associated with this number of broken filaments is about 1.46 for a three-dimensional square array. Accordingly, the stress level in the fibers immediately adjacent to the broken elements was 51.32 x 10^3 kg/cm^2 (730 ksi). It can be argued that an analysis that depends on the principles of elasticity may not be applicable to the present case. It is almost certain that the theoretical load concentration value of 6.7 calculated using a two-dimensional elastic theory is higher than that actually generated, for the matrix probably deforms plastically and a stress of 51.32 x 10^3 kg/cm^2 (730 ksi) is larger than the strength of any of fibers tested. However, neglecting dynamic effects, the same argument can be applied to the stress concentration factor of 1.46 calculated as being generated around three adjacent fiber breaks. Thus, although the agreement between the values of the stresses generated in fibers adjacent to a machined slot and those generated around a much smaller number of broken fibers may appear fortuitous, the effect is certainly worthy of a more detailed investigation. Indeed, the application of the principles of

fracture mechanics to failure of unidirectionally reinforced boron-aluminum composites might be profitably examined.

ii. Effect of Cyclic Temperature Variations

Comparison of the upper and lower strength bounds calculated for as-received and thermally fatigued materials with the strength values determined experimentally has been presented in Table LI. The tensile strength of composite specimens fabricated from as-received materials was observed to approach the expected upper strength bounds in these materials. We therefore concluded that the procedures used in the fabrication of these materials had been carefully controlled to produce a material which exhibited optimum properties. The experimental values of the transverse strengths were also very close to those theoretically expected from a perfectly bonded composite. We believe that the variation in both the longitudinal and transverse strengths of some specimens indicated that the strength of the matrix fiber bond varied at different positions in the panel. This effect presumably results from variations in the fabrication technique. For example, should the cleanliness of the boron fibers surface vary, weak interfacial bonds would result. It appears, however, that the attainment of maximum longitudinal and transverse strengths in the as-received materials may not be possible in these boron reinforced alloys, since the failure of the composite may change from a cumulative to a crack propagation mode as these strength values of individual specimen increases.

Cyclic temperature changes using a maximum temperature of 425 °C cause the experimental strength values to decrease. The major cause of this effect is undoubtedly due to the decrease in the strength of the reinforcements. However, it should also be noted that the strength values move away from the upper bound to approach, and in some cases to equal, the lower bound of strength. This effect must be caused by an increase in the ineffective, or stress transfer length, resulting from a degradation in the matrix-fiber bond. The ratcheting process undoubtedly reduces the effective bonded area, and it must also reduce the already small load-bearing capacity of the matrix. Obviously, the matrix is losing its efficiency, and the magnitude of its synergistic strengthening effect is reduced significantly. Under these conditions of reduced stress transfer, the crack propagation mode of failure would be unlikely.

CONCLUSIONS

Applying 6000 thermal cycles to three aluminum alloys reinforced with about 44 v/o unidirectional boron fibers resulted in the following conclusions:

1. The strength of 0.0135 cm (0.0053 inch) diameter boron fibers, extracted from as-received or thermally fatigued aluminum alloys, can be described by a Weibull distribution.
2. The strength of as-received or thermally cycled boron-fiber-reinforced-aluminum specimens is best described by means of upper and lower strength bounds. And, the experimental strength values approach the upper bound as the effective matrix-fiber bond strength increases.
3. The failure mode of reinforced specimens probably changes from a cumulative to a crack propagation mode as the experimental strengths approach the upper bound.
4. Cyclic temperature variations between room temperature and 315°C produce a negligible effect on the mechanical properties of reinforced 1100, 6061, and 2024 aluminum alloys.
5. Cyclic temperature variations between room temperature and 365°C produced a negligible effect on the mechanical properties of the reinforced 1100 alloy. Some of the properties of reinforced 6061 were reduced significantly. However, some of the properties of the reinforced 2024 specimens were reduced markedly.

6. Cyclic temperature variations between room temperature and 425°C caused significant degradation of both the longitudinal and transverse properties of the reinforced 1100 material. However, dramatic property degradation occurred in most of the 6061 and all of the 2024 specimens.
7. A drop in mechanical properties occurs by simply heating reinforced boron-aluminum alloys to 425°C for nine hours. However, thermal fatigue causes ratcheting of the matrix surface and, if this becomes severe, dramatic property degradation occurs.
8. The strength degradation can be explained in terms of decreased fiber strengths, decreased effective strength of the matrix-fiber bond and a decrease in both the load and stress transferring capacity of the matrix.

REFERENCES

[1] Wright, M. A., "Effect of Thermal Cycling on the Mechanical Properties of Various B-Al Alloys", Paper presented at Mini-Symposium on Composium Materials, NASA, Huntsville, August 14-15, 1972.

[2] Wright, M. A., "Failure of Composites", Paper presented at American Society of Metals Annual Meeting, Cleveland, Ohio, October 16-20, 1972.

[3] Wright, M. A., and J. Wills, "The Effect of Cyclic Temperature Variations on the Mechanical Properties of Various Boron-Aluminum Alloys", in preparation.

[4] Wright, M. A., and B. H. Intwala, "The Effect of Elevated Temperatures on the Mechanical Properties of Boron-Aluminum", Submitted to J. of Mat. Science.

[5] Mehan, R. L., "Fabrication and Evaluation of Sapphire Whisker Reinforced Aluminum Composites", Metal Matrix Composites, ASTM Special Publication, No. 438, Philadelphia, 1968.

[6] Shahinian, P., "Thermal Fatigue of Boron-Aluminum Composites", SAMPE Quarterly, 2:28-35, June, 1970.

[7] Anthony, K. C., and W. H. Chang, "Mechanical Properties of Al-B Composites", Transactions of the American Society of Metals, 61:550-558, September, 1968.

[8] Volk, H. F., Nara, H. R., and D. P. Hanley, "Integrated Research on Carbon Composite Materials", TR, ARML-TR-66-310, PT V, Volume 1, January, 1971.

[9] Kreider, K. G., Dardi, L. D., and K. Prewo, "Metal Matrix Composite Technology", Air Force Materials Laboratory, TR-70-193, Wright-Patterson Air Force Base, Ohio, July, 1970.

[10] Pepper, R. T., Upp, J. W., Rossi, R. C., and E. G. Kendall, "The Tensile Properties of a Graphite-Fiber-Reinforced Al-Si Alloy", Met. Trans., Z, 117, 1971.

[11] Coleman, B. D., "On the Strength of Classical Fibers and Fiber Bundles", Journal of the Mechanics and Physics of Solids, 7:60-70, November, 1958.

[12] Rosen, B. W., "Tensile Failure of Fibrous Composites", AIAA Journal, 2:1985-1991, November, 1964.

[13] Chen, P. E., and J. M. Lin, "Transverse Properties of Fibrous Composites", Materials Research and Standards, Volume 9, No. 8, 29-33.

[14] Daniels, H. E., "The Statistical Theory of the Strength of Bundles of Threads", Proceedings of the Royal Society, 183:405-535, 1945.

[15] Herring, H. W., "Selected Mechanical and Physical Properties of Boron Filaments", NASA TN D-3202, 1966.

[16] Corten, H. T., "Micromechanics and Fracture Behavior of Composites", Modern Composite Materials, Addison-Wesley Publishing Company, 1967, pp. 27-105.

[17] Klein, M. J., and A. G. Metcalfe, "Effect of Interfaces in Metal Matrix Composites on Mechanical Properties", TR-AFML-TR-71-189, October, 1971.

[18] Hedgepeth, J. M., "Stress Concentration in Filamentary Composites", NASA-TND-882, May, 1961.

[19] Hedgepeth, J. M., and P. Van Dyke, "Local Stress Concentrations in Imperfect Filamentary Composite Materials", Journal of Composite Materials, 1:294-309, July, 1967.

[20] Zweben, C., and B. W. Rosen, "A Statistical Theory of Material Strength with Application to Composite Materials", Journal of the Mechanics and Physics of Solids, 18:189-206, June, 1970.

[21] Zweben, C., "Tensile Failure of Fiber Composites", AIAA Journal, 4:2325-2331, December, 1968.

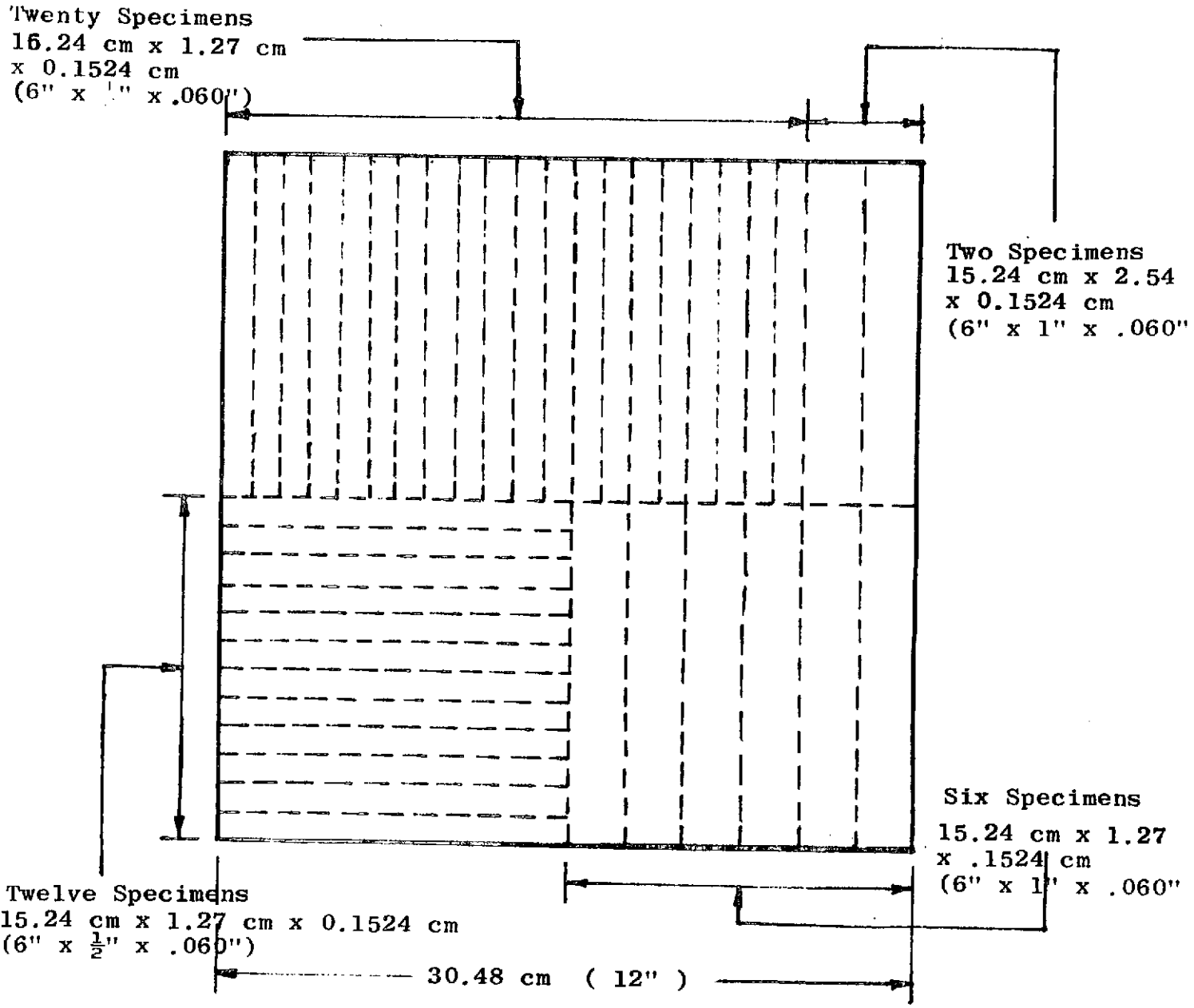

FIGURE 1

Fabricated panel configuration showing individual specimen positions

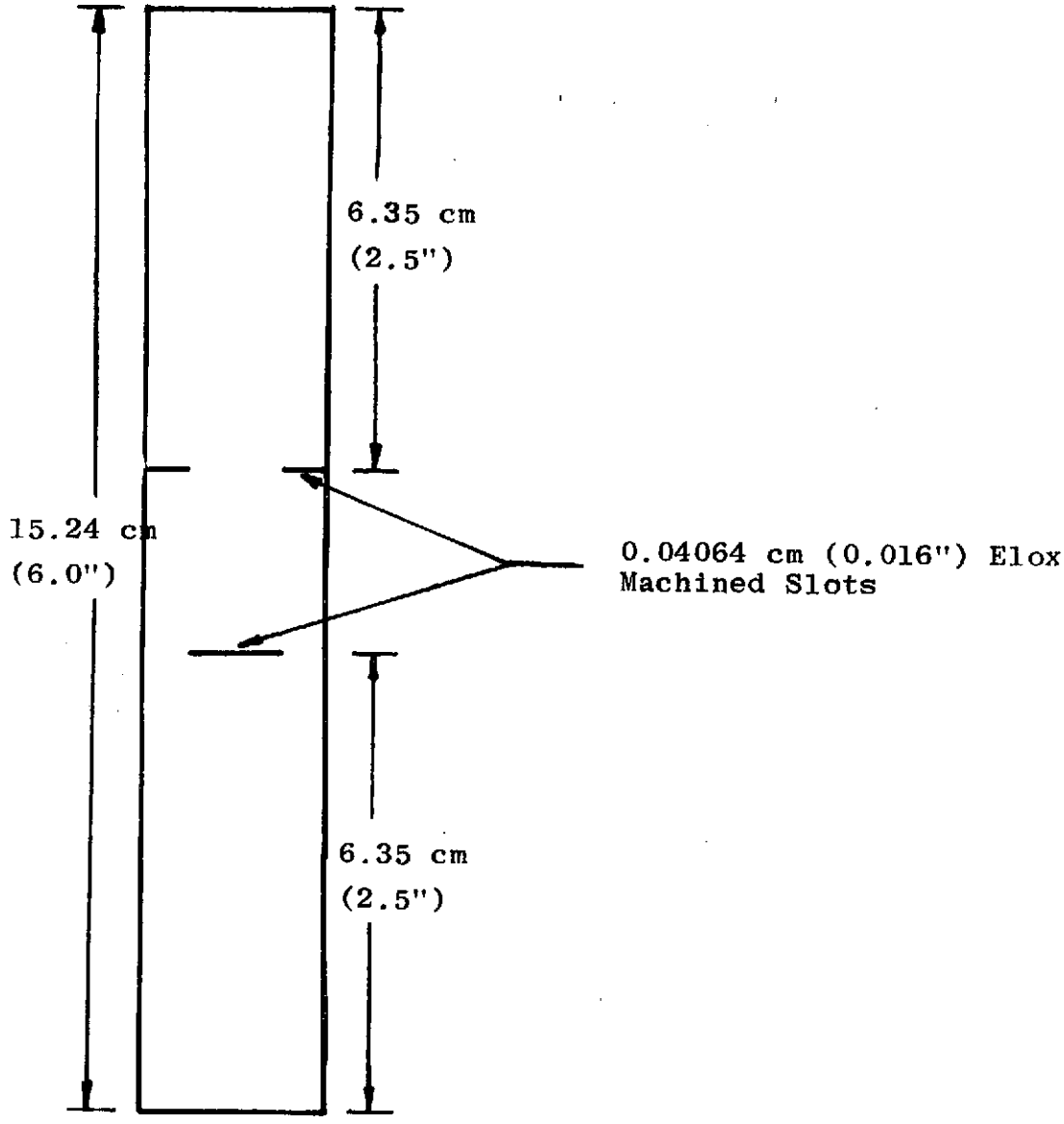

FIGURE 2

Shear Specimen

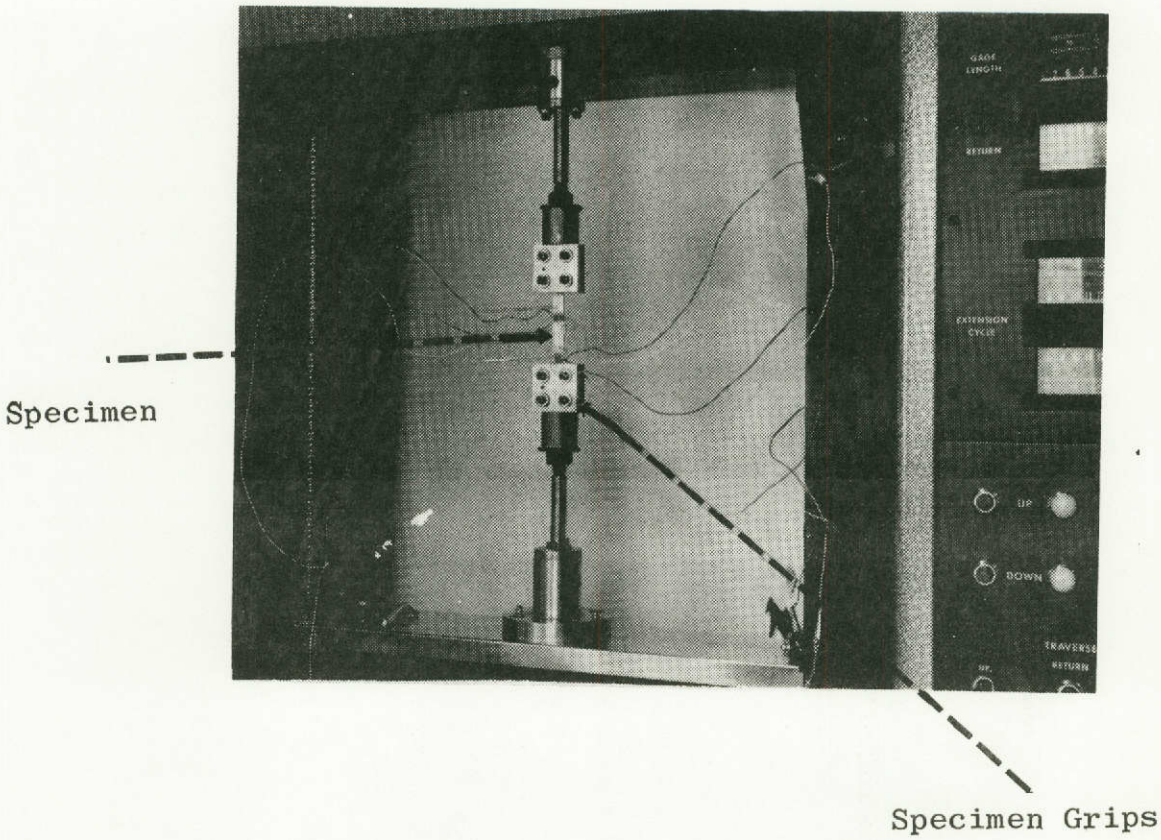

Figure 3

Tensile testing arrangement (rigid grips)

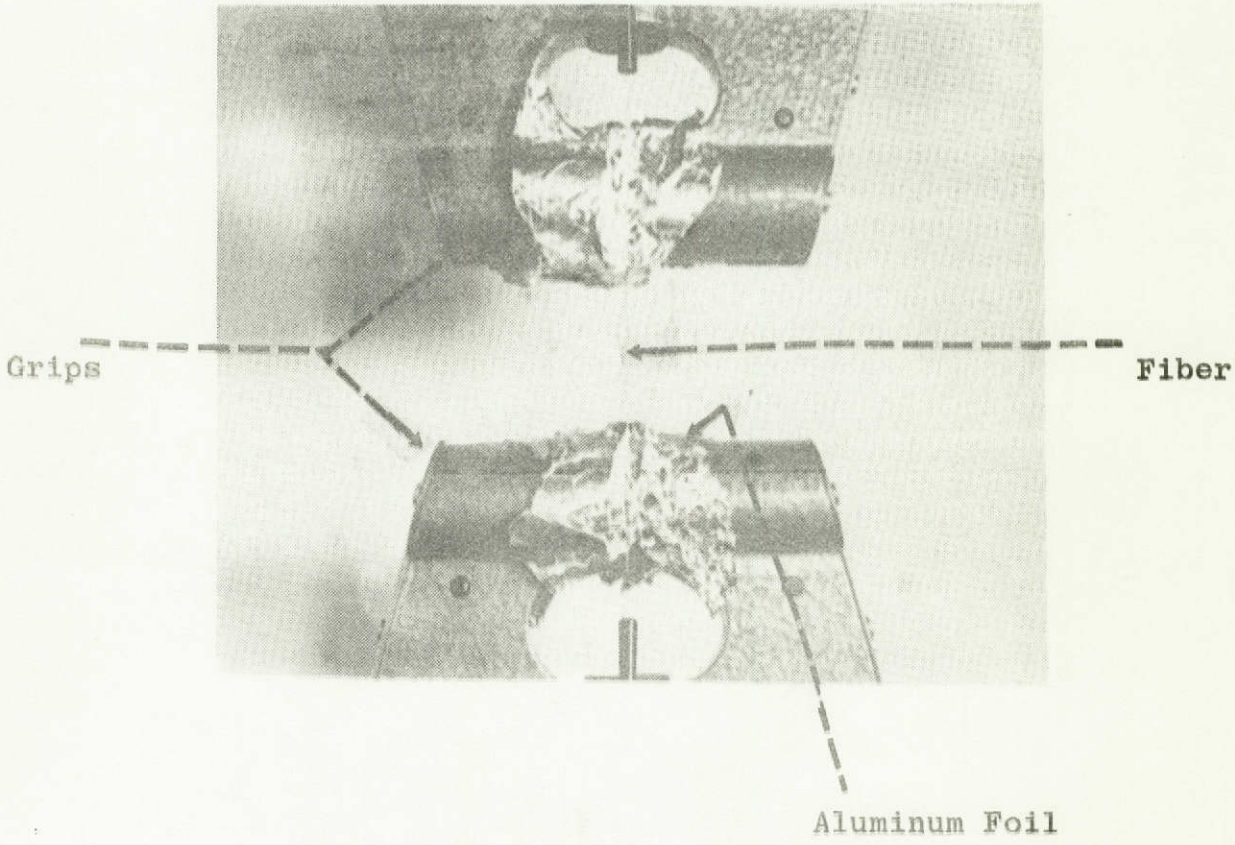

Figure 4

Grip arrangement for testing individual fibers

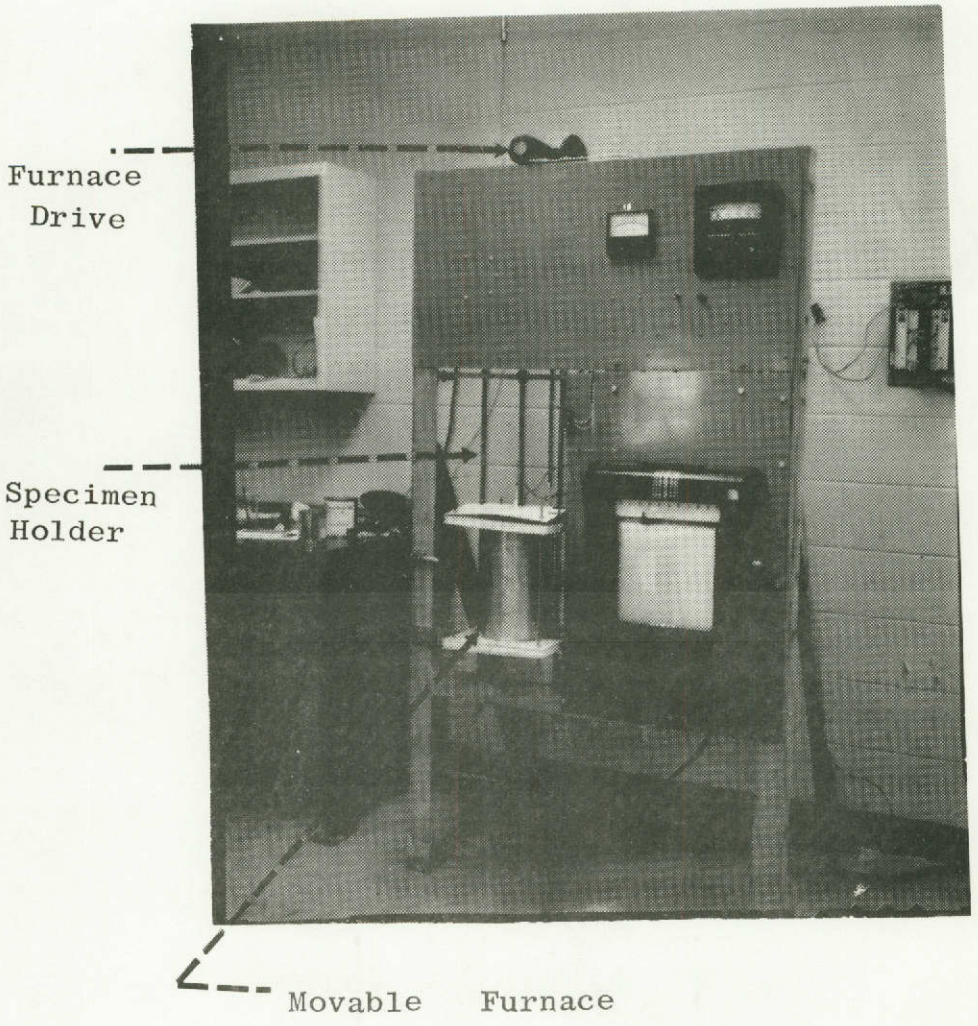

Figure 5

Thermal fatigue apparatus--zero static load

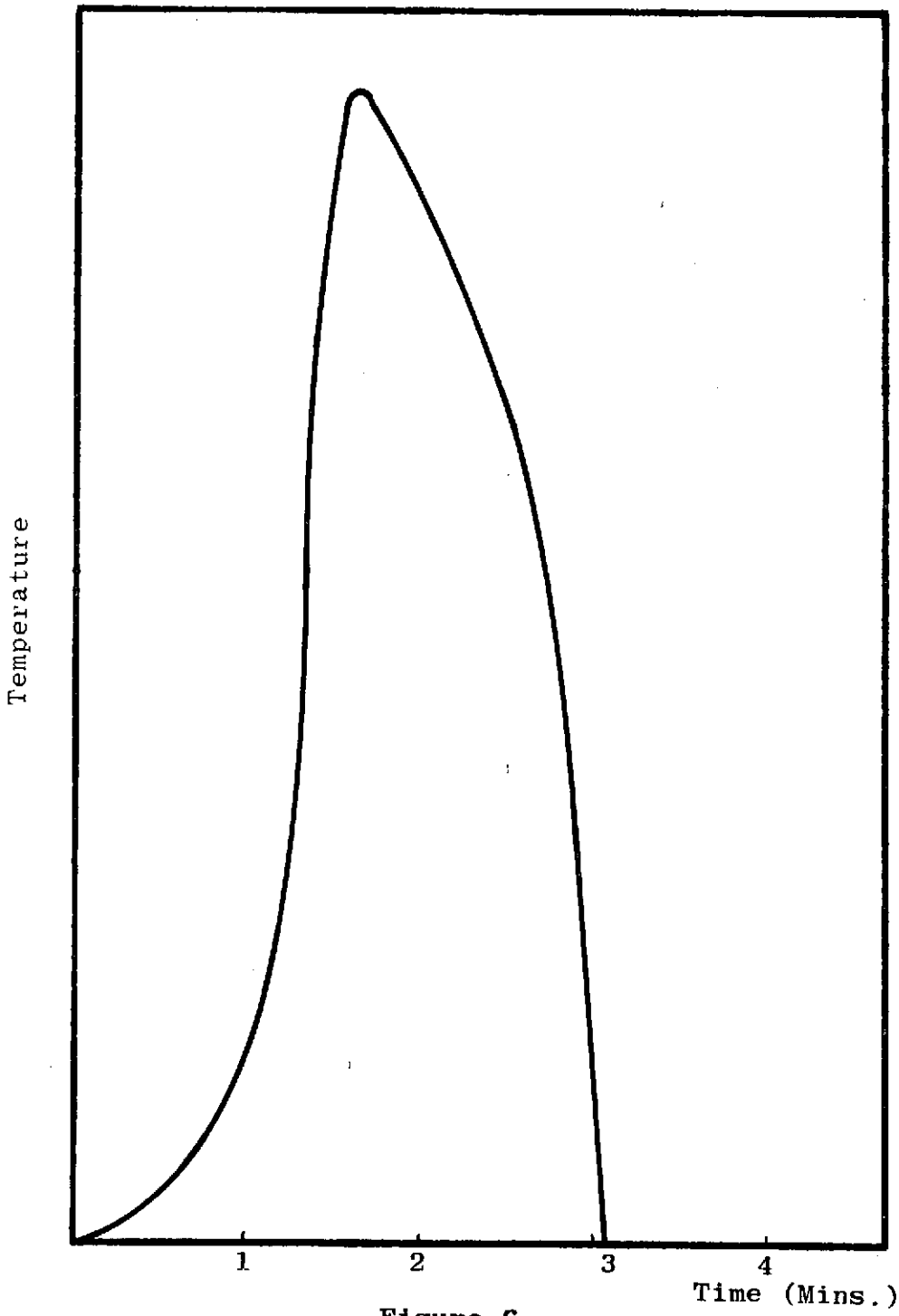

Figure 6

Heating and Cooling Curve
obtained from
Thermal Fatigue Apparatus

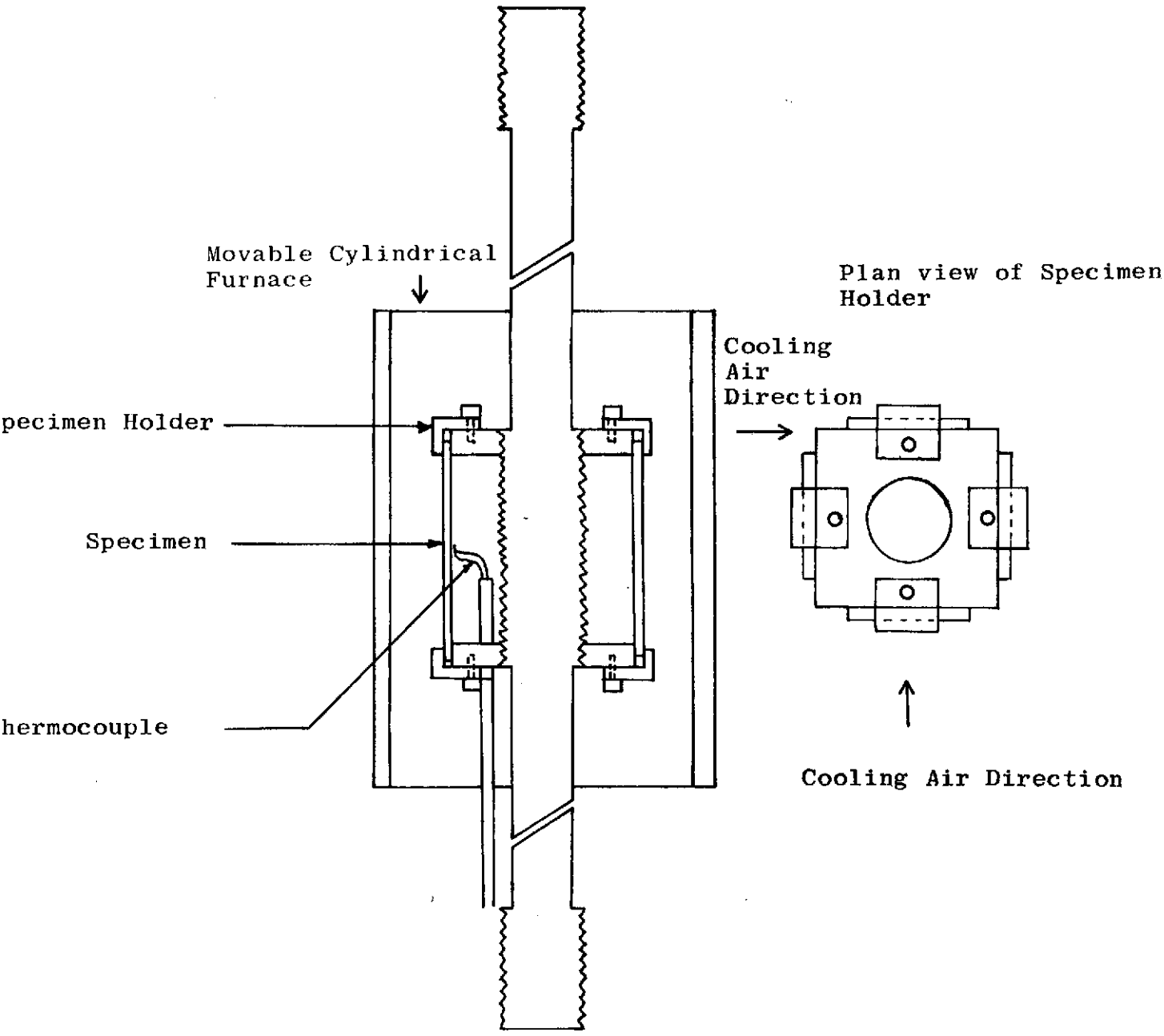

Figure 7

Specimen Holder--zero static load tests

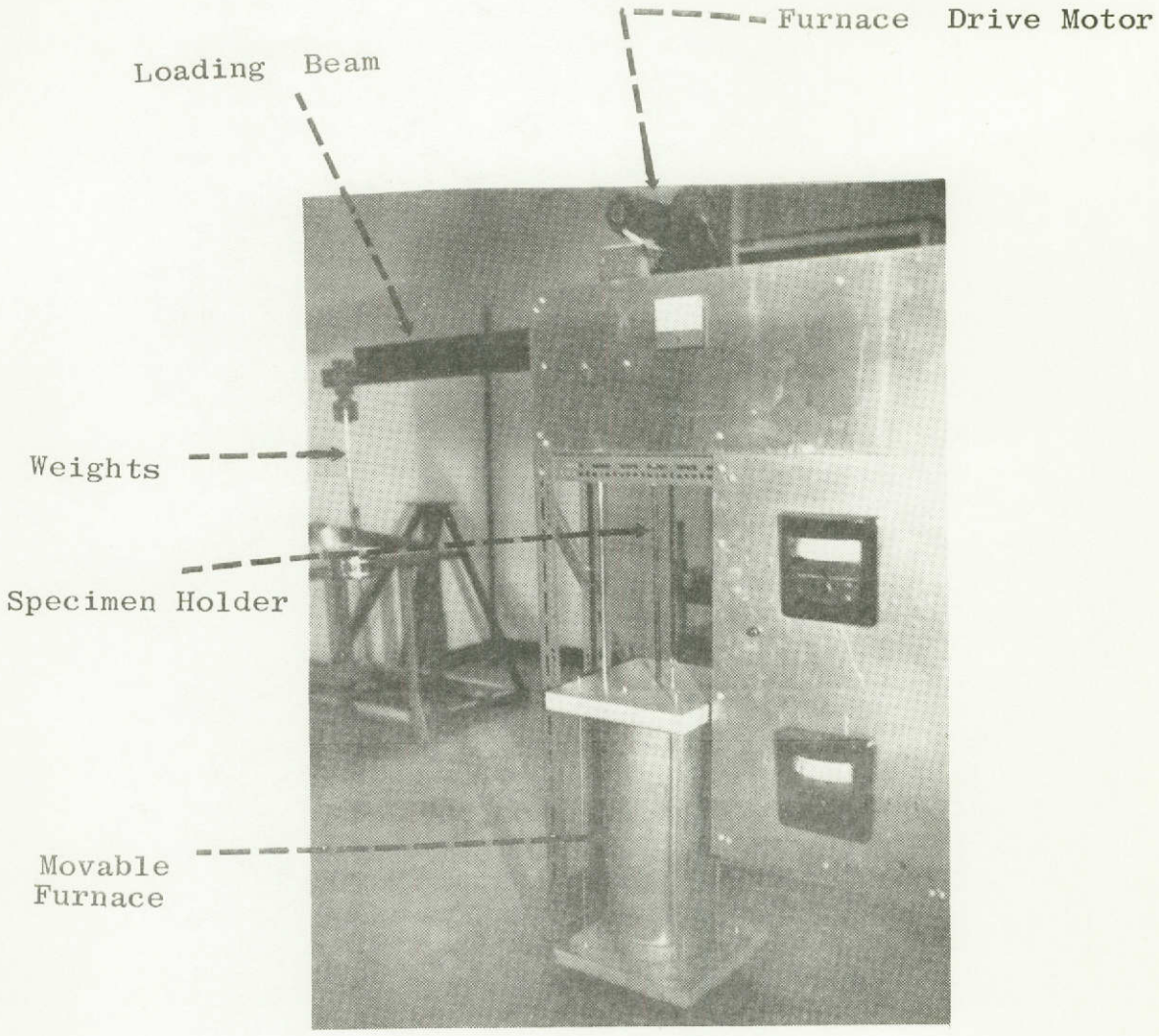

Figure 8

Apparatus capable of subjecting unidirectional loads to specimens also subjected to cyclic temperature variations

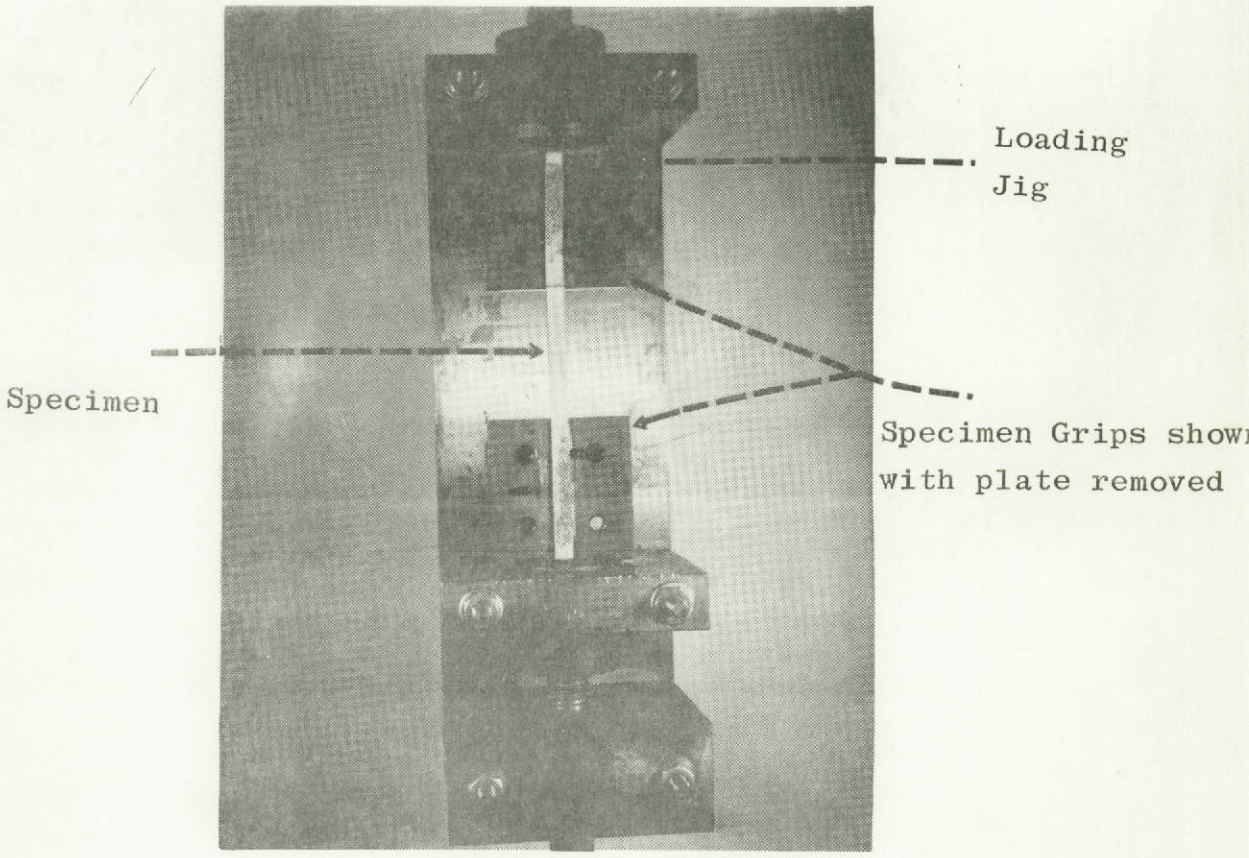

Figure 9

Loading jig for placing specimens in thermal fatigue apparatus--positive static load

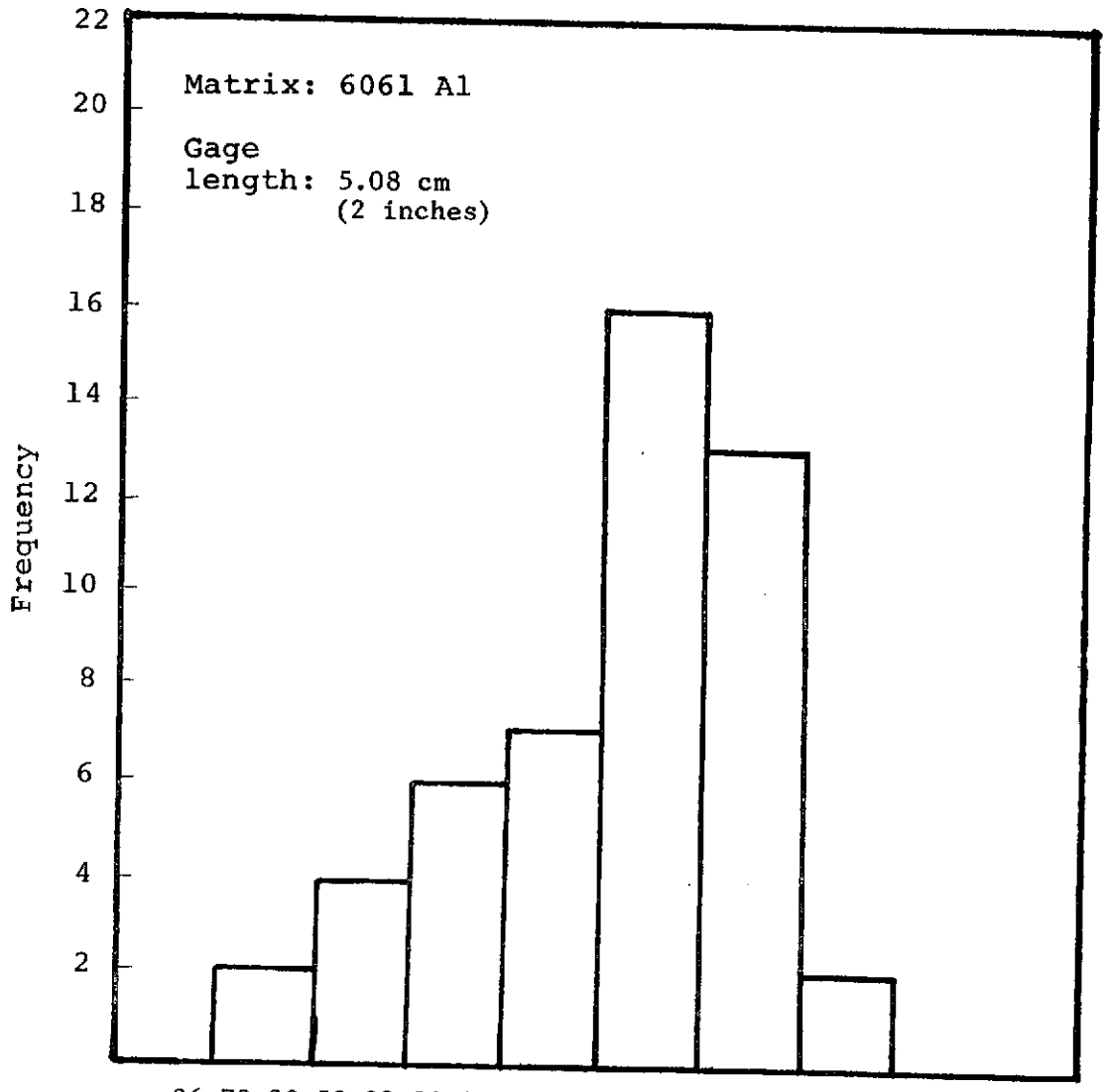

Figure 10

The Strength of Fibers Extracted from an As Received Boron-6061 Aluminum Composite Gage Length 5.08 cm (2 Inches)

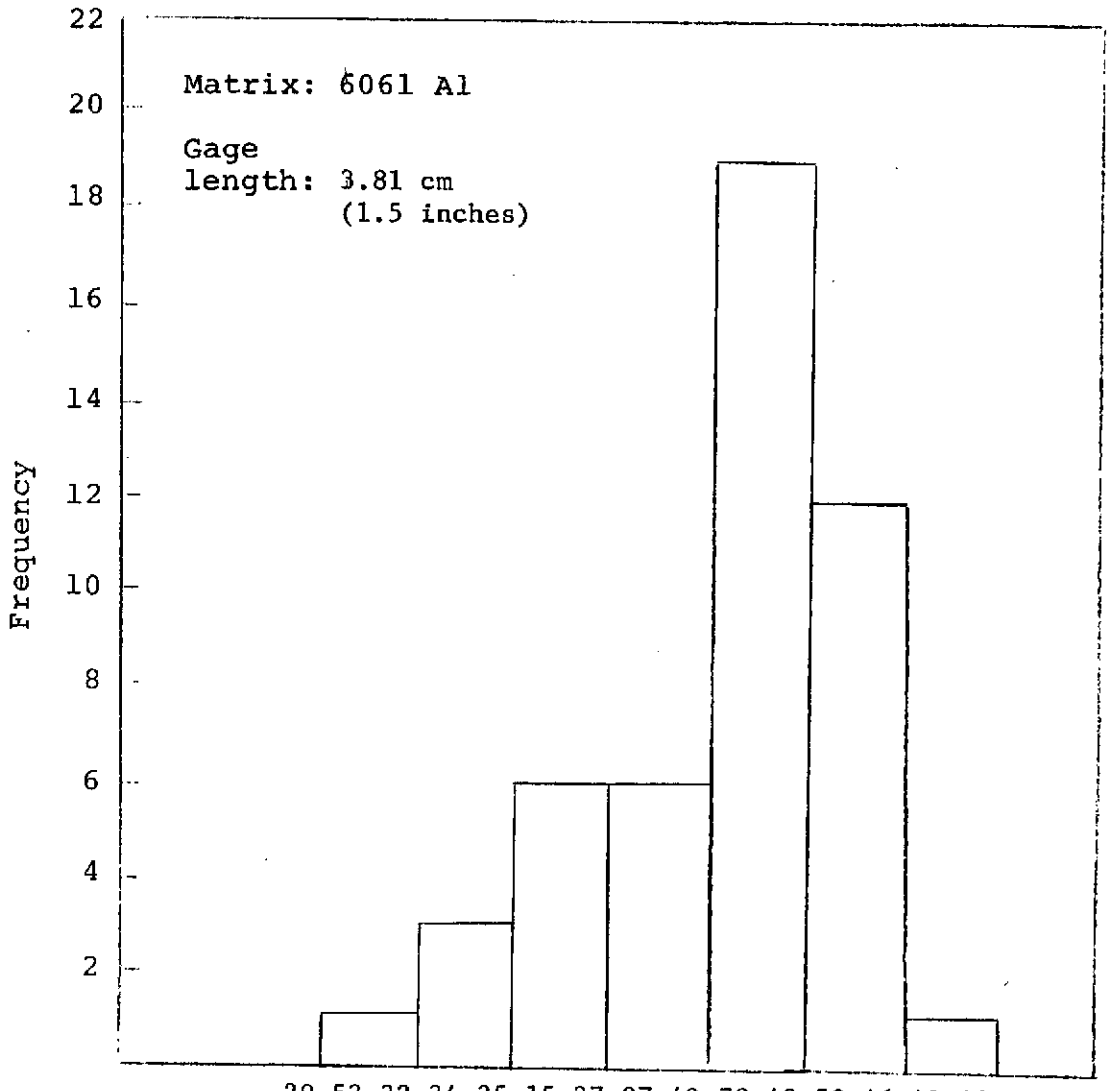

Figure 11

The Strength of Fibers Extracted from an As-Received Boron-6061 Aluminum Composite Gage Length 3.81 cm (1.5 Inches)

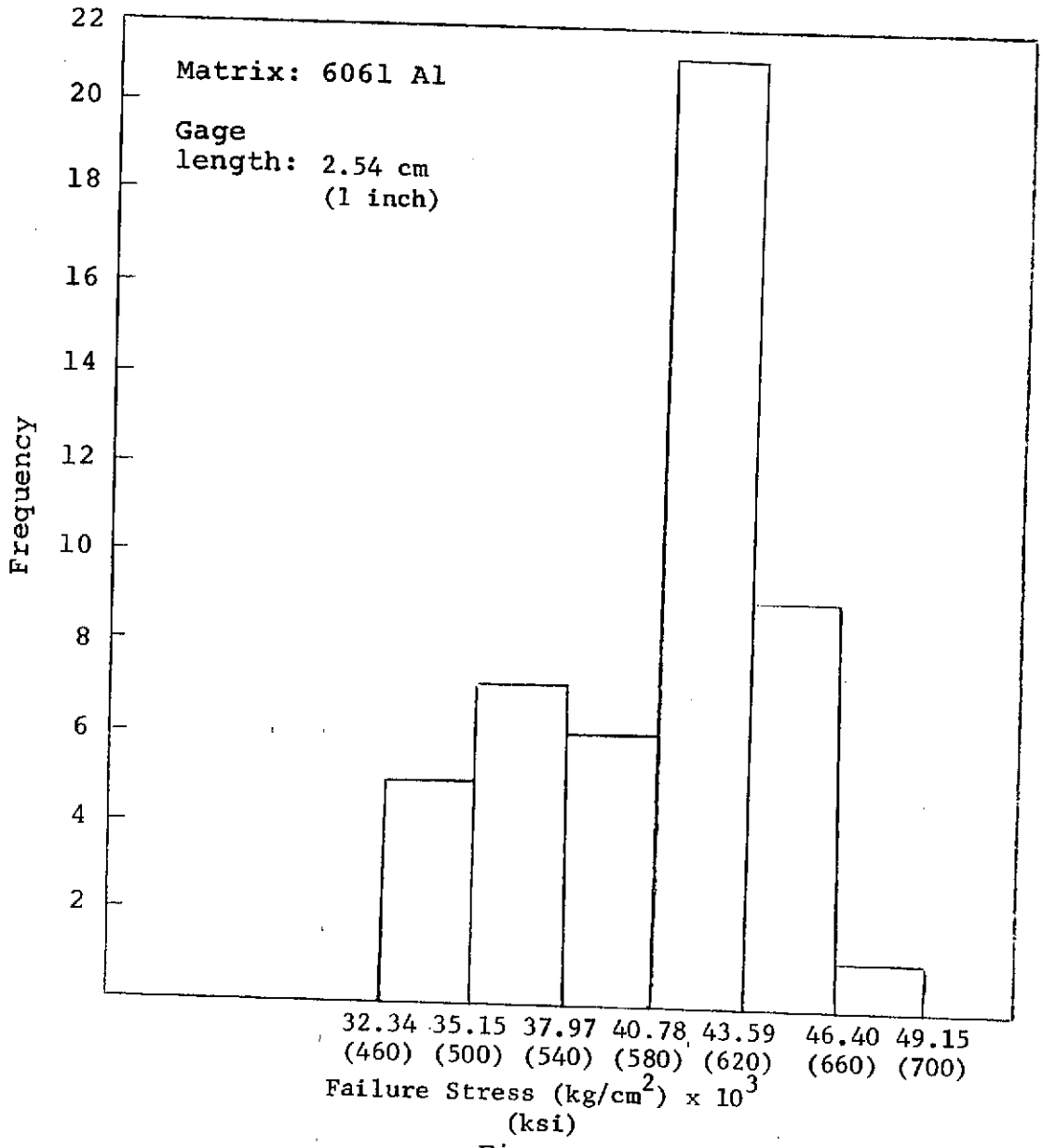

Figure 12

The Strength of Fibers Extracted from an As Received Boron 6061 Aluminum Composite
Gage Length 2.54 cm
(1 Inch)

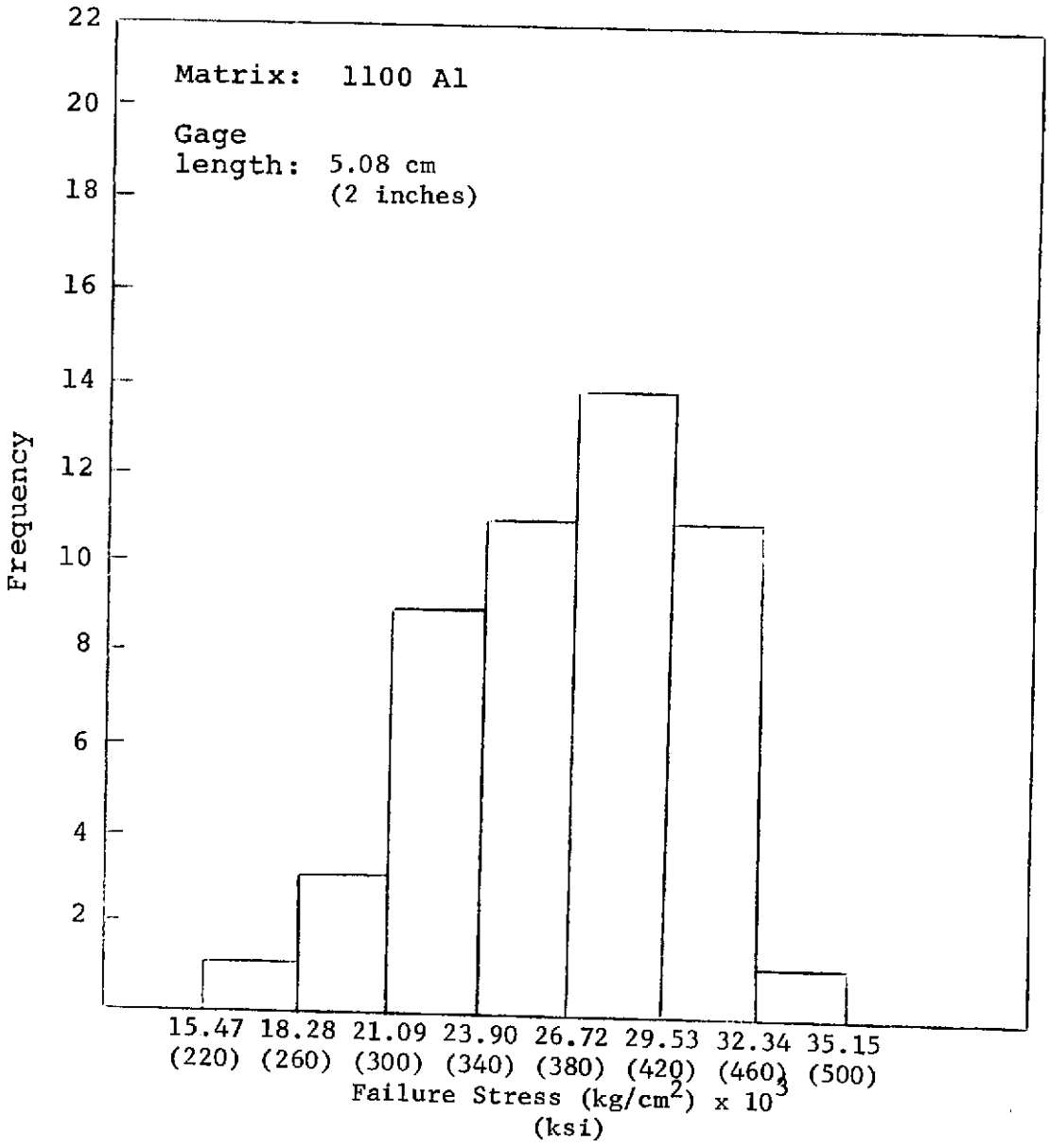

Figure 13

The Strength of Fibers Extracted from an As-Received Boron-1100 Aluminum Composite
Gage Length 5.08 cm
(2 Inches)

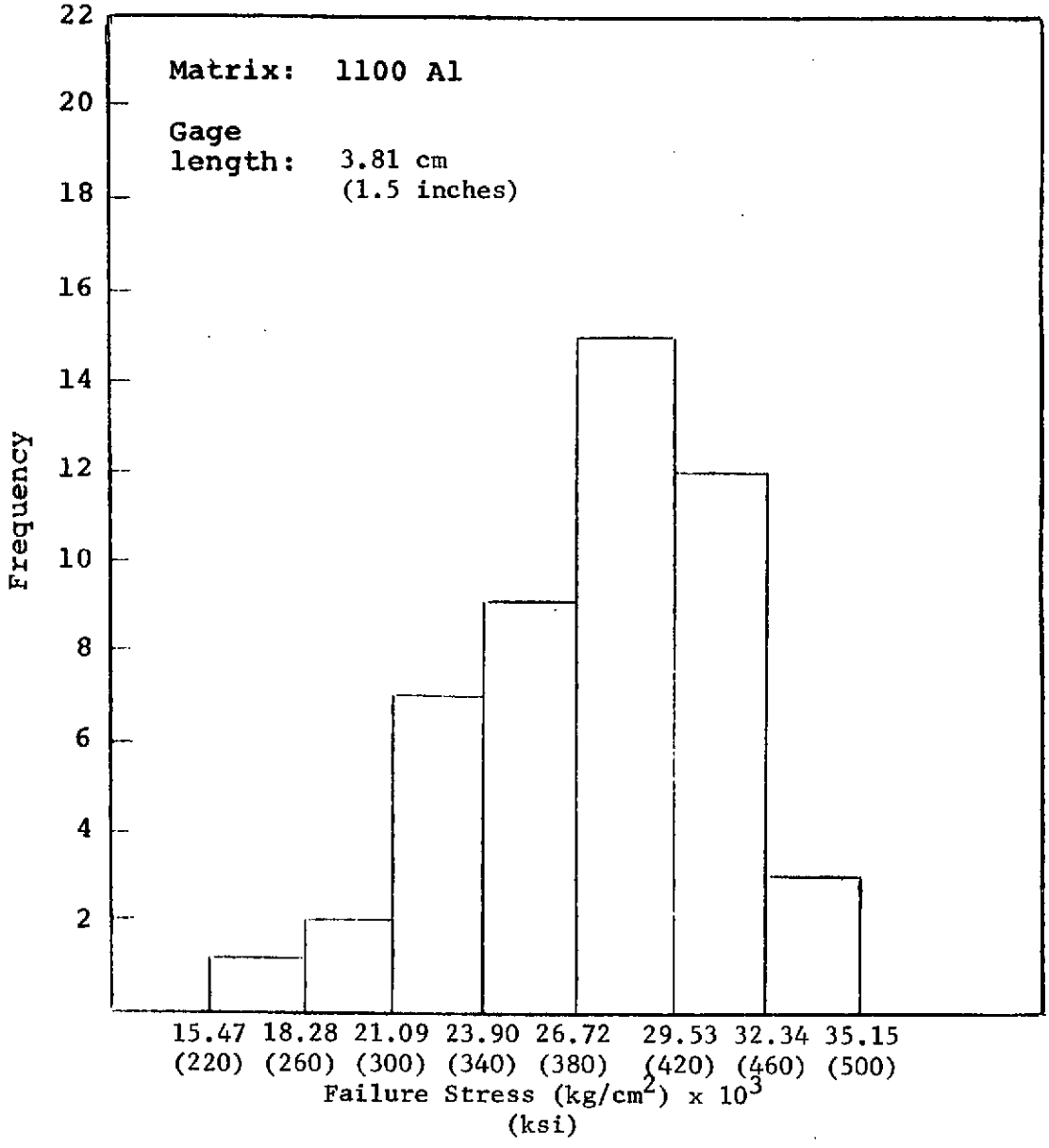

Figure 14

The Strength of Fibers Extracted from an As Received Boron 1100 Aluminum Composite
Gage Length 3.81 cm
(1.5 Inches)

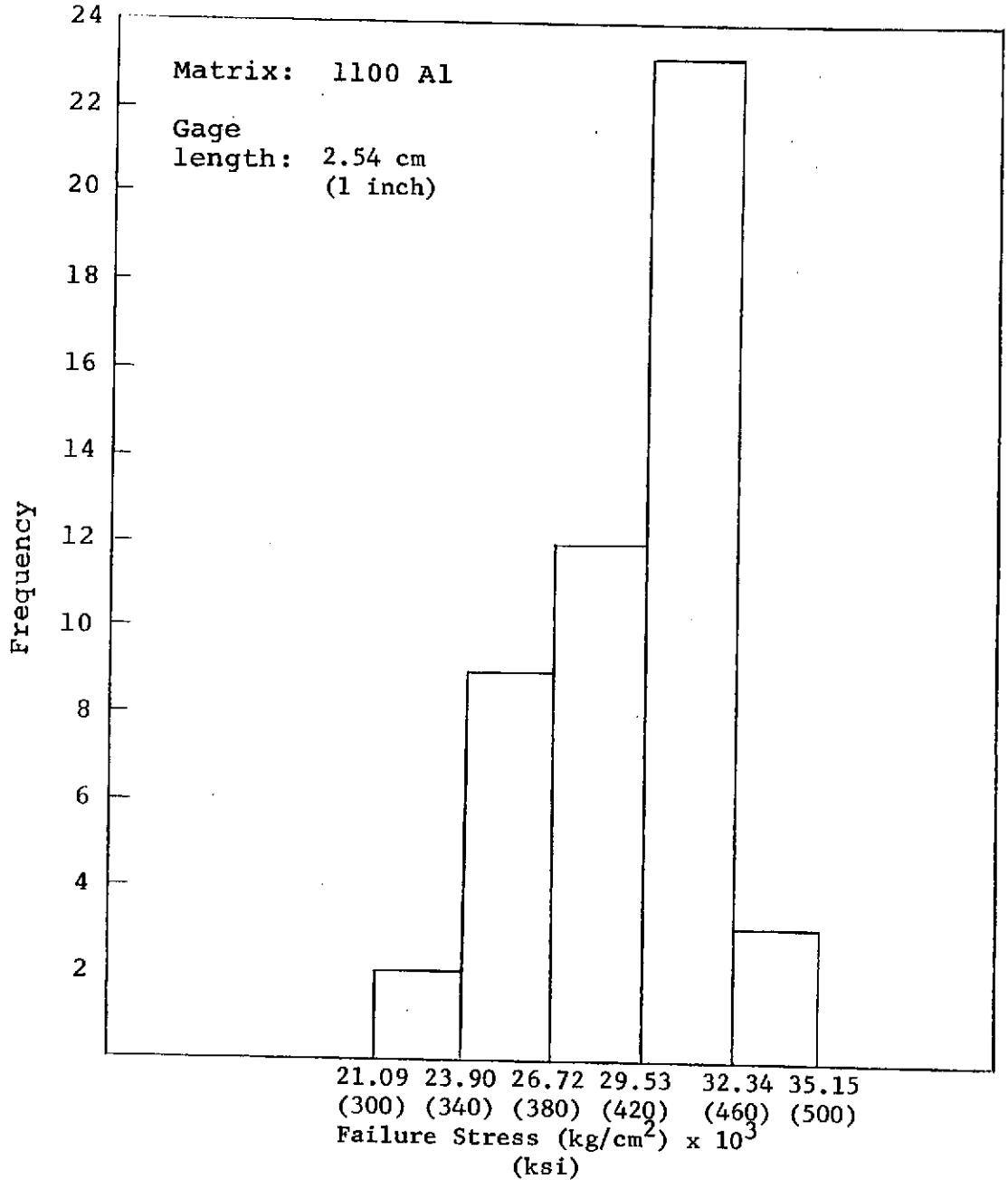

Figure 15

The Strength of Fibers Extracted from an As Received Boron 1100 Aluminum Composite
Gage Length 2.54cm
(1 Inch)

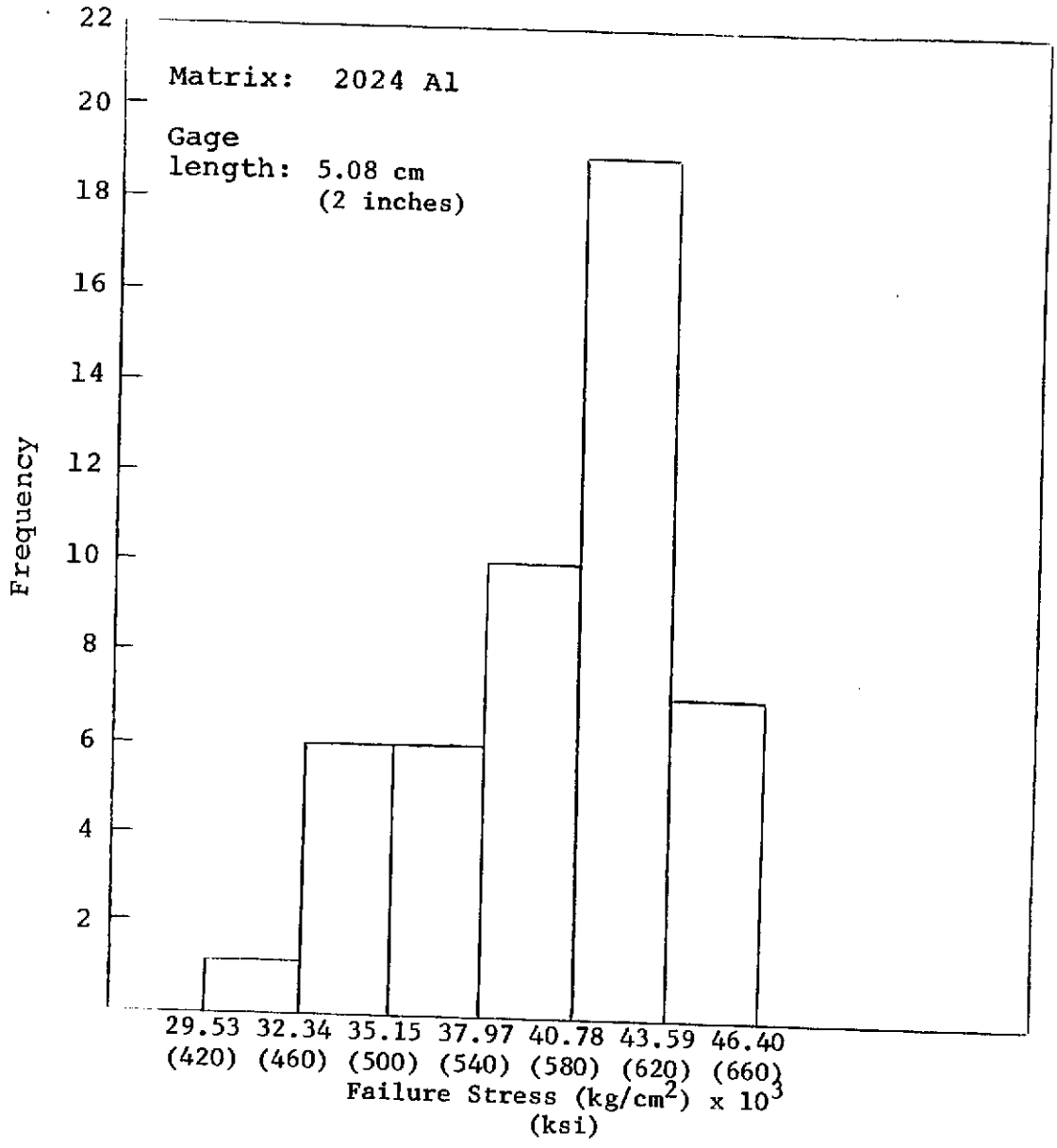

Figure 16

The Strength of Fibers Extracted from an As Received Boron 2024 Aluminum Composite Gage Length 5.08 cm (2 Inches)

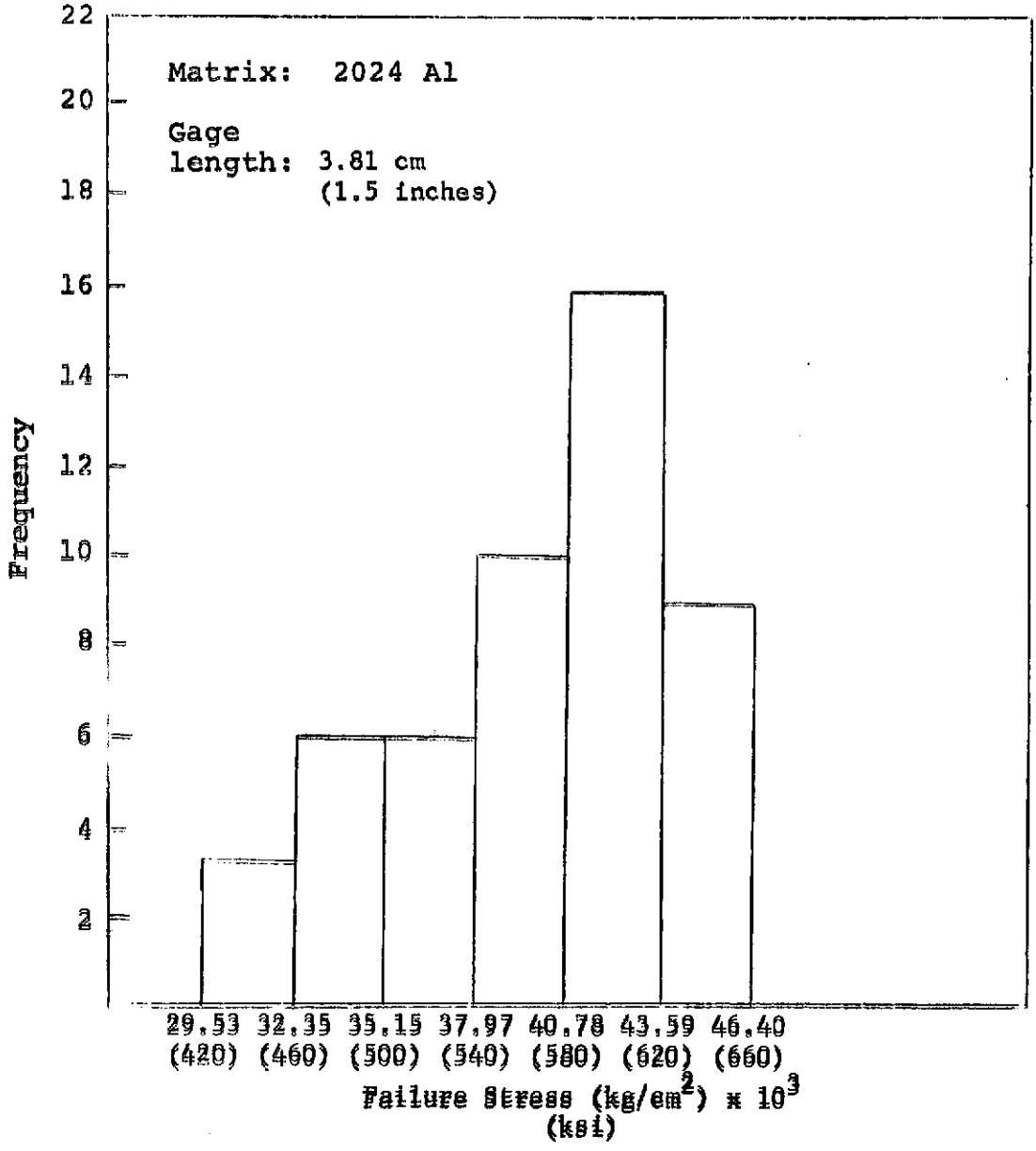

Figure 17

The Strength of Fibers Extracted from an As Received Boron 2024 Aluminum Composite
Gage Length 3.81 cm
(1.5 Inches)

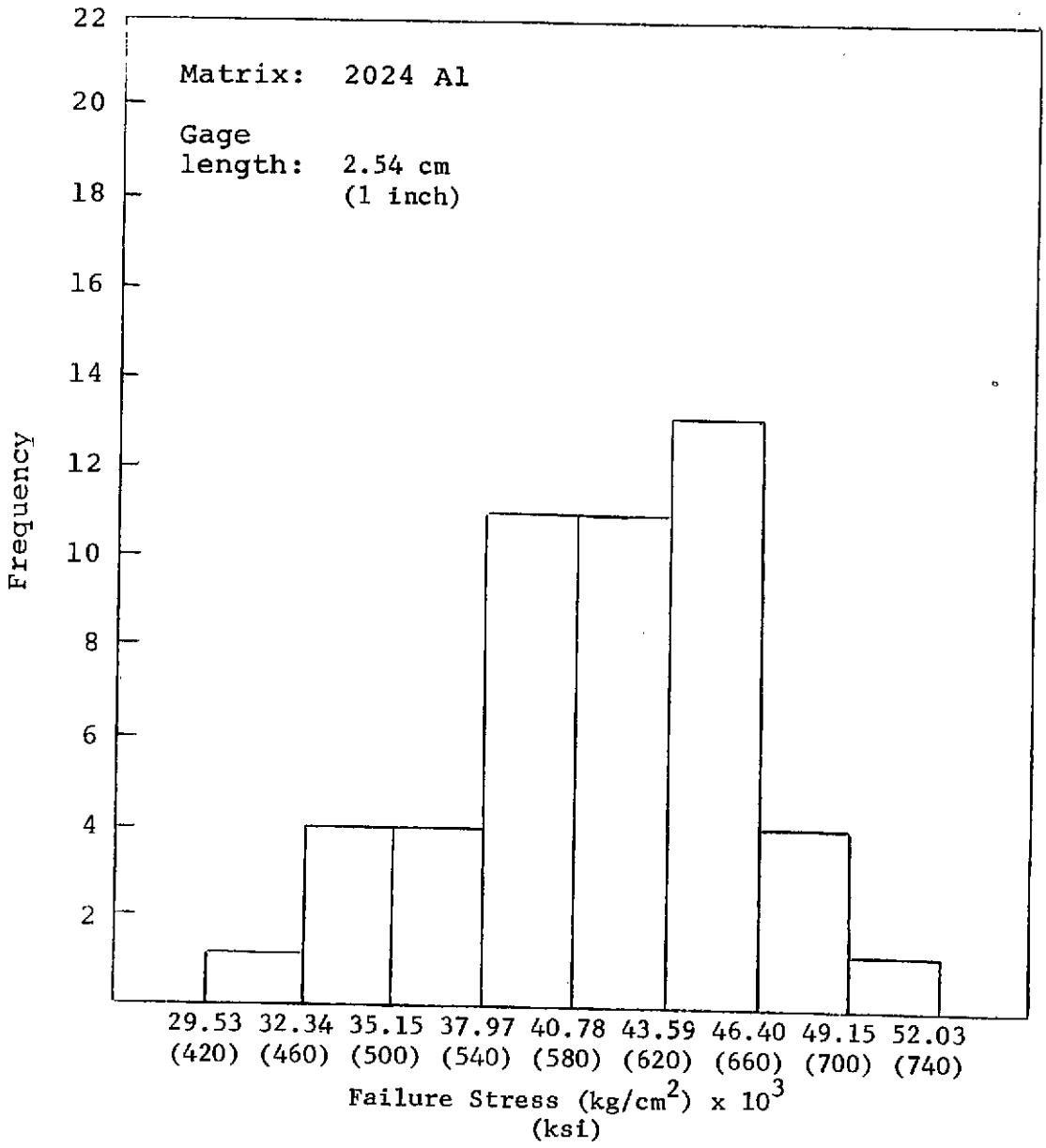

Figure 18

The Strength of Fibers Extracted from an As Received Boron 2024 Aluminum Composite
Gage Length 2.54 cm
(1 Inch)

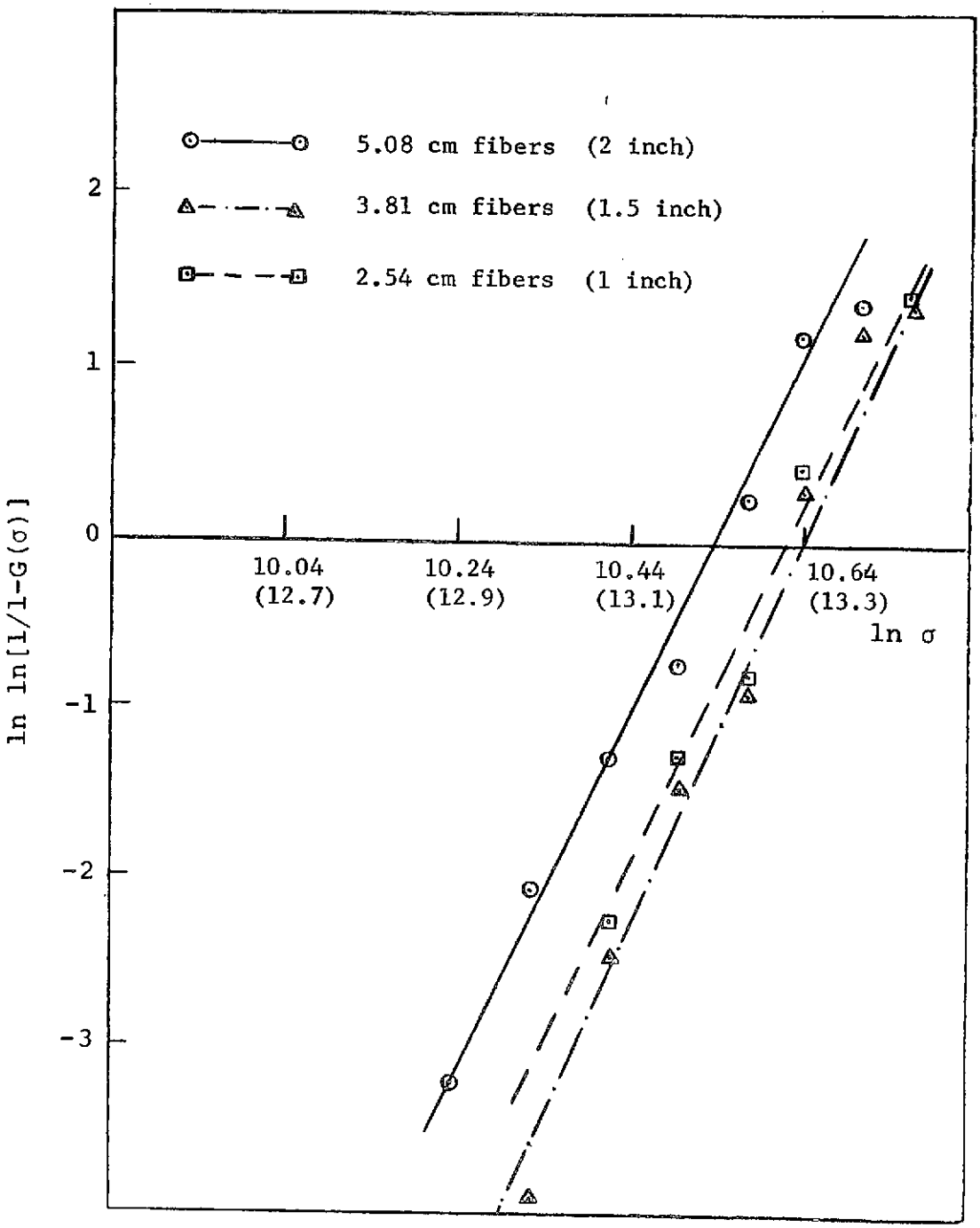

Figure 19

Weibull Distribution of the Strength of Fibers Extracted from As Received Reinforced 6061 Aluminum

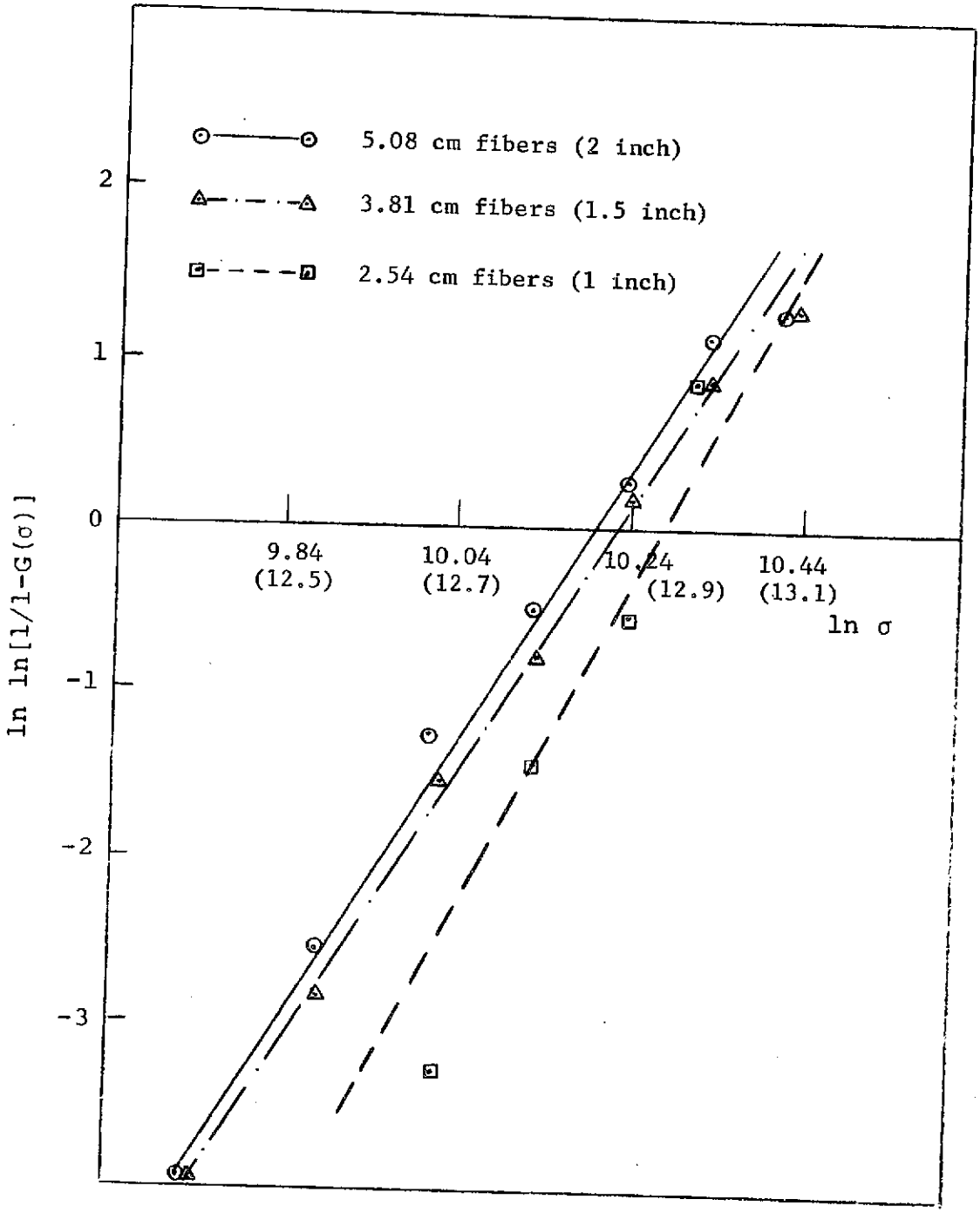

Figure 20

Weibull Distribution of the Strengths of Fibers Extracted from As Received Reinforced 1100 Aluminum

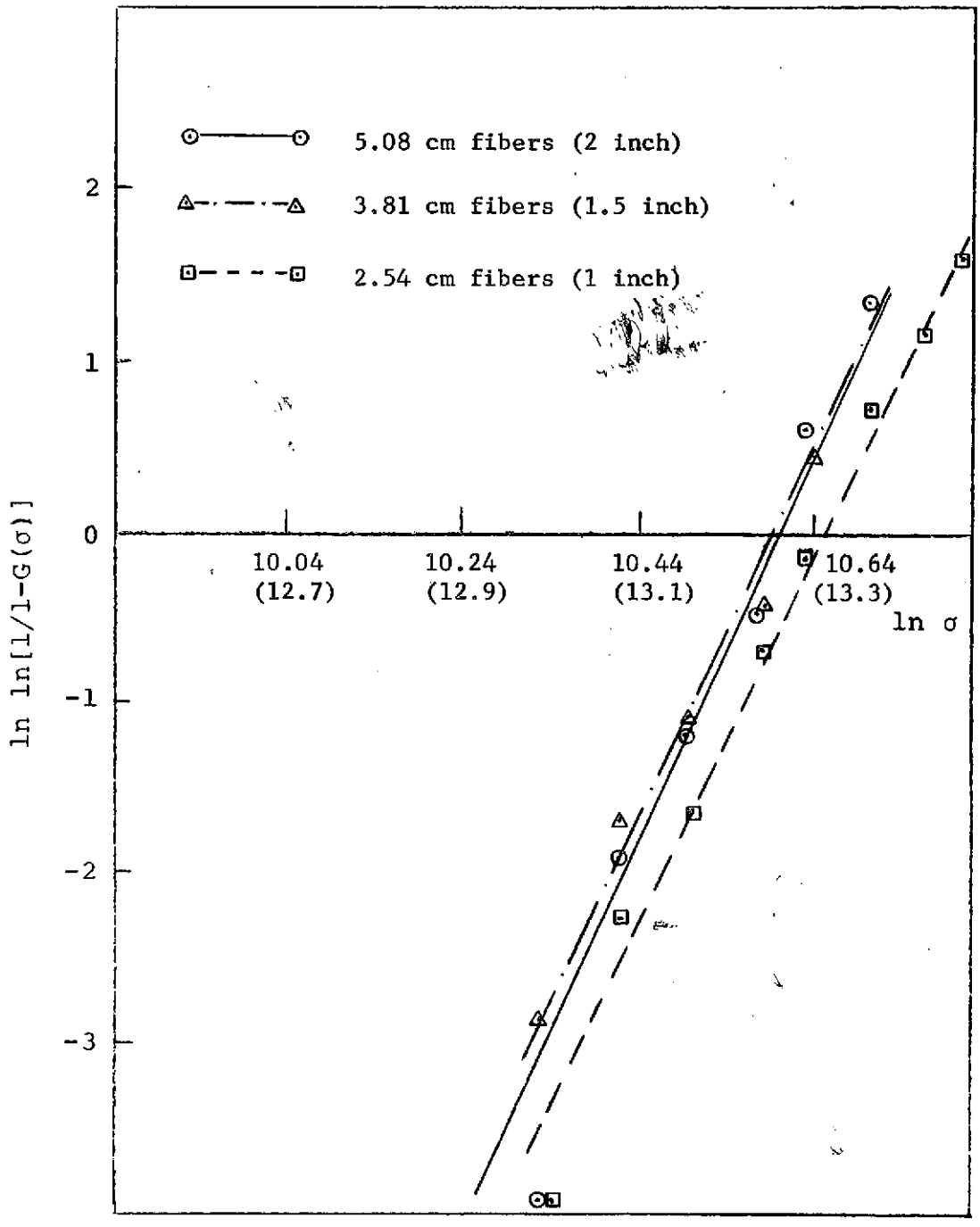

Figure 21

Weibull Distribution of the Strengths of Fibers Extracted from As Received Reinforced 2024 Aluminum

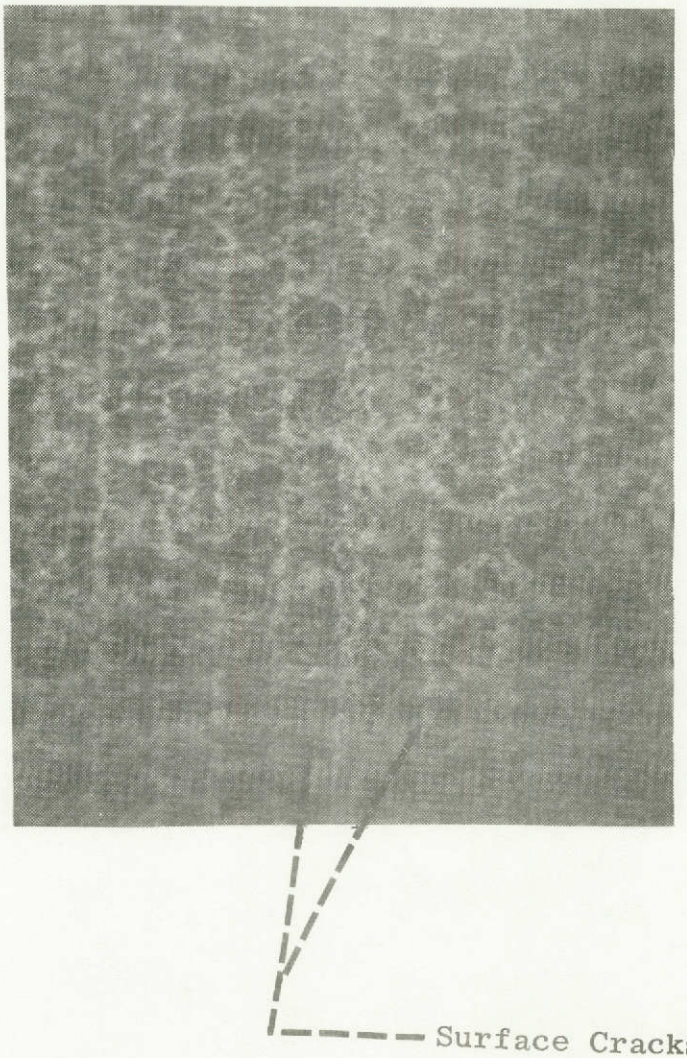

Figure 22

Surface of specimen subjected to 2500 thermal cycles (RT - 315°C)

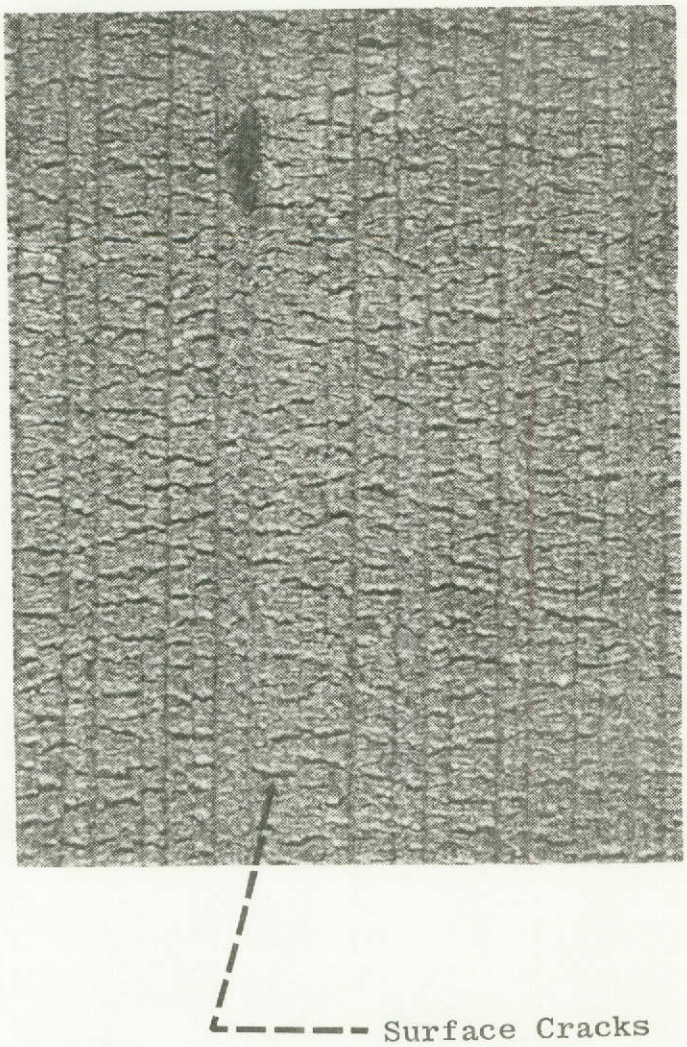

Figure 23

Surface of specimen subjected to 6000 thermal cycles, X20 (RT - 315°C)

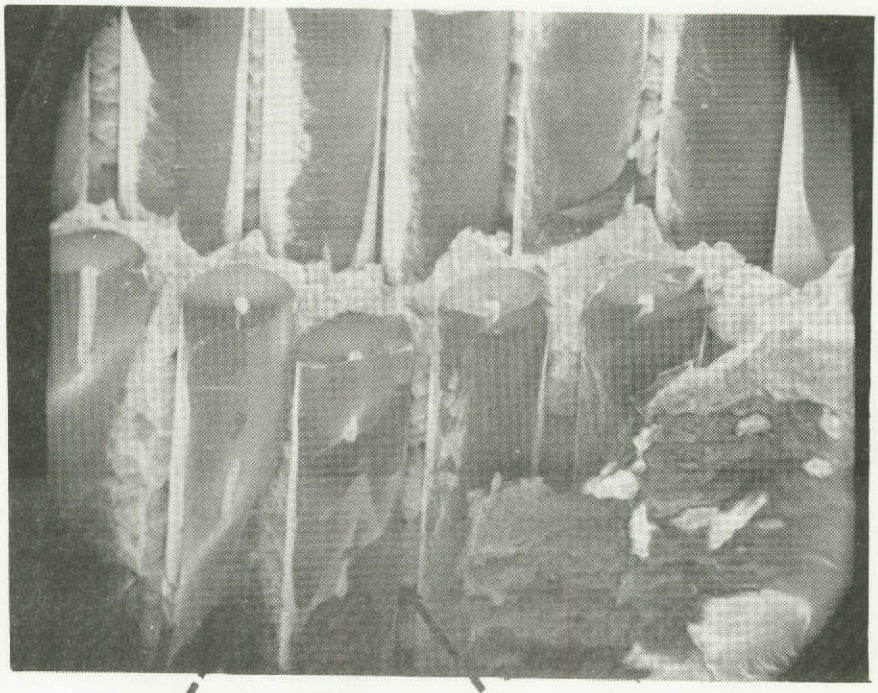

Figure 24

Specimen of reinforced 2024 material subjected to 6000 thermal cycles showing internal ratcheting of the matrix, X100

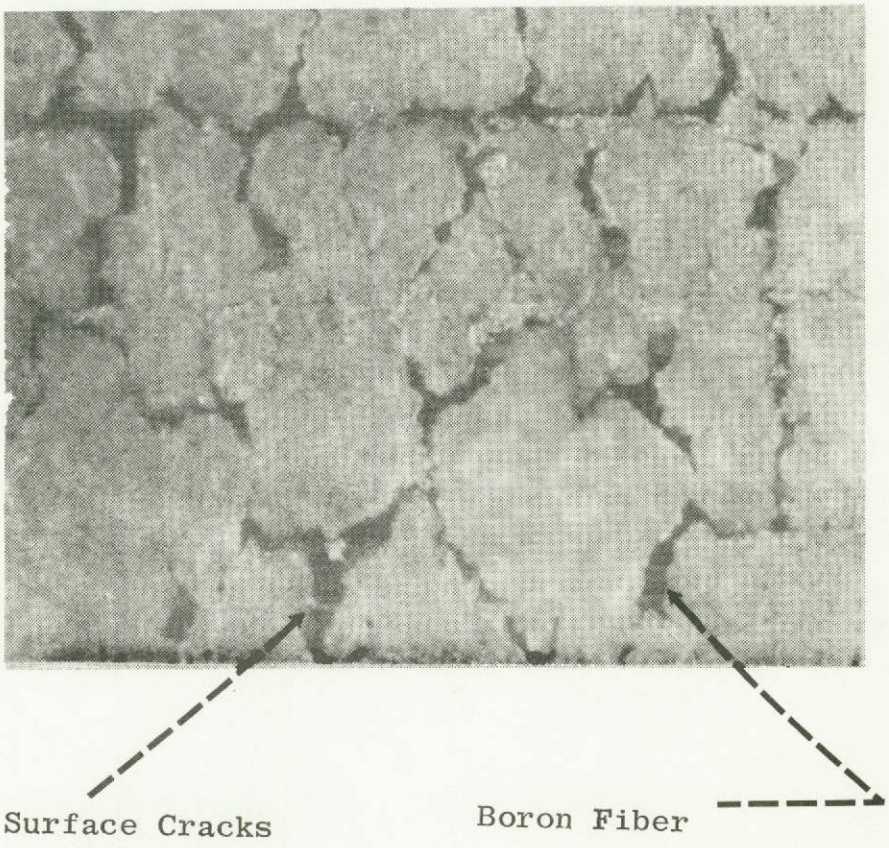

Figure 25

Magnified view of section of the surface of a thermally cycled 2024 Al-Boron specimen

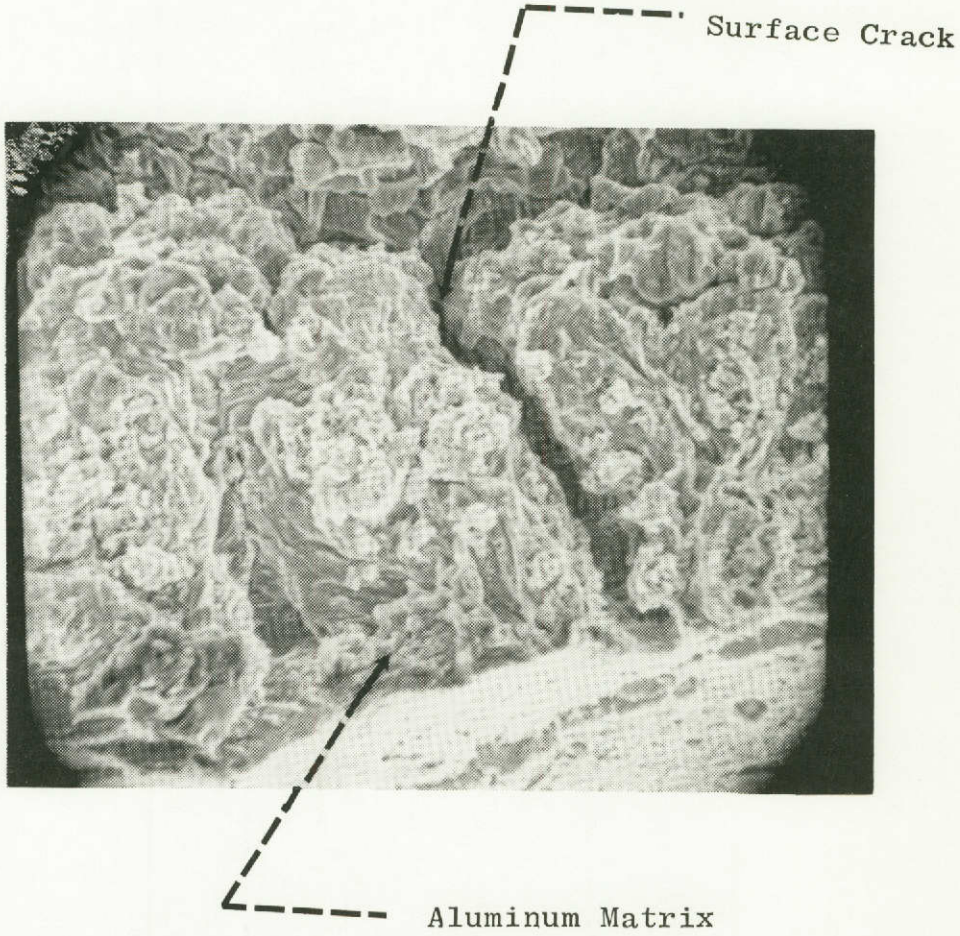

Figure 26

Cracking in surface of thermally cycled Boron reinforced 2024 alloy, X1000

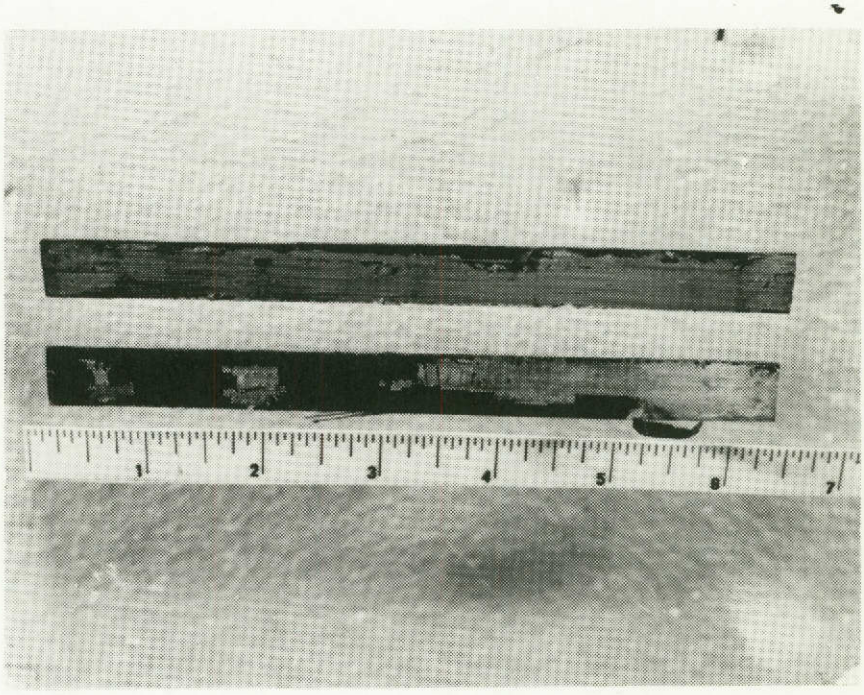

Figure 27

Specimens of reinforced 2024 materials thermally cycled between room temperature and 425°C showing disintegrated surface layers

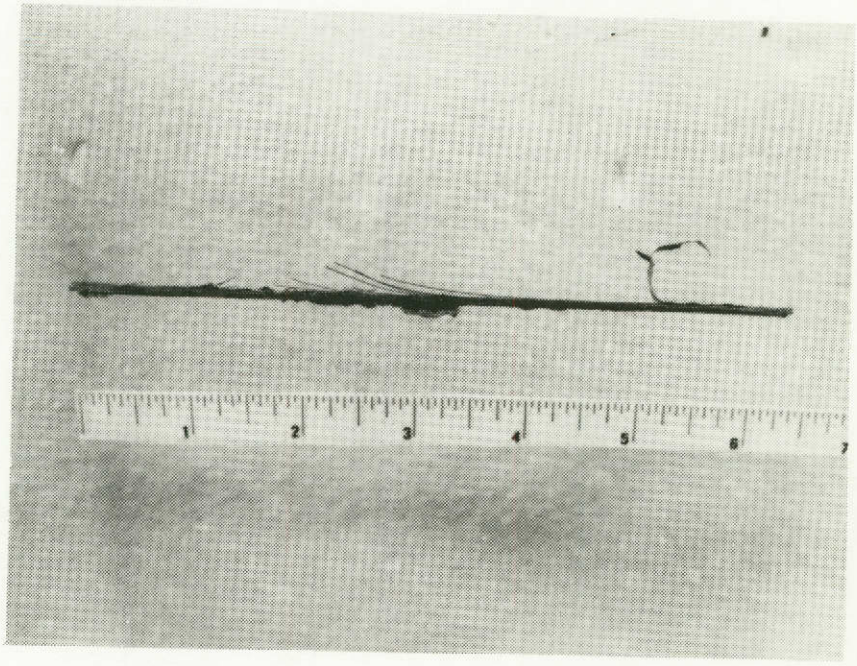

Figure 28

Specimen of reinforced 2024 material thermally cycled between room temperature and 425°C showing broken fibers

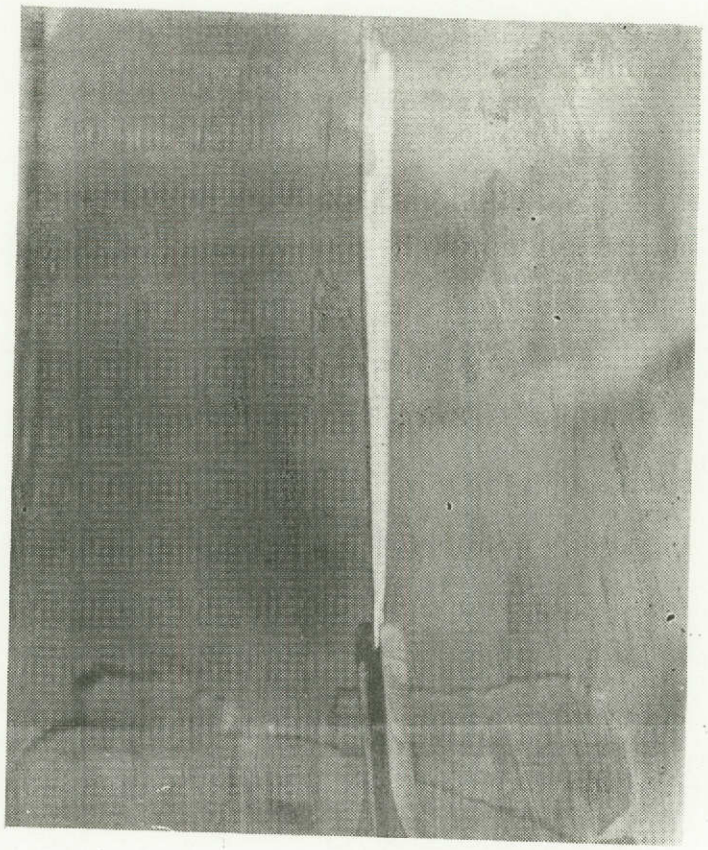

Figure 29

Twist produced in specimen by thermal cycling operation

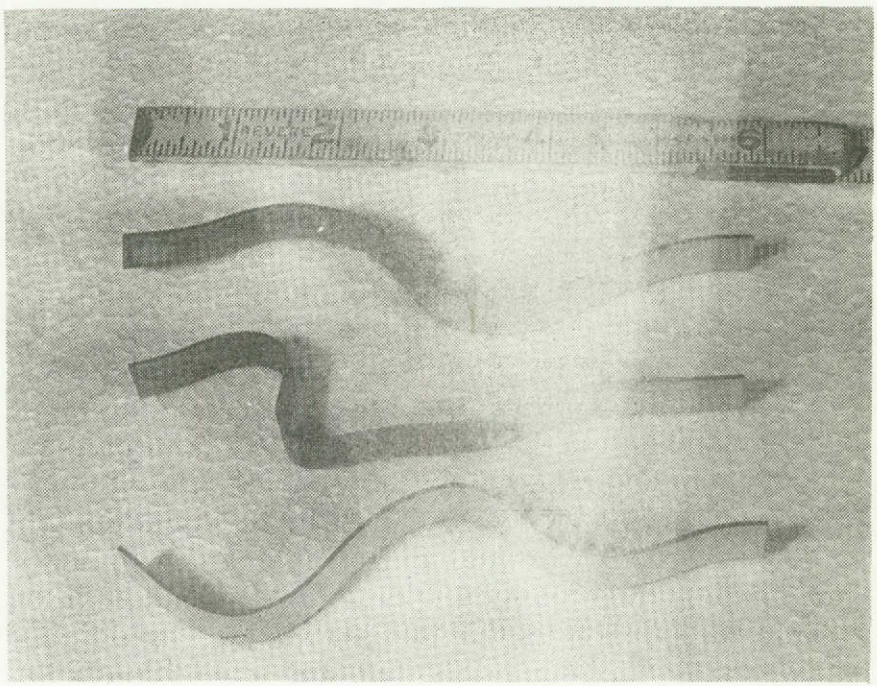

Figure 30

Transverse specimen showing distortions produced by thermal fatigue, RT - 425°C

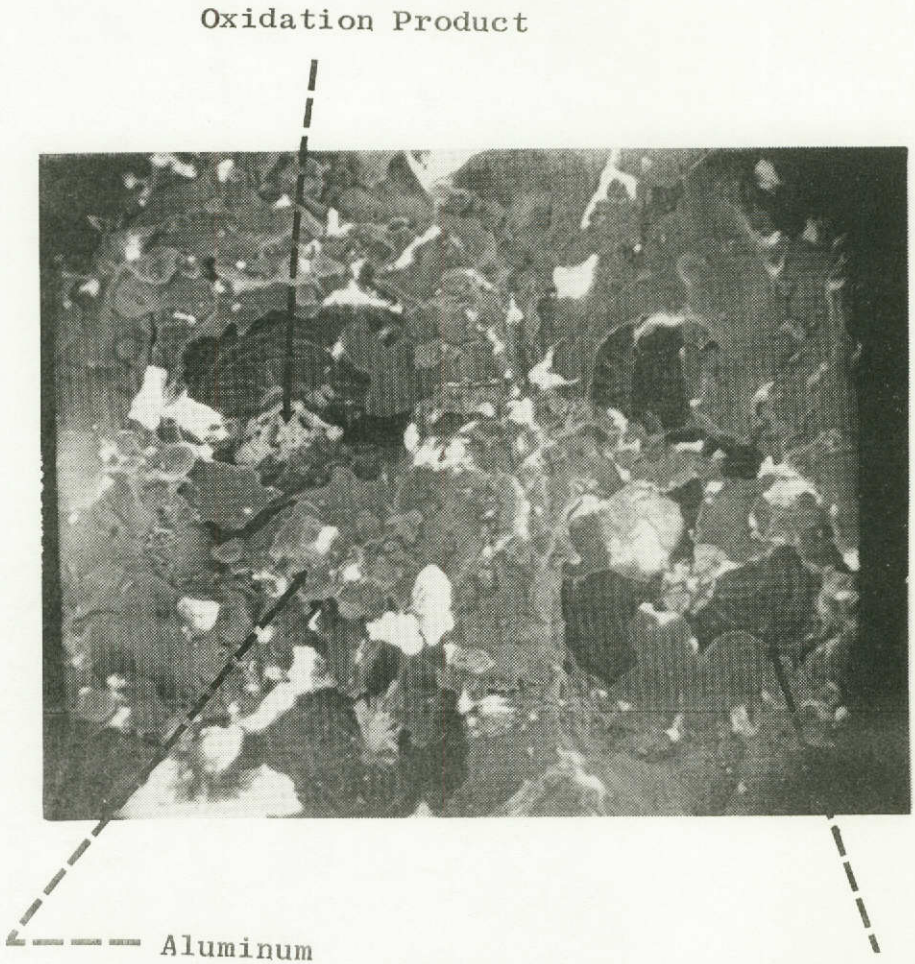

Figure 31

Exposed Boron fiber ends in transverse specimen subjected to 6000 thermal cycles, RT - 425°C. Illustrates oxidation products, X1000.

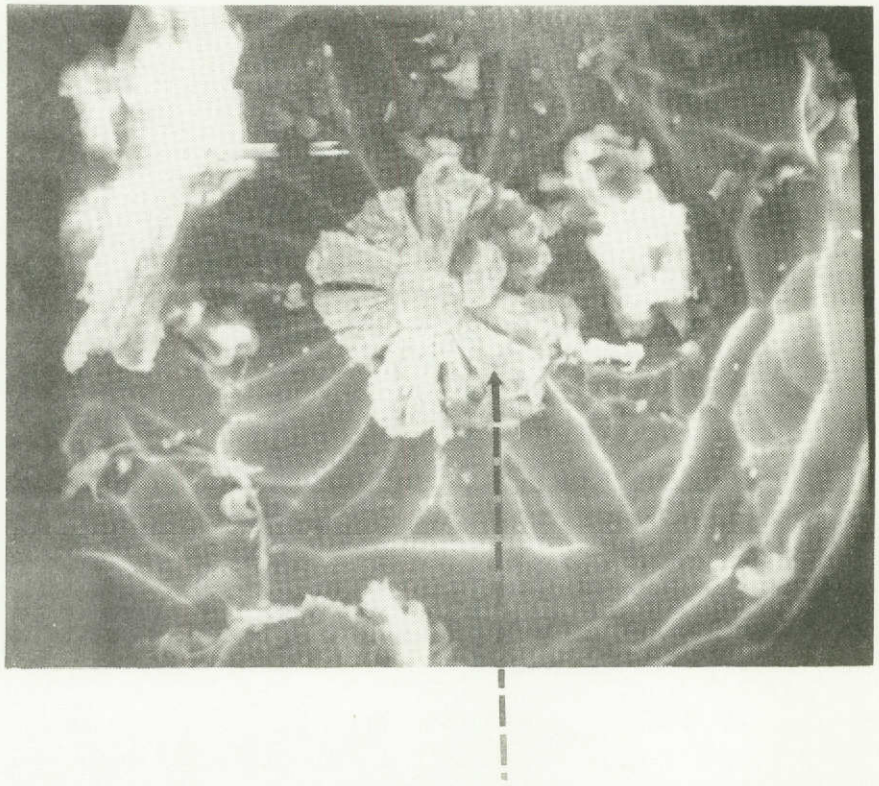

Figure 32

Oxidation products formed from original tungsten fiber. Specimen thermally cycled 6000 times, RT - 425°C, X1350

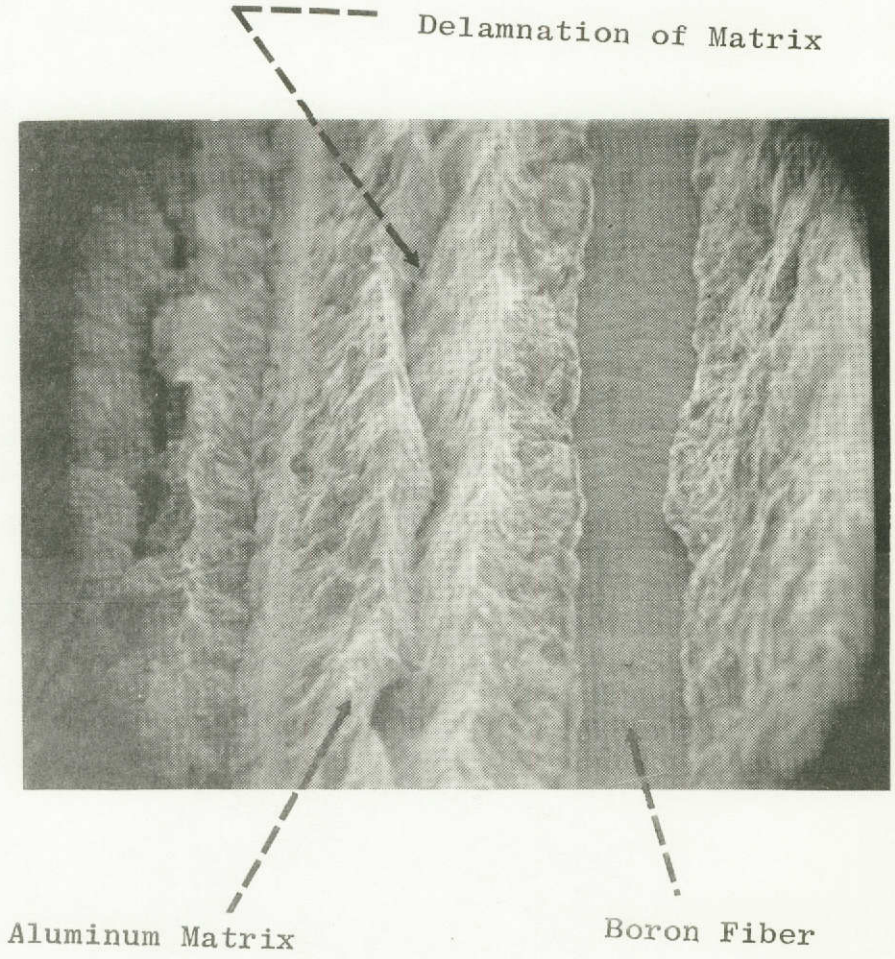

Figure 33

Failure of transverse specimen showing clean surface of exposed Boron fiber, X200

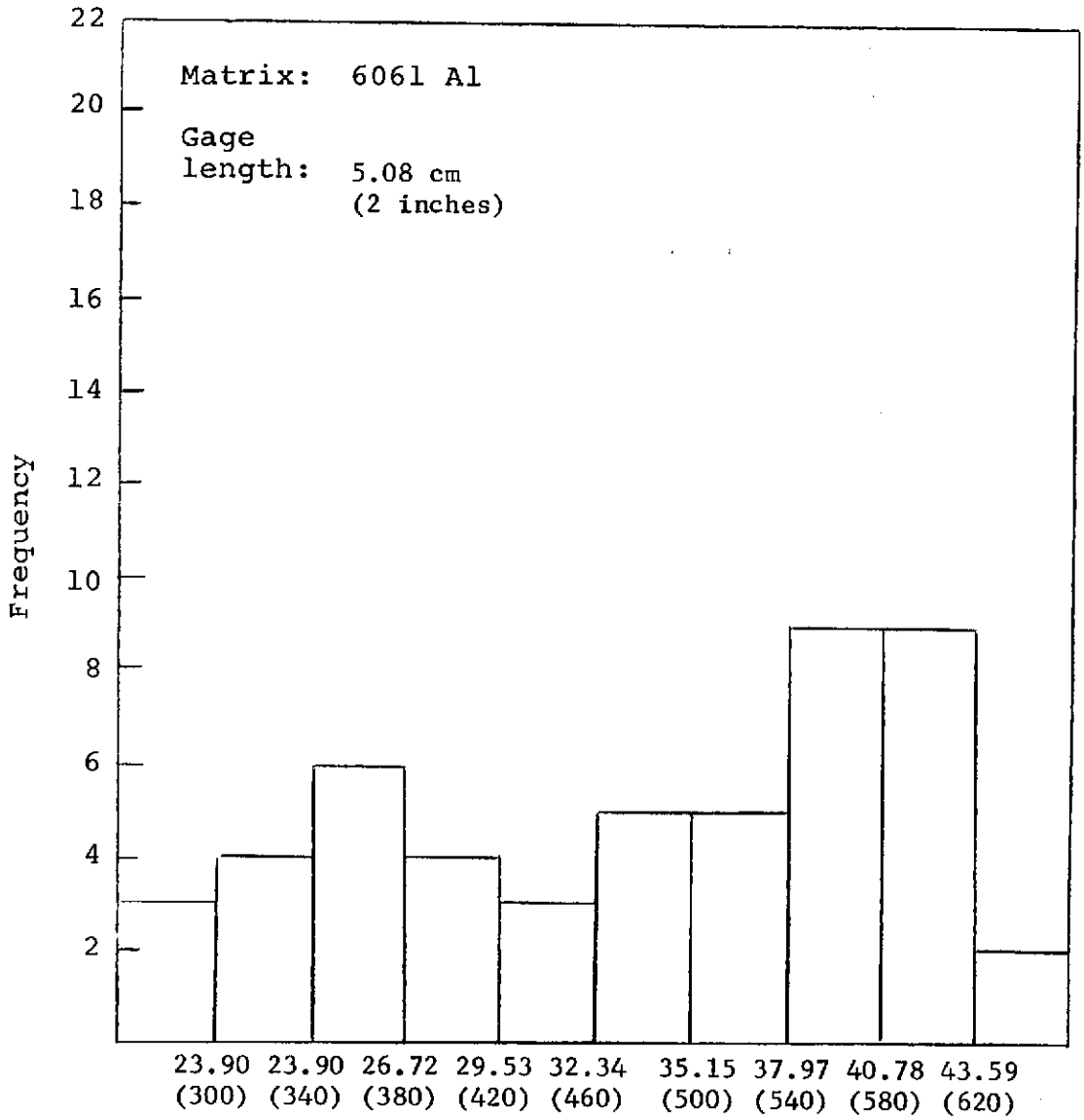

Figure 34

The Strength of Fibers Extracted from a Thermally Cycled Boron 6061 Aluminum Composite
Gage Length 5.08 cm
(2 Inches)

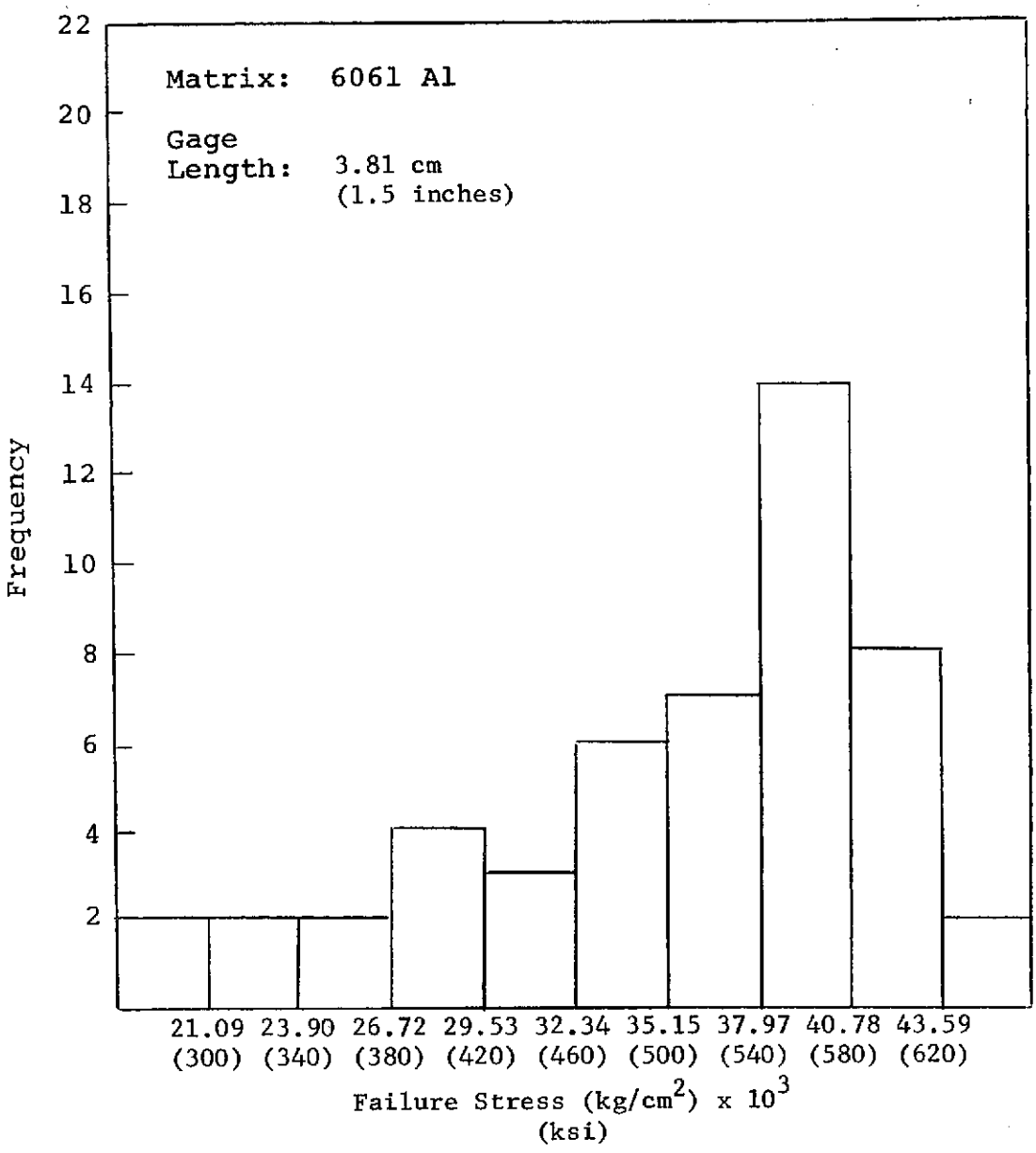

Figure 35

The Strength of Fibers Extracted from a Thermally Cycled Boron 6061 Aluminum Composite
Gage Length 3.81 cm
(1.5 Inches)

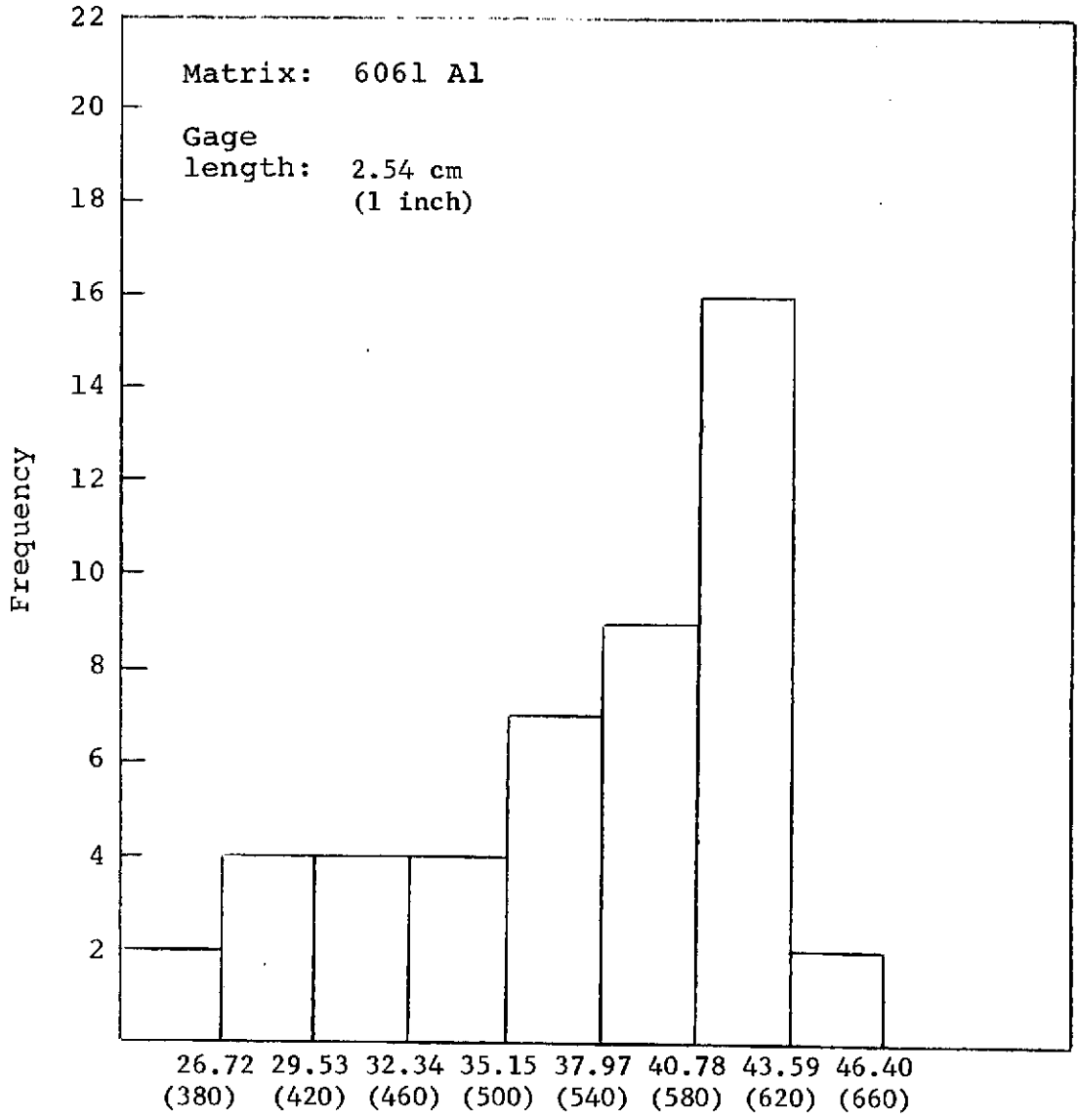

Figure 36

The Strength of Fibers Extracted from a Thermally Cycled Boron 6061 Aluminum Composite
Gage Length 2.54 cm
(1 Inch)

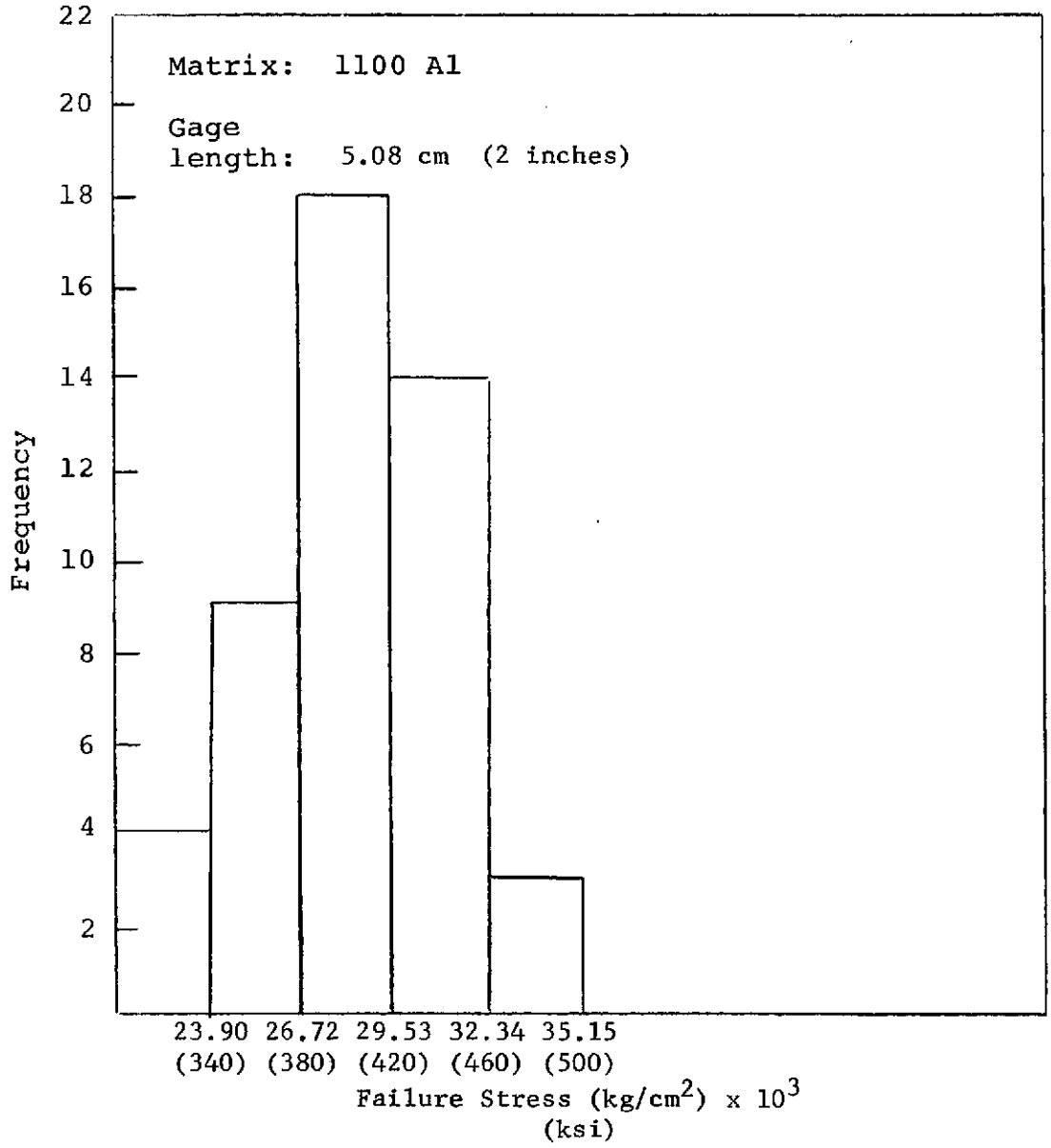

Figure 37

The Strength of Fibers Extracted from a Thermally Cycled Boron 1100 Aluminum Composite
Gage Length 5.08 cm
(2 Inches)

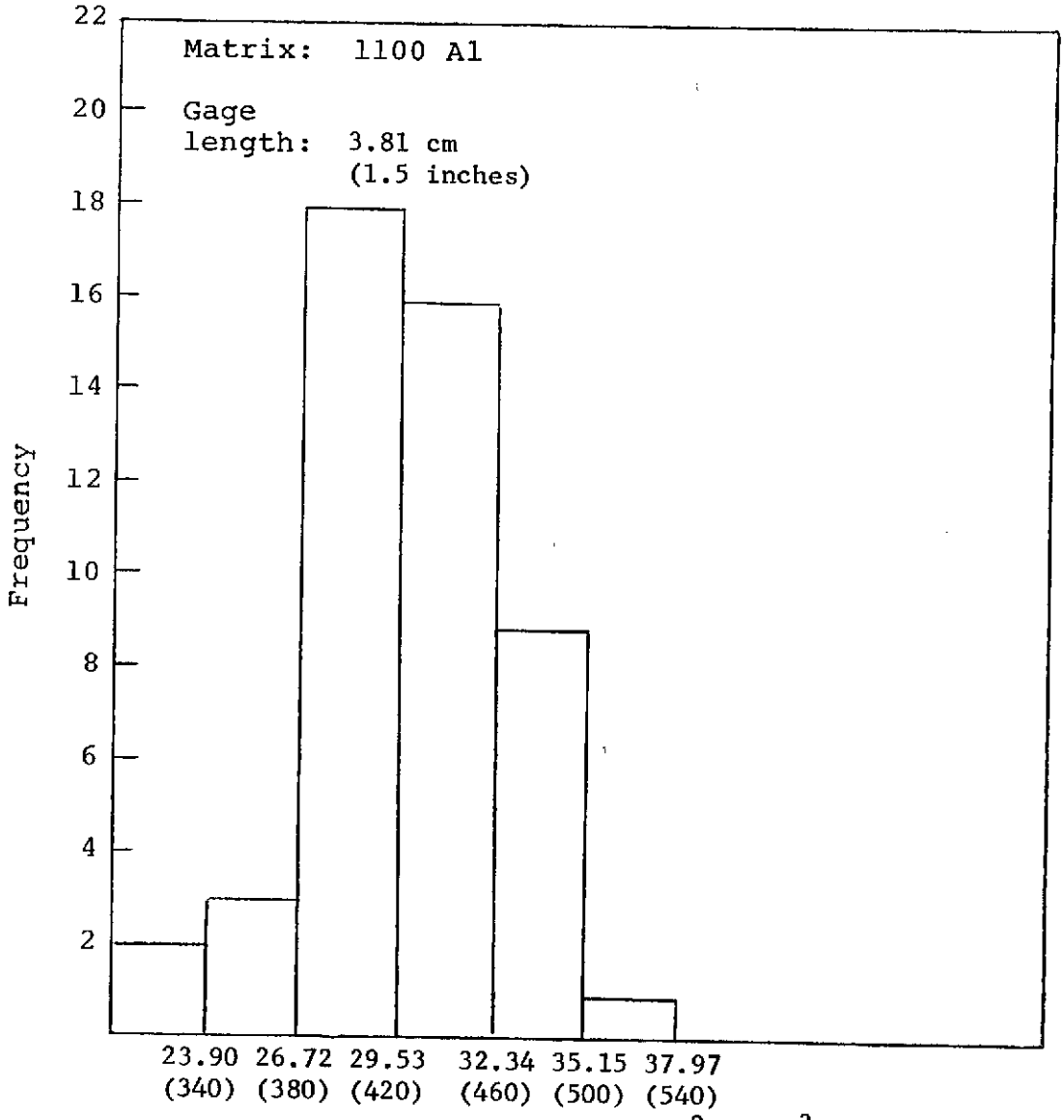

Figure 38

The Strength of Fibers Extracted from a Thermally Cycled Boron 1100 Aluminum Composite
Gage Length 3.81 cm
(1.5 Inches)

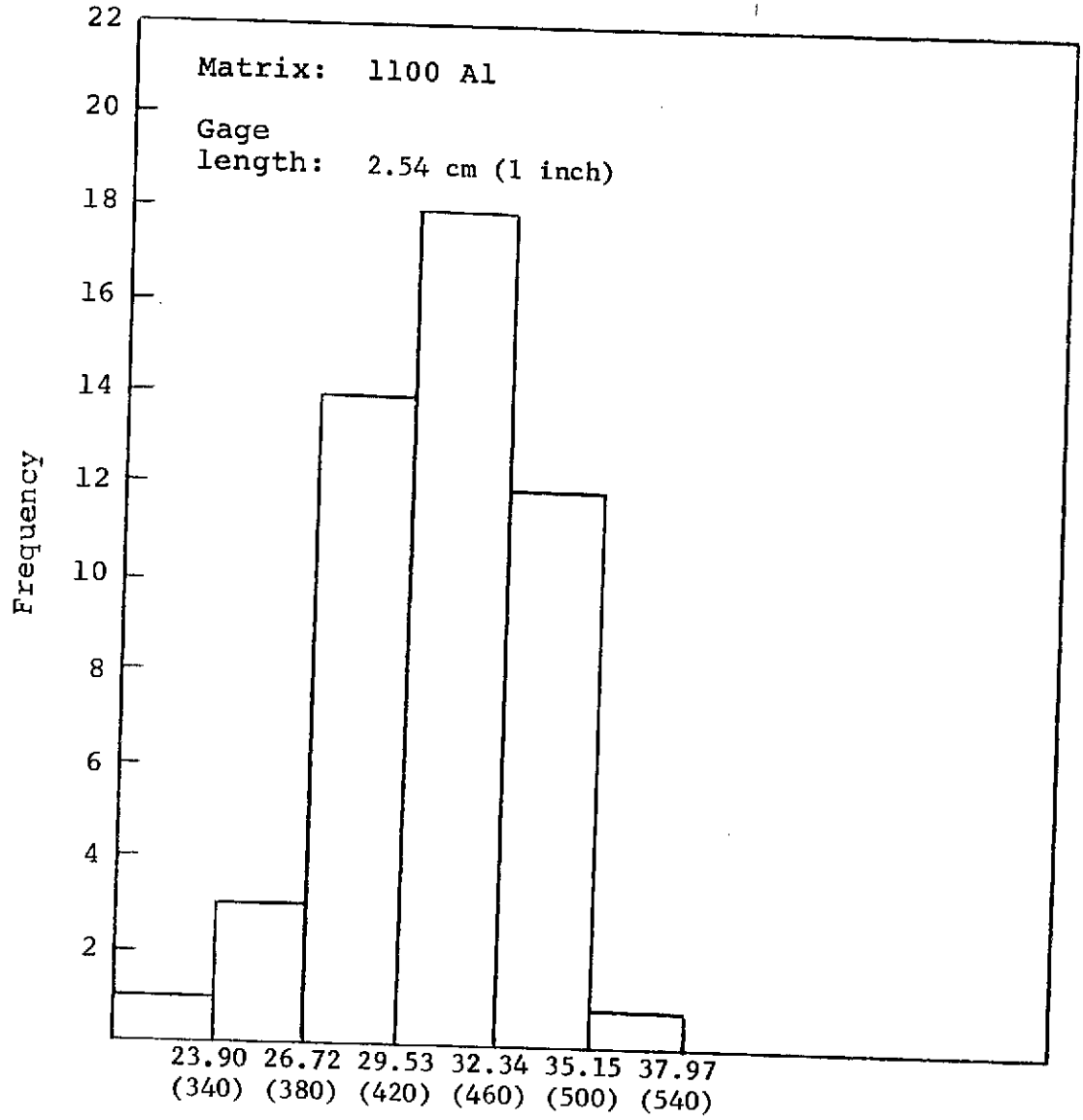

Figure 39

The Strength of Fibers Extracted from a Thermally Cycled Boron 1100 Aluminum Composite
Gage Length 2.54 cm
(1 Inch)

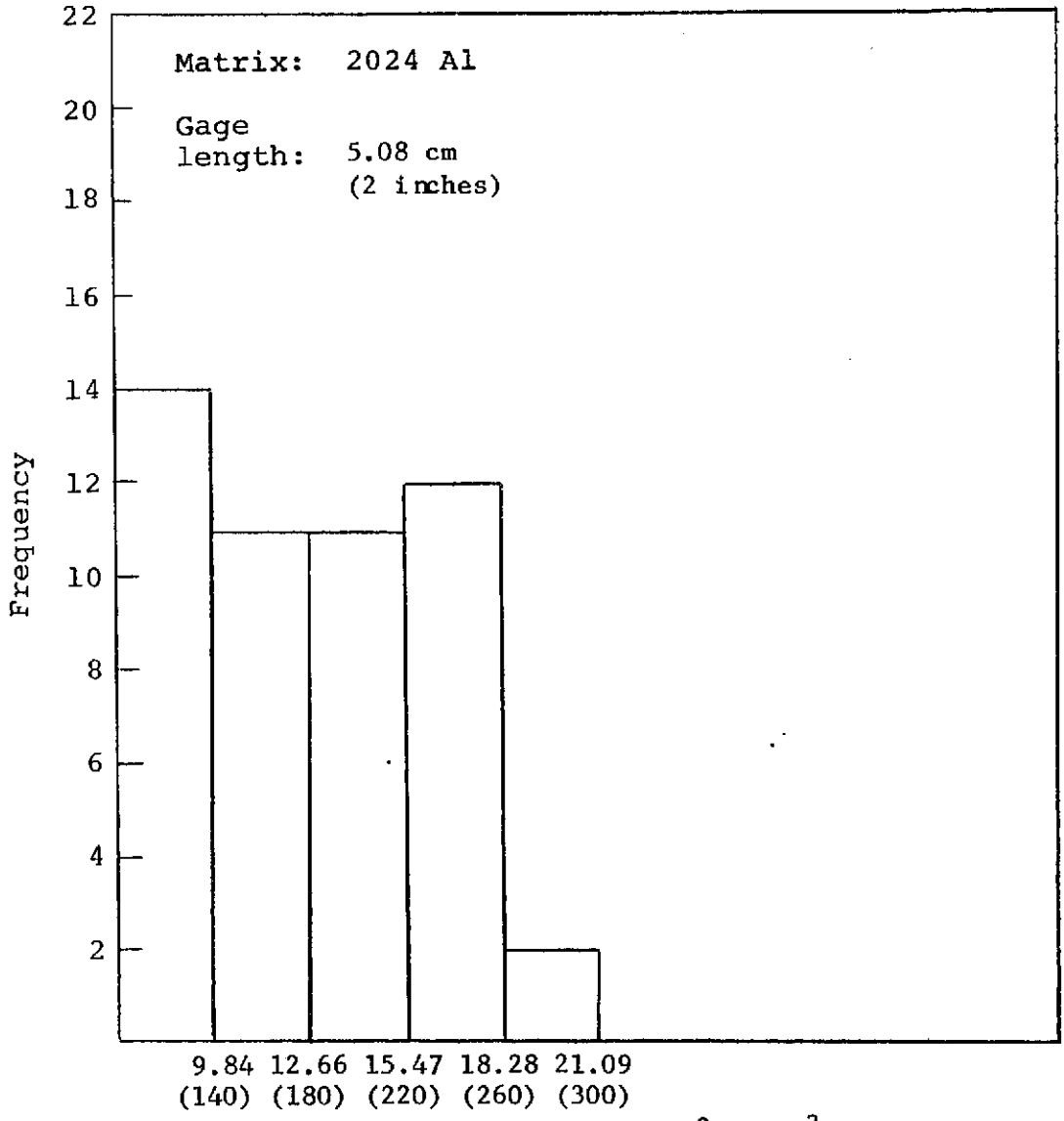

Figure 40

The Strength of Fibers Extracted from a Thermally Cycled Boron 2024 Aluminum Composite
Gage Length 5.08 cm
(2 Inches)

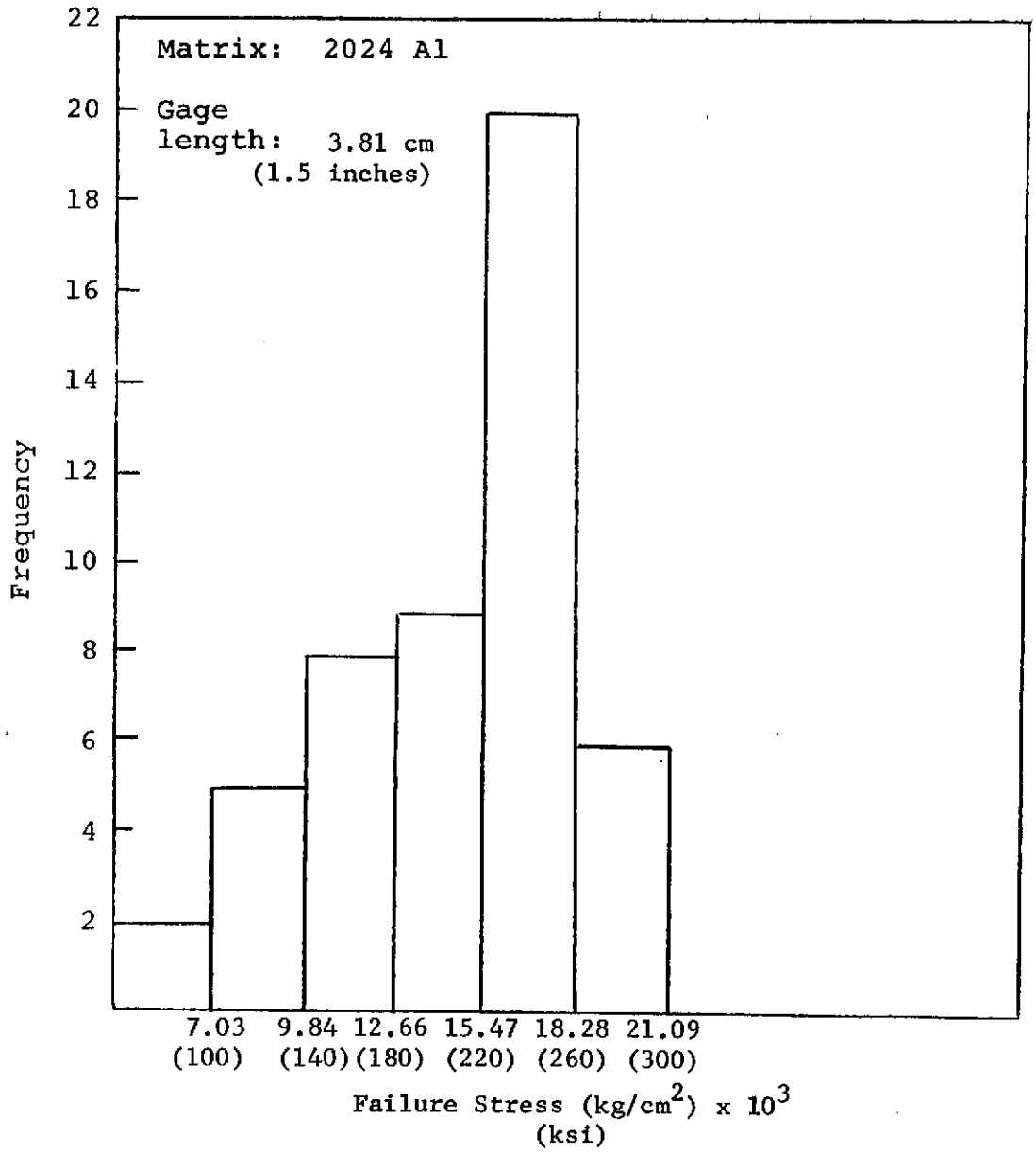

Figure 41

The Strength of Fibers Extracted from a Thermally Cycled Boron 2024 Aluminum Composite
Gage Length 3.81 cm
(1.5 Inches)

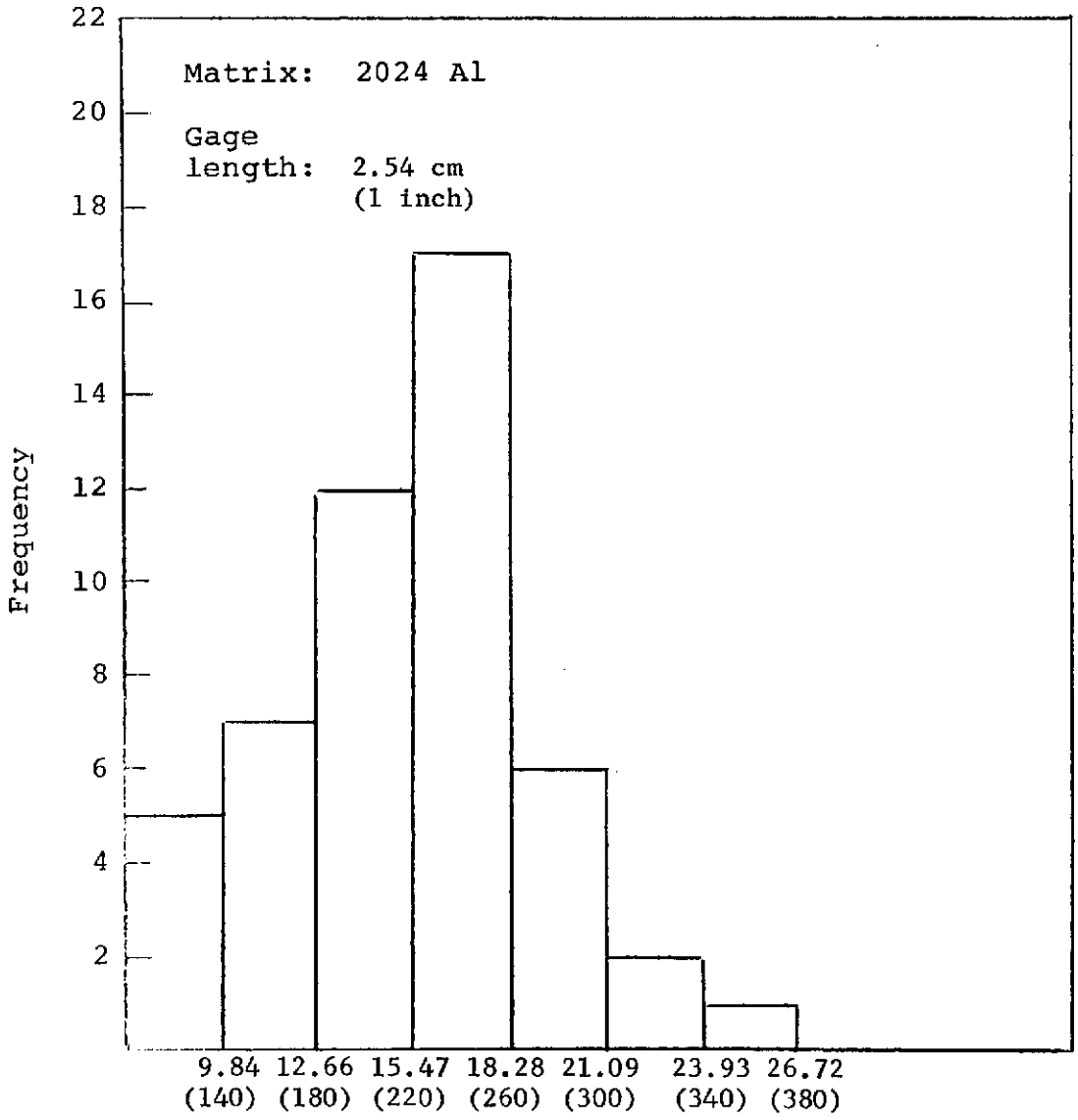

Figure 42

The Strength of Fibers Extracted from a Thermally Cycled Boron 2024 Aluminum Composite
Gage Length 2.54 cm
(1 Inch)

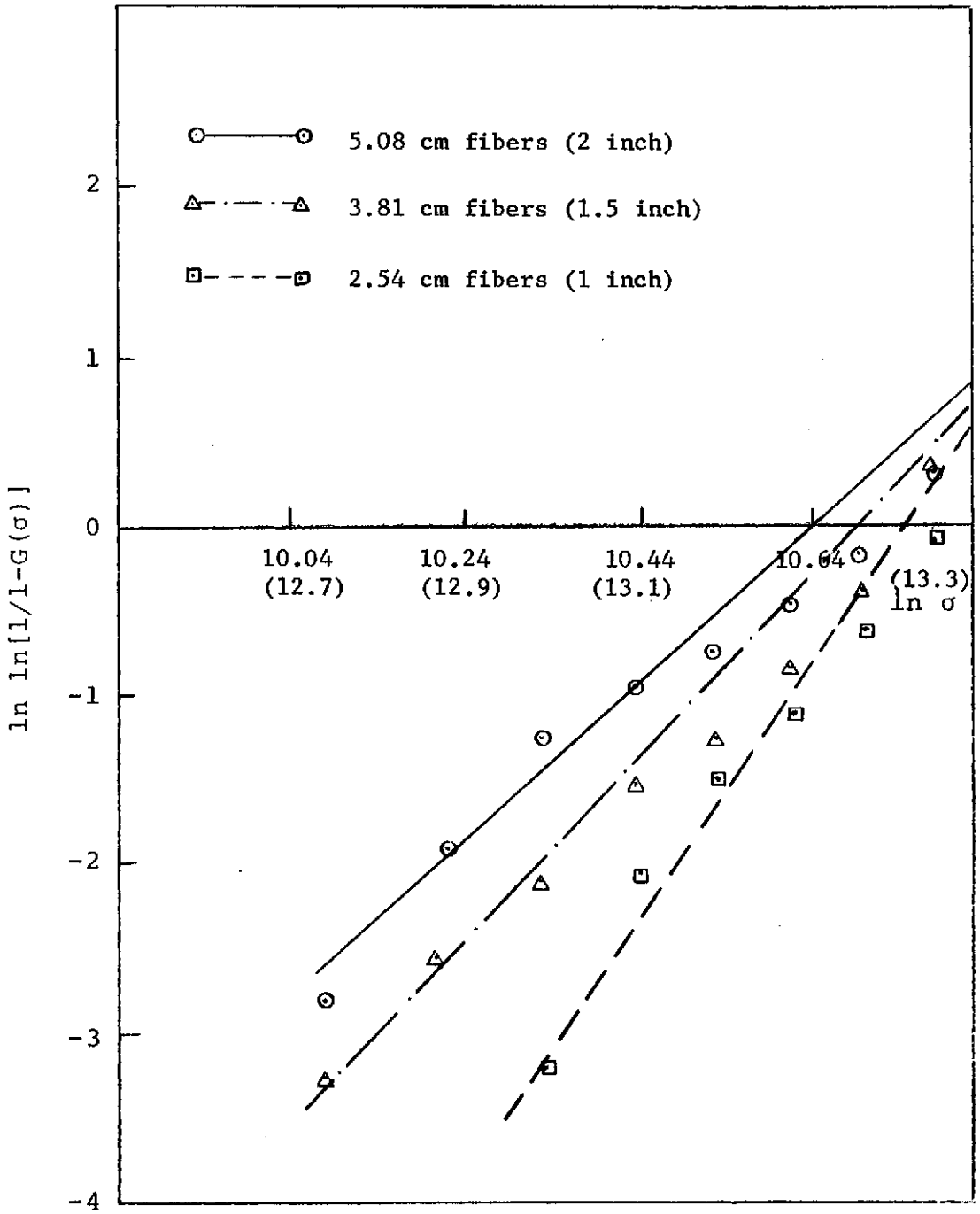

Figure 43

Weibull Distribution of the Strengths of Fibers Extracted from Thermally Cycled Reinforced 6061 Aluminum

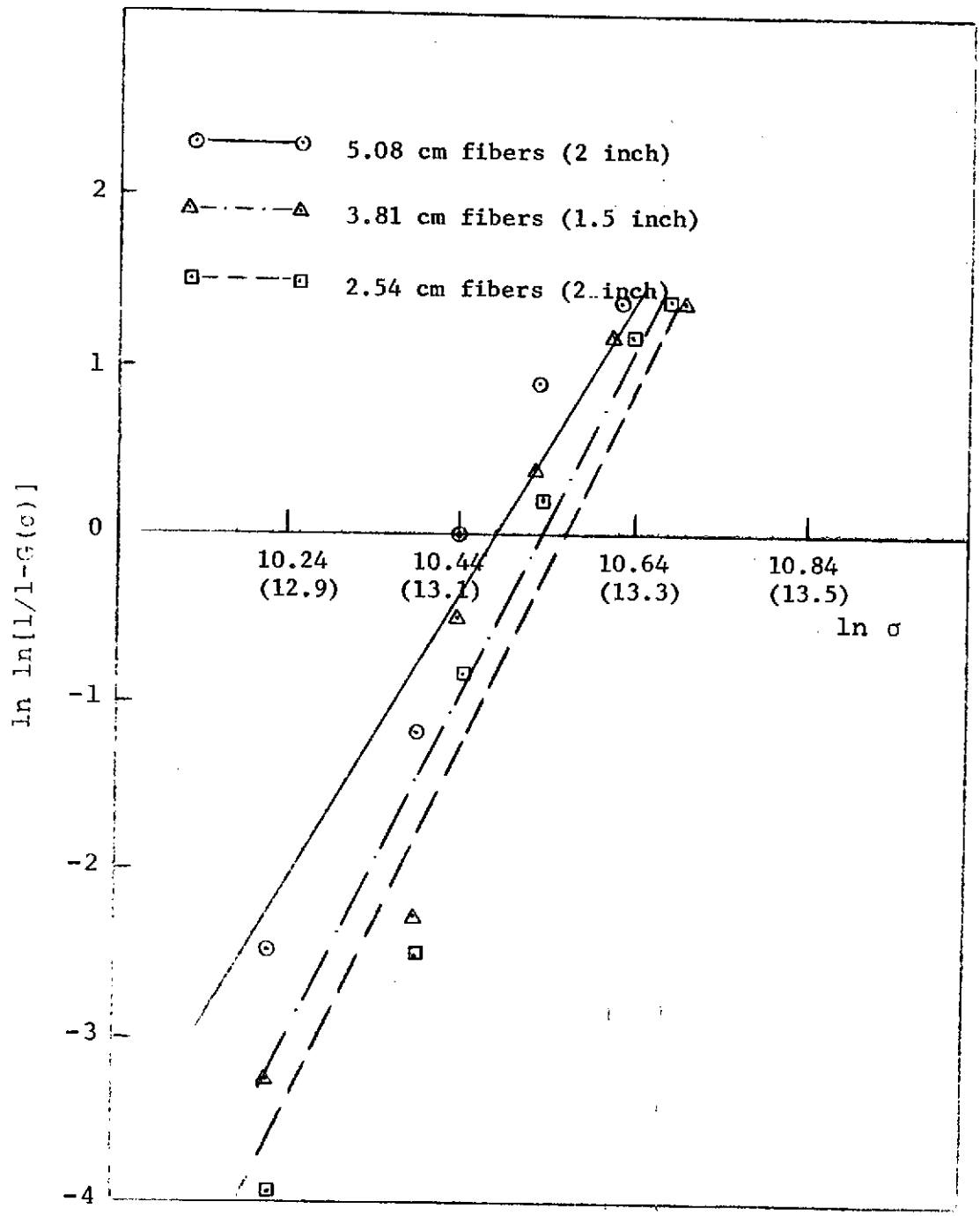

Figure 44

Weibull Distribution of the Strengths of Fibers Extracted from Thermally Cycled Reinforced 1100 Aluminum

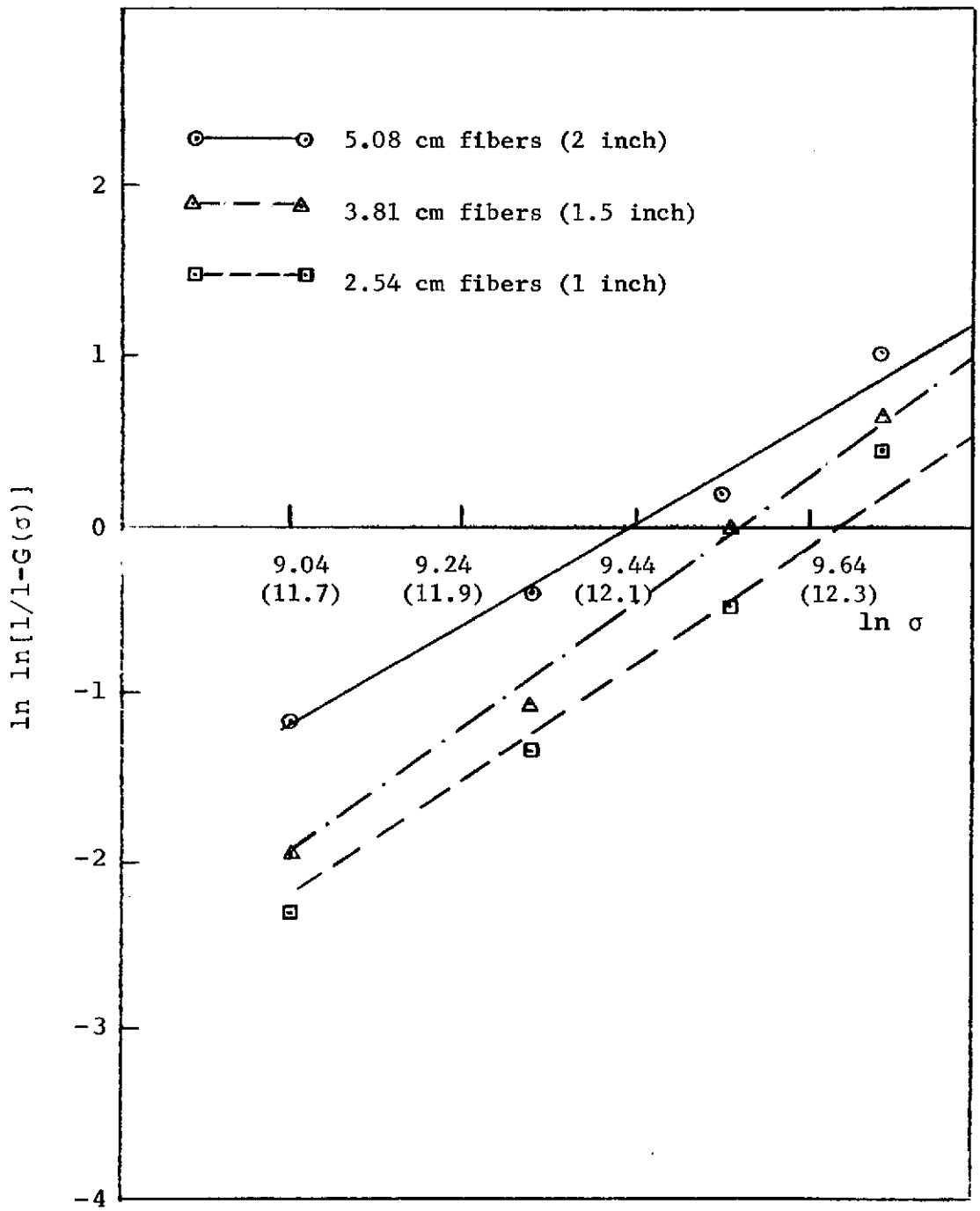

Figure 45

Weibull Distribution of the Strengths of Fibers Extracted from Thermally Cycled Reinforced 2024 Aluminum

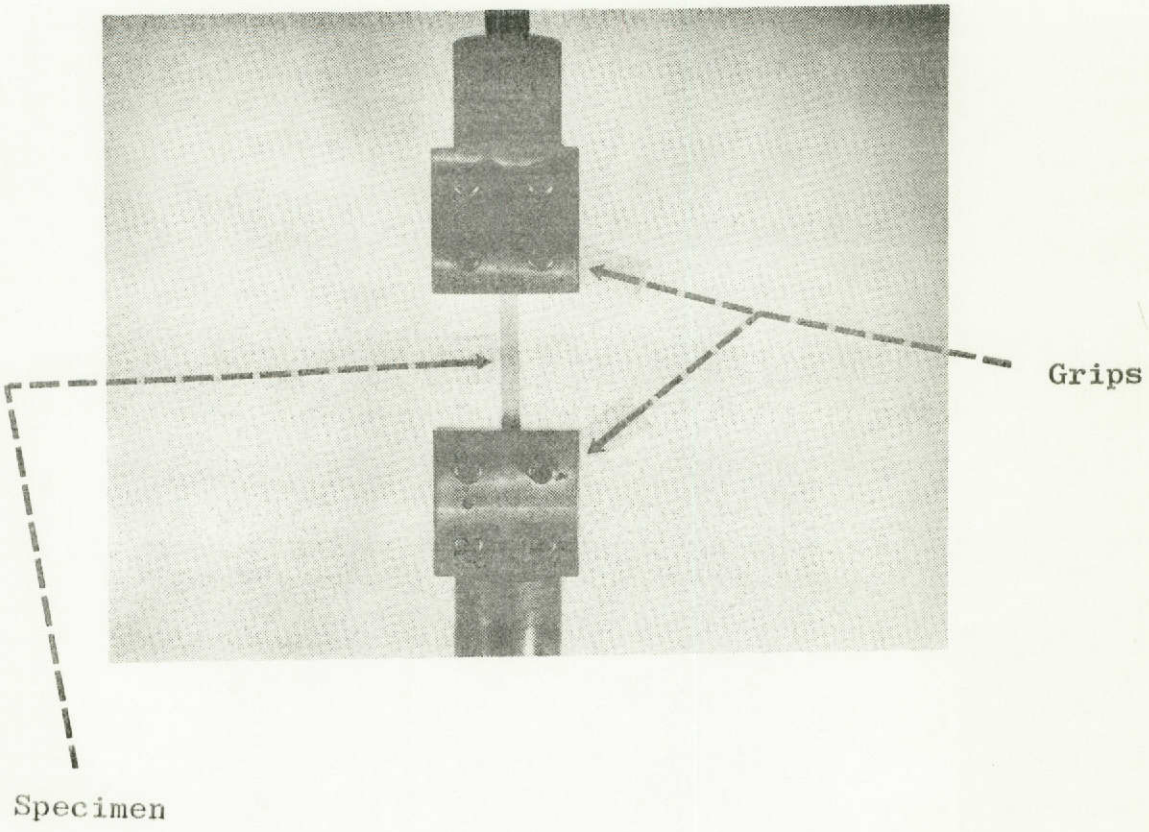

Figure 46

Specimen gripping arrangement for thermal fatigue apparatus...applied static load

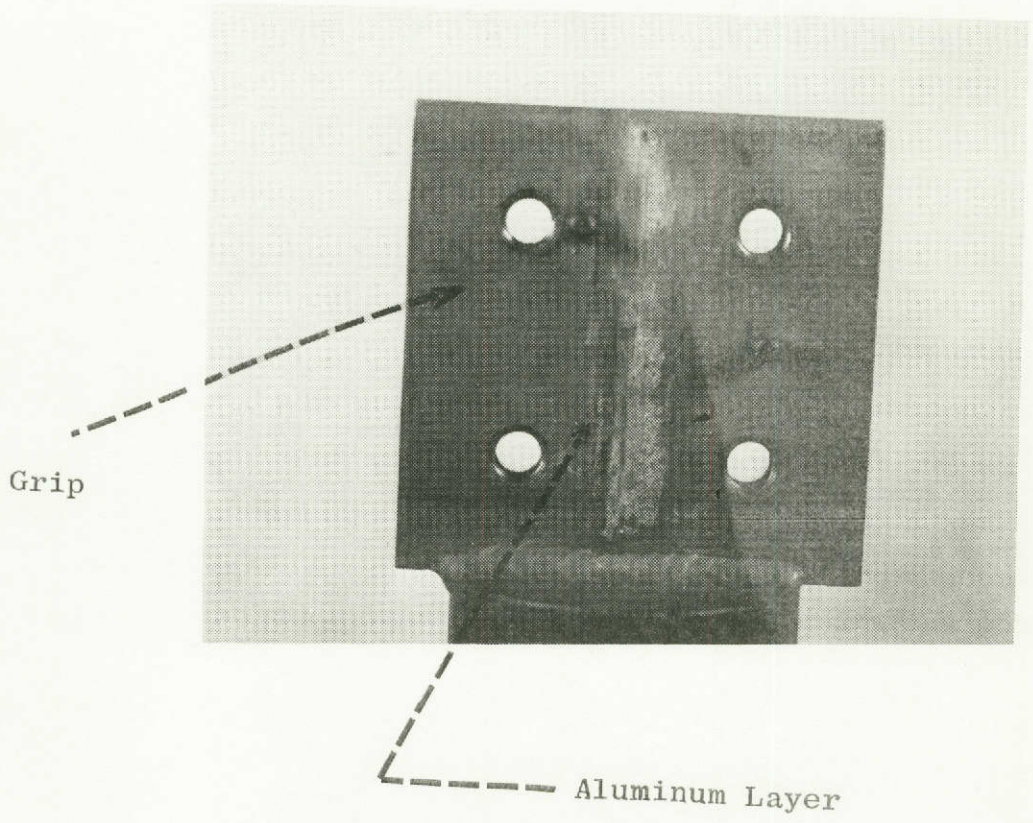

Figure 47

Grip surface, showing transferred Aluminum layer

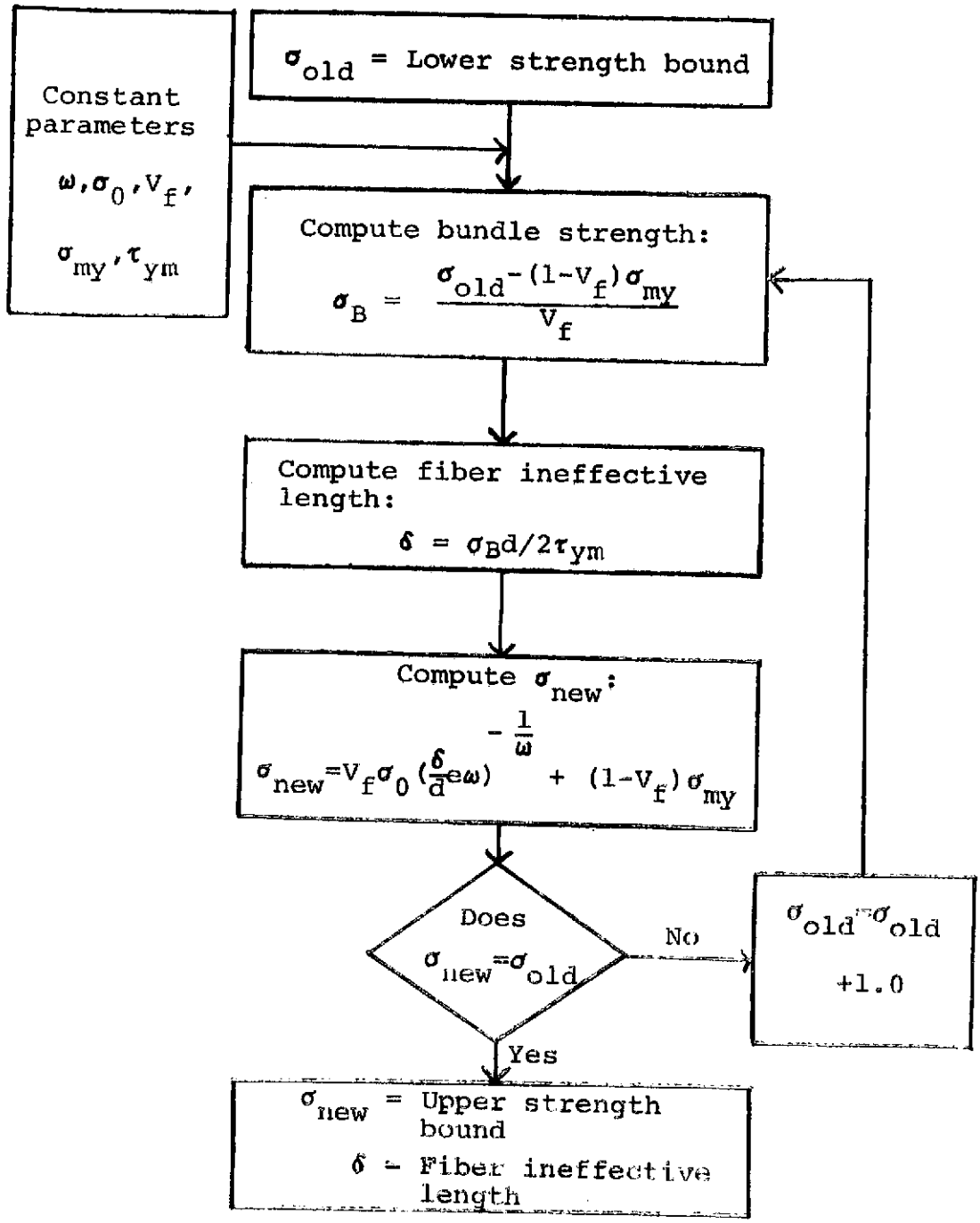

Figure 48

Flow Chart for Computation ineffective length, δ, and Upper Strength Bound, σ_{new}.

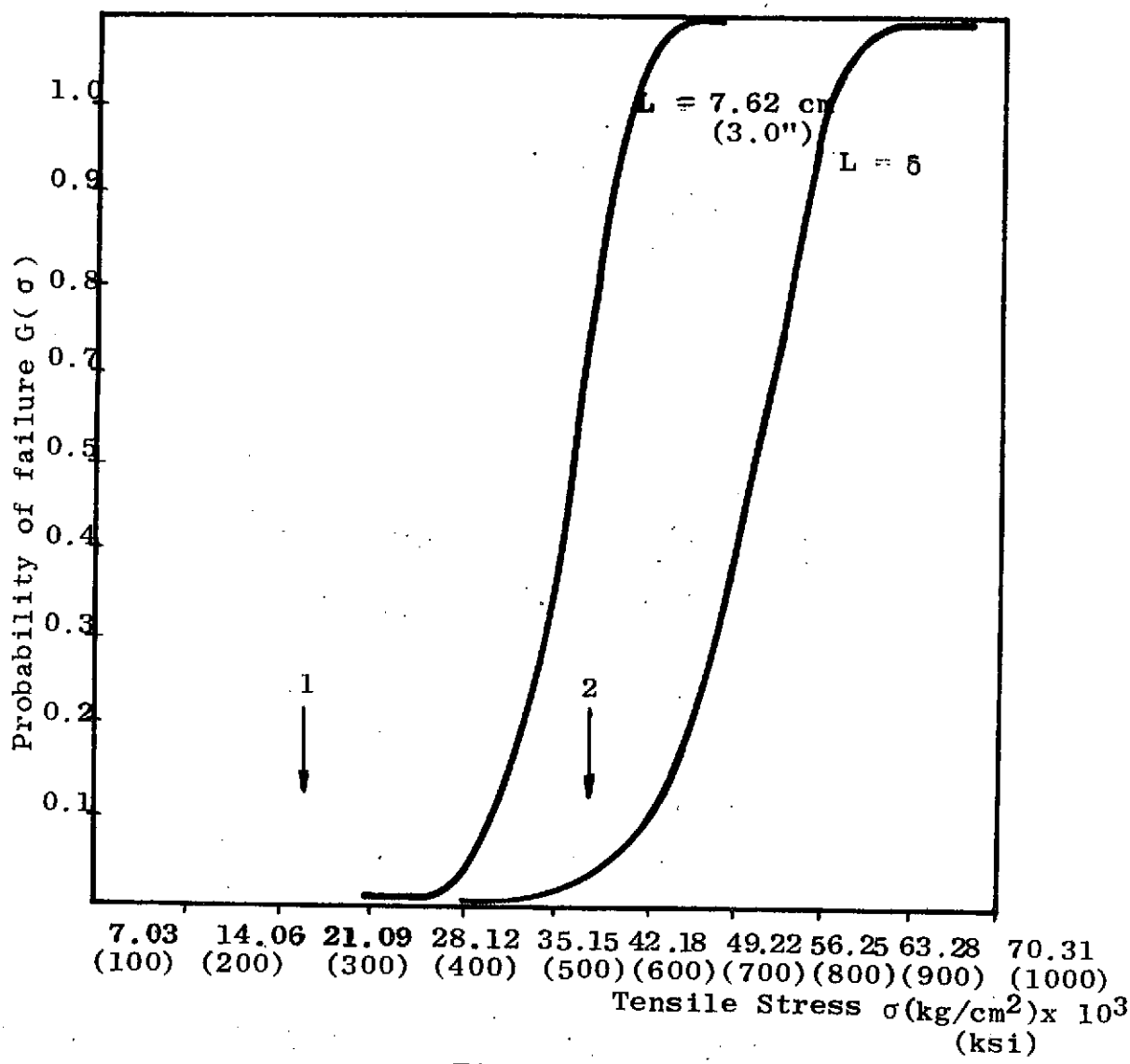

Figure 49

Probability of failure of different length fibers extracted from 6061 alloy (as received) (1 = failure stress, bundle; 2 = failure stress, composite)

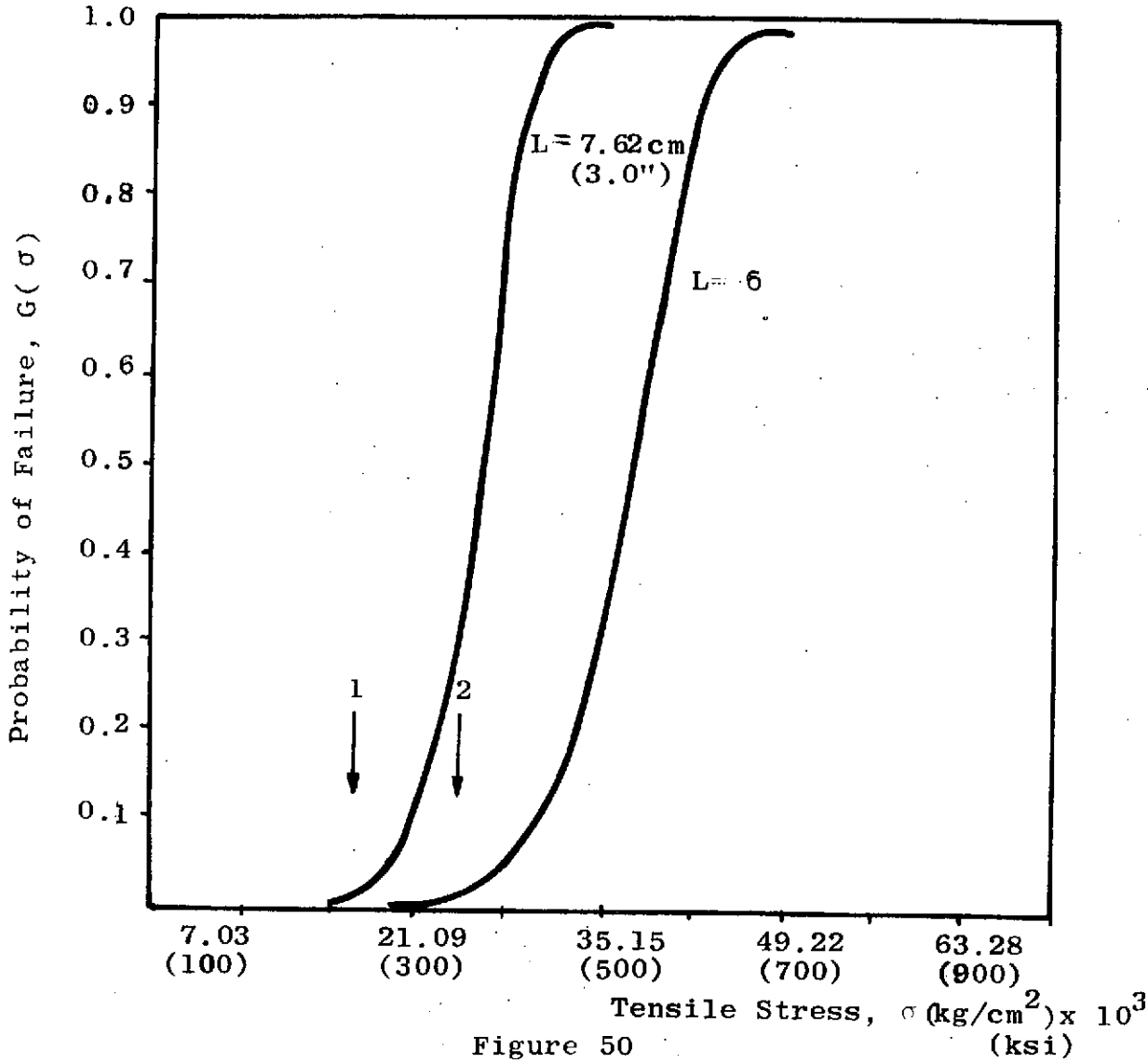

Figure 50

Probability of failure of different length fibers extracted from 1100 alloy (as received)

(1 Failure Stress, Bundle; 2 Failure Stress, Composite.)

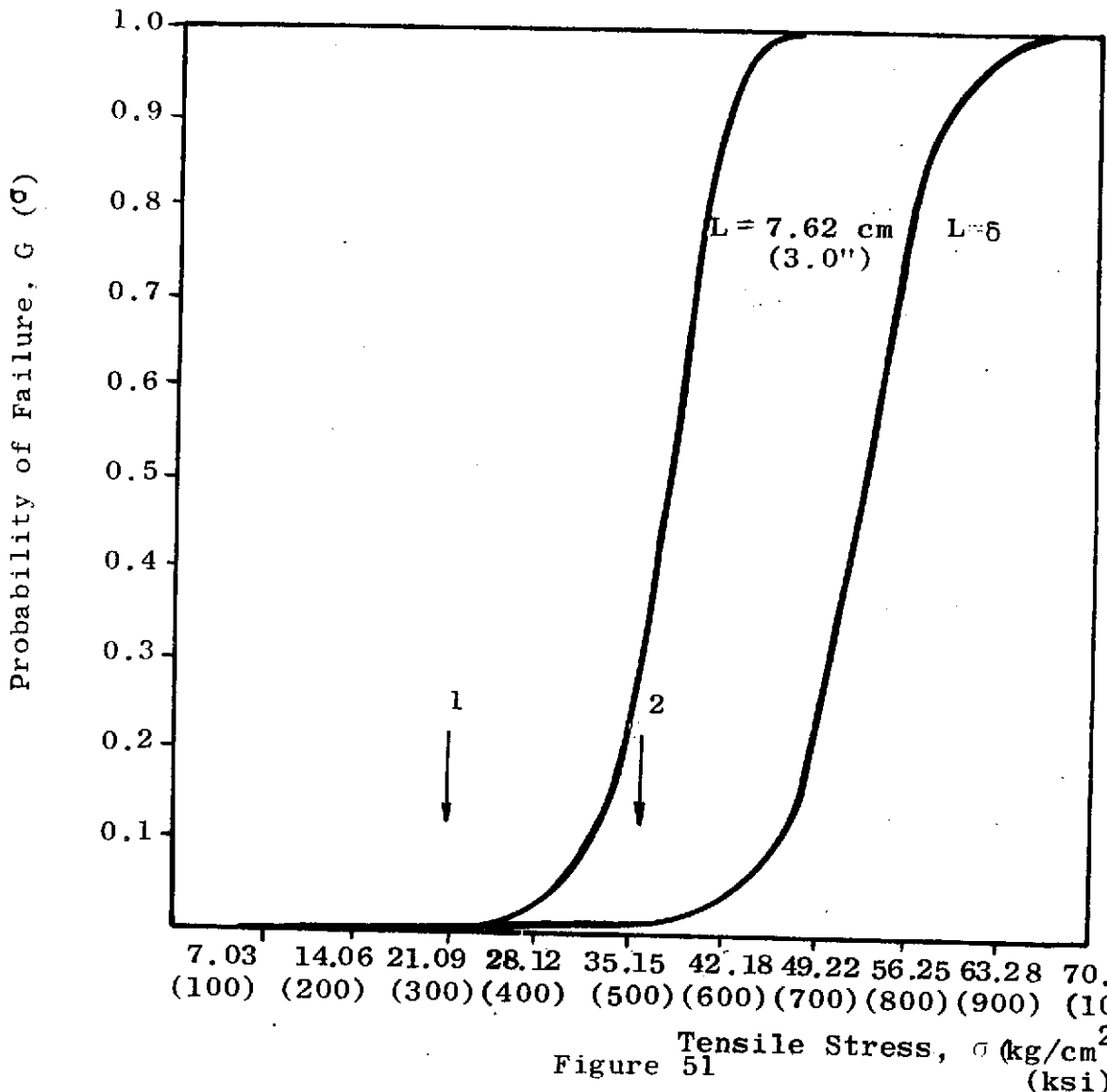

Figure 51

Probability of failure of different length fibers extracted from 2024 alloy (as received).

(1 = Failure Stress, Bundle; 2 = Failure Stress, Composite.)

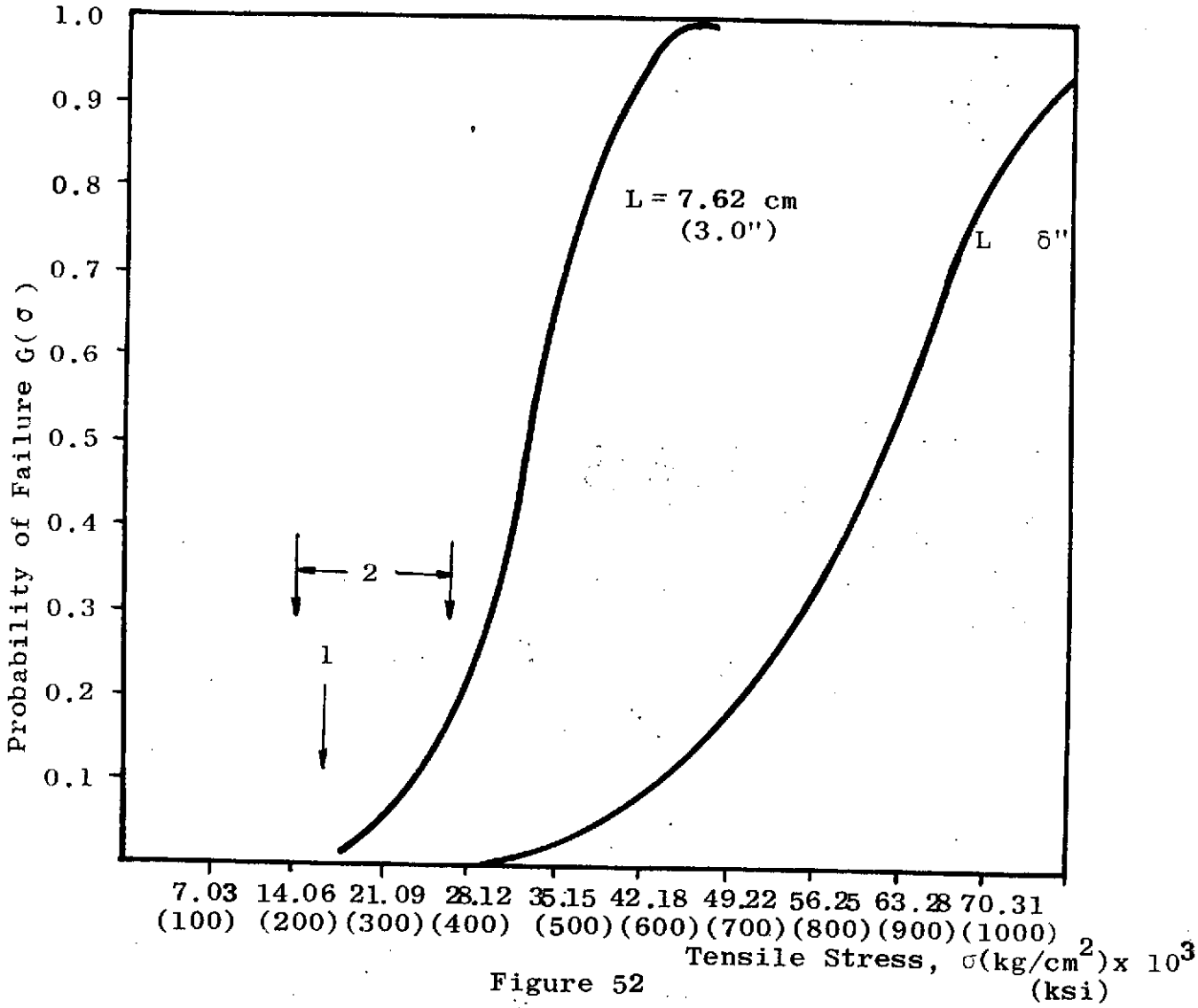

Figure 52

Probability of failure of different length fibers extracted from 6061 alloy (thermally fatigued) (1 = failure stress, bundle; 2 = failure stress, composite)

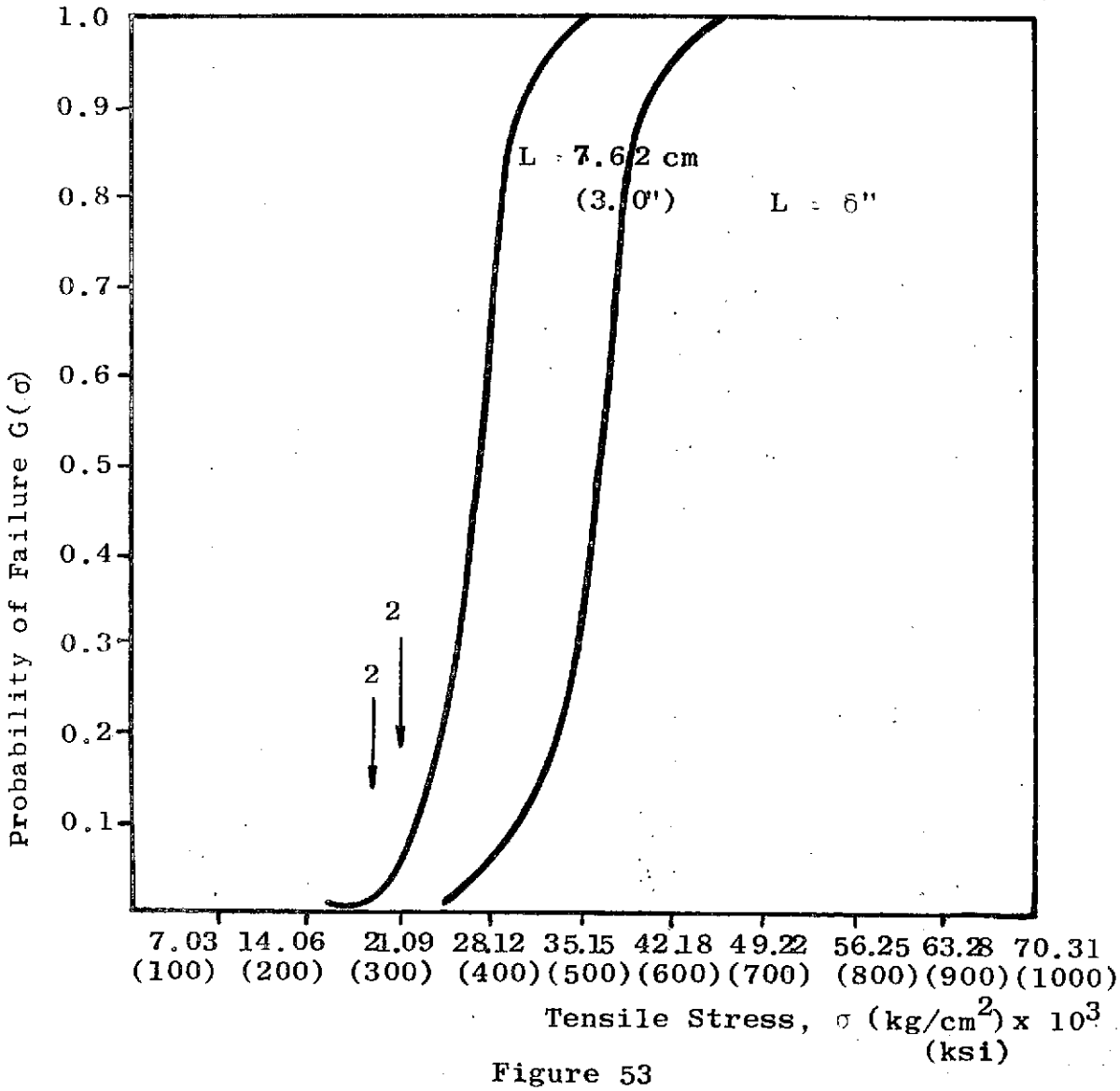

Figure 53

Probability of failure of different length fibers extracted from 1100 alloy (thermally fatigued) (1 = failure stress, bundle; 2 = failure stress, composite)

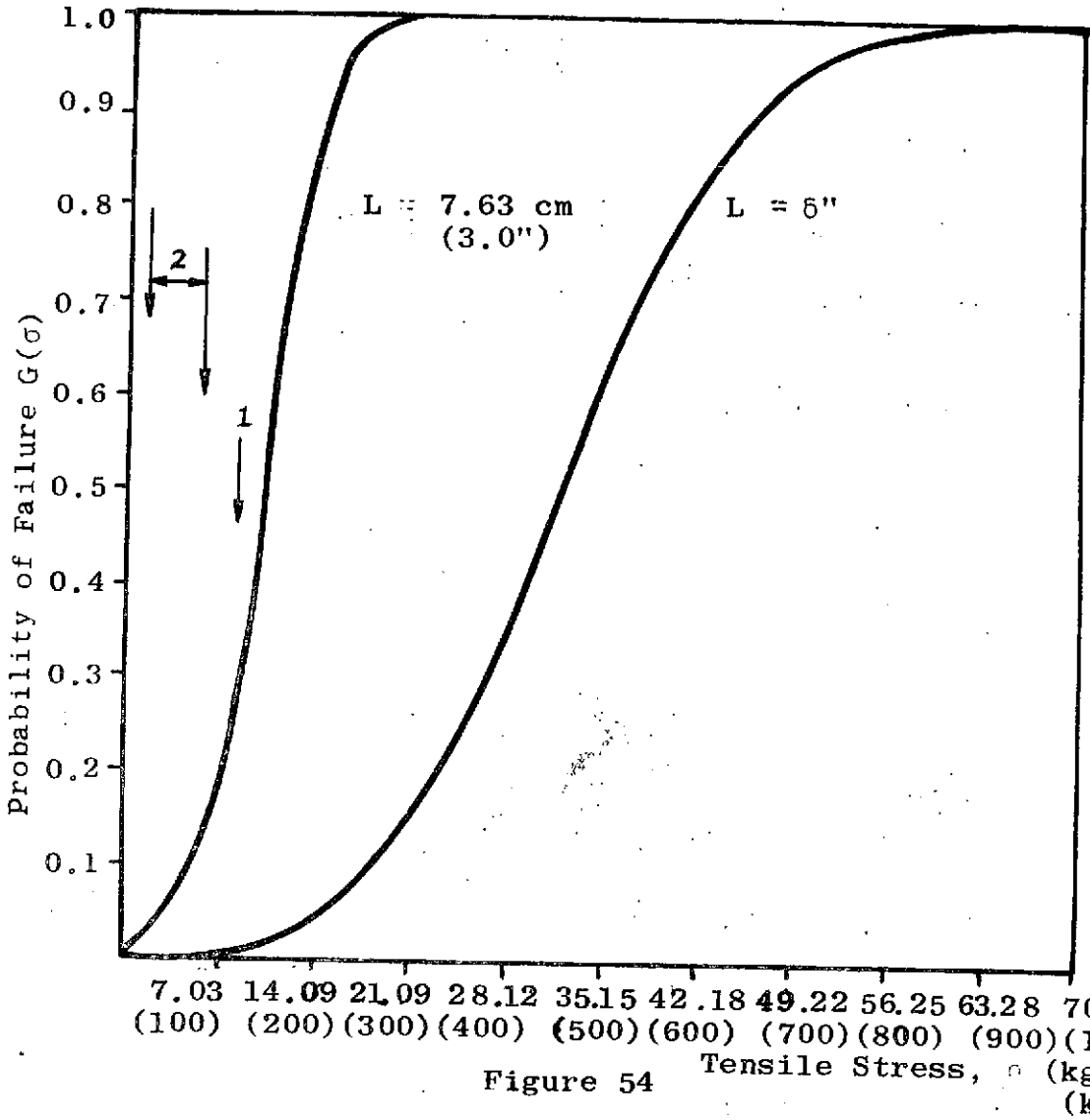

Figure 54

Probability of failure of different length fibers extracted from 2024 alloy (thermally fatigued) (1 = failure stress, bundle; 2 = failure stress, composite)

TABLE I

PROPERTIES OF AS-RECEIVED 6061, 1100, and 2024 ALUMINUM ALLOYS REINFORCED WITH 44 V/O BORON FIBERS.

	1100	6061	2024
Longitudinal Strength, σ_1, $kg/cm^2 \times 10^{-3}$ ($psi \times 10^{-3}$)	10.15 (144.30*) 10.90 (155.0)	14.58 (207.32) 17.30 (246.00)	- 15.55 (221.2)
Longitudinal Modulus, E_{11} $kg/cm^2 \times 10^{-6}$ ($psi \times 10^{-6}$)	2.004 (28.50*)	2.334 (33.20)	2.250 (32.00)
Poissons Ratio, ν_{12}	0.27	0.22	0.22
Transverse Strength, σ_2, $kg/cm^2 \times 10^{-3}$ ($psi \times 10^{-3}$)	0.569 (8.097) 0.489 (6.955)	1.502 (21.36) 1.314 (18.69)	0.775 (11.02) 1.561 (22.2)
Transverse Modulus, E_{22} $kg/cm^2 \times 10^{-6}$ ($psi \times 10^{-6}$)	1.174 (16.7) -	1.169 (16.63) 0.963 (13.70)	1.603 (22.8) -
Poissons Ratio, ν_{21}	-	0.13	0.15
Shear Strength, τ_{12}, $kg/cm^2 \times 10^{-3}$ ($psi \times 10^{-3}$)	0.555 (7.90) 0.600 (8.54)	1.005 (14.30)	1.420 (20.20) 1.420 (20.20)
Density grm/cc	2.63	2.65	2.61

*Contained 39 v/o reinforcement

TABLE II

FAILURE STRESS OF BORON FIBERS EXTRACTED FROM 6061 ALUMINUM: GAGE LENGTH 5.08 cm (2 inches)

Fiber No.	Failure Stress $kg/cm^2 \times 10^3$	Fiber No.	Failure Stress $kg/cm^2 \times 10^3$	Fiber No.	Failure Stress $kg/cm^2 \times 10^3$
1	34.61 (492.3)	18	38.34 (545.3)	35	40.48 (575.7)
2	40.88 (581.5)	19	41.43 (589.3)	36	36.11 (513.6)
3	38.56 (548.5)	20	38.24 (543.9)	37	38.24 (543.9)
4	32.64 (606.5)	21	36.65 (521.3)	38	41.21 (586.1)
5	38.82 (552.1)	22	41.43 (589.3)	39	41.43 (589.3)
6	35.95 (511.3)	23	37.47 (553.0)	40	38.40 (546.2)
7	41.75 (593.8)	24	40.79 (580.2)	41	30.27 (430.6)
8	43.86 (623.8)	25	31.95 (454.6)	42	26.30 (374.0)
9	33.46 (475.9)	26	39.04 (555.3)	43	27.88 (396.6)
10	34.26 (487.3)	27	40.95 (582.5)	44	34.68 (493.2)
11	40.73 (579.3)	28	42.07 (598.3)	45	40.73 (579.3)
12	39.67 (564.3)	29	39.20 (557.5)	46	34.35 (488.6)
13	36.97 (525.8)	30	33.46 (475.9)	47	26.93 (383.0)
14	37.45 (532.6)	31	29.57 (420.6)	48	43.02 (611.9)
15	40.09 (570.2)	32	37.54 (534.0)	49	39.61 (563.4)
16	30.60 (435.1)	33	42.23 (600.6)	50	40.63 (577.9)
17	36.49 (519.0)	34	42.18 (600.0)		

*Numbers in parentheses are (ksi).

TABLE III

FAILURE STRESS OF BORON FIBERS EXTRACTED FROM 6061 ALUMINUM: GAGE LENGTH 3.81 cm (1.5 INCHES)

Fiber No.	Failure Stress $kg/cm^2 \times 10^3$		Fiber No.	Failure Stress $kg/cm^2 \times 10^3$		Fiber No.	Failure Stress $kg/cm^2 \times 10^3$	
1	43.91	(624.6)	18	42.23	(600.6)	35	43.82	(623.2)
2	39.84	(566.6)	19	38.34	(545.3)	36	32.29	(459.2)
3	43.44	(617.8)	20	39.67	(564.3)	37	39.67	(564.3)
4	25.59	(364.0)	21	43.44	(617.8)	38	27.19	(386.7)
5	44.61	(634.6)	22	41.43	(589.3)	39	34.89	(496.3)
6	42.16	(599.7)	23	43.30	(658.6)	40	39.67	(564.3)
7	36.81	(523.5)	24	43.12	(613.3)	41	44.46	(632.3)
8	42.16	(599.7)	25	44.62	(634.6)	42	35.70	(507.7)
9	44.23	(629.1)	26	45.41	(645.9)	43	42.32	(601.9)
10	42.64	(606.5)	27	43.02	(611.9)	44	41.05	(583.8)
11	43.18	(614.2)	28	42.86	(609.6)	45	32.92	(468.2)
12	45.03	(640.5)	29	41.90	(596.0)	46	36.59	(520.4)
13	42.23	(600.6)	30	25.02	(355.8)	47	40.79	(580.2)
14	42.64	(606.5)	31	37.45	(532.6)	48	44.23	(629.1)
15	33.94	(482.7)	32	45.41	(645.9)	49	37.86	(538.5)
16	37.45	(532.6)	33	43.02	(611.9)	50	44.55	(633.7)
17	41.59	(591.5)	34	38.72	(550.7)			

* Numbers in parentheses are (ksi).

TABLE IV

FAILURE STRESS OF BORON FIBERS EXTRACTED FROM 6061 ALUMINUM: GAGE LENGTH 2.54 cm (1 INCH)

Fiber No.	Failure Stress $kg/cm^2 \times 10^3$		Fiber No.	Failure Stress $kg/cm^2 \times 10^3$		Fiber No.	Failure Stress $kg/cm^2 \times 10^3$	
1	35.79	(509.0)	18	42.23	(600.6)	35	32.74	(465.7)
2	34.26	(487.3)	19	44.23	(629.1)	36	43.82	(623.2)
3	37.61	(534.9)	20	39.04	(555.3)	37	43.02	(611.9)
4	41.75	(593.8)	21	43.02	(611.9)	38	29.44	(618.7)
5	43.82	(623.2)	22	43.34	(616.4)	39	47.10	(669.9)
6	42.18	(600.0)	23	43.02	(611.9)	40	45.57	(648.2)
7	43.02	(611.9)	24	41.52	(590.6)	41	34.51	(490.9)
8	36.65	(521.3)	25	44.79	(637.0)	42	41.05	(583.8)
9	40.00	(568.9)	26	43.02	(611.9)	43	40.63	(577.9)
10	39.67	(564.3)	27	43.02	(611.9)	44	43.60	(620.1)
11	43.18	(614.2)	28	38.72	(550.7)	45	42.07	(598.3)
12	44.14	(627.8)	29	33.47	(504.5)	46	37.45	(532.6)
13	37.45	(532.6)	30	41.43	(589.3)	47	25.11	(357.2)
14	38.09	(541.7)	31	43.82	(623.2)	48	42.70	(607.4)
15	44.46	(632.3)	32	42.54	(605.1)	49	32.92	(468.2)
16	34.35	(488.6)	33	42.80	(608.7)	50	41.43	(589.3)
17	35.31	(502.2)	34	42.32	(601.9)			

* Numbers in parenthesis are (ksi).

TABLE V

FAILURE STRESS OF BORON FIBERS EXTRACTED FROM 1100 ALUMINUM: GAGE LENGTH 5.08 cm (2 INCHES)

Fiber No.	Failure Stress $kg/cm^2 \times 10^3$		Fiber No.	Failure Stress $kg/cm^2 \times 10^3$		Fiber No.	Failure Stress $kg/cm^2 \times 10^3$	
1	28.78	(409.3)	18	26.13	(371.7)	35	28.88	(410.7)
2	34.04	(484.1)	19	23.10	(328.6)	36	28.88	(410.7)
3	24.06	(342.2)	20	30.27	(430.6)	37	23.90	(340.0)
4	28.84	(410.2)	21	31.19	(443.6)	38	23.91	(304.1)
5	23.10	(328.6)	22	20.23	(287.8)	39	23.04	(327.7)
6	30.91	(439.7)	23	32.25	(458.7)	40	26.28	(373.9)
7	25.97	(369.4)	24	31.71	(451.0)	41	28.59	(406.6)
8	25.49	(362.6)	25	23.17	(329.5)	42	28.68	(407.9)
9	19.60	(278.8)	26	24.92	(354.4)	43	27.69	(393.9)
10	26.55	(377.6)	27	32.12	(456.9)	44	29.16	(414.7)
11	21.77	(309.6)	28	23.33	(331.8)	45	25.43	(361.7)
12	20.02	(284.7)	29	27.41	(389.8)	46	29.51	(419.7)
13	24.47	(348.1)	30	29.03	(412.9)	47	17.85	(253.9)
14	27.76	(394.8)	31	27.38	(389.4)	48	21.13	(300.5)
15	26.01	(369.9)	32	31.17	(443.3)	49	28.68	(407.9)
16	30.56	(434.7)	33	29.93	(340.4)	50	30.88	(439.2)
17	30.02	(427.0)	34	32.25	(458.7)			

* Numbers in parentheses are (ksi).

TABLE VI

FAILURE STRESS OF BORON FIBERS EXTRACTED FROM 1100 ALUMINUM: GAGE LENGTH 3.81 cm (1.5 INCHES)

Fiber No.	Failure Stress $kg/cm^2 \times 10^3$		Fiber No.	Failure Stress $kg/cm^2 \times 10^3$		Fiber No.	Failure Stress $kg/cm^2 \times 10^3$	
1	29.09	(413.8)	18	25.11	(357.2)	35	20.65	(293.7)
2	29.80	(423.8)	19	27.51	(391.2)	36	31.07	(441.9)
3	30.11	(428.3)	20	25.33	(360.3)	37	26.29	(373.9)
4	32.69	(465.0)	21	29.42	(418.4)	38	30.53	(434.2)
5	28.14	(400.2)	22	17.15	(243.9)	39	29.42	(418.4)
6	25.17	(358.0)	23	23.90	(339.9)	40	24.79	(352.6)
7	29.48	(419.3)	24	23.04	(327.7)	41	28.05	(398.9)
8	34.45	(488.6)	25	27.88	(396.6)	42	32.44	(461.4)
9	30.27	(430.6)	26	29.09	(413.8)	43	31.07	(441.9)
10	28.30	(402.5)	27	28.30	(402.5)	44	24.86	(353.6)
11	23.74	(337.7)	28	30.91	(439.7)	45	23.52	(334.5)
12	26.70	(379.8)	29	29.96	(426.1)	46	31.07	(441.9)
13	26.55	(377.6)	30	31.81	(452.4)	47	24.86	(353.6)
14	29.73	(422.9)	31	23.10	(328.6)	48	22.71	(323.0)
15	14.34	(204.0)	32	30.27	(430.6)	49	22.71	(323.0)
16	27.98	(398.0)	33	26.86	(382.1)	50	27.72	(394.3)
17	19.76	(281.0)	34	27.98	(398.0)			

* Numbers in parentheses are (ksi).

TABLE VII

FAILURE STRESS OF BORON FIBERS EXTRACTED FROM 1100 ALUMINUM: GAGE LENGTH 2.54 cm (1 INCH)

Fiber No.	Failure Stress $kg/cm^2 \times 10^3$		Fiber No.	Failure Stress $kg/cm^2 \times 10^3$		Fiber No.	Failure Stress $kg/cm^2 \times 10^3$	
1	19.38	(275.6)	18	30.31	(431.1)	35	27.82	(395.7)
2	26.16	(372.1)	19	30.34	(431.5)	36	29.48	(419.3)
3	29.99	(426.5)	20	30.56	(434.7)	37	31.01	(441.0)
4	30.59	(435.1)	21	32.19	(457.8)	38	26.13	(371.7)
5	31.84	(452.8)	22	28.52	(405.7)	39	25.18	(358.1)
6	31.87	(453.3)	23	28.68	(407.9)	40	22.63	(321.8)
7	31.58	(449.2)	24	31.17	(443.3)	41	33.40	(475.0)
8	28.62	(407.0)	25	29.48	(419.3)	42	32.03	(455.5)
9	25.43	(361.7)	26	25.11	(357.2)	43	24.54	(349.0)
10	29.99	(426.5)	27	30.37	(432.0)	44	26.93	(383.0)
11	31.42	(446.9)	28	26.22	(373.0)	45	22.95	(326.4)
12	29.80	(423.8)	29	33.30	(473.7)	46	27.88	(396.6)
13	30.11	(428.3)	30	27.88	(396.6)	47	29.57	(420.6)
14	30.98	(440.6)	31	31.81	(452.4)	48	31.48	(447.8)
15	28.52	(405.7)	32	31.07	(441.9)	49	26.39	(375.3)
16	27.79	(395.3)	33	25.81	(367.1)	50	25.18	(358.1)
17	30.82	(438.3)	34	33.14	(471.4)			

* Numbers in parentheses are (ksi).

TABLE VIII

FAILURE STRESS OF BORON FIBERS EXTRACTED FROM 2024 ALUMINUM: GAGE LENGTH 5.08 cm (2 INCHES)

Fiber No.	Failure Stress $kg/cm^2 \times 10^3$		Fiber No.	Failure Stress $kg/cm^2 \times 10^3$		Fiber No.	Failure Stress $kg/cm^2 \times 10^3$	
1	25.91	(368.5)	18	41.36	(588.3)	35	38.72	(550.7)
2	35.06	(498.6)	19	40.57	(577.0)	36	42.80	(608.7)
3	43.18	(614.2)	20	41.84	(595.1)	37	34.26	(487.3)
4	41.84	(595.1)	21	42.23	(600.6)	38	45.41	(645.9)
5	34.89	(496.3)	22	40.63	(577.9)	39	45.51	(647.3)
6	38.97	(554.3)	23	33.46	(475.9)	40	38.66	(549.8)
7	32.29	(459.2)	24	42.23	(600.6)	41	44.23	(629.1)
8	37.38	(531.7)	25	44.39	(631.4)	42	41.55	(591.5)
9	44.71	(635.9)	26	41.84	(595.1)	43	42.07	(598.3)
10	43.38	(602.8)	27	43.82	(623.2)	44	36.49	(519.0)
11	43.38	(602.8)	28	43.12	(613.3)	45	43.18	(614.2)
12	37.28	(530.3)	29	36.26	(515.8)	46	37.28	(530.3)
13	45.25	(643.6)	30	38.09	(541.7)	47	39.93	(567.9)
14	38.09	(541.7)	31	32.98	(469.1)	48	33.56	(477.3)
15	38.34	(545.3)	32	40.88	(581.5)	49	37.13	(528.1)
16	42.00	(597.4)	33	42.32	(601.9)	50	38.40	(546.2)
17	41.52	(590.6)	34	42.80	(608.7)			

* Numbers in parentheses are (ksi).

TABLE IX

FAILURE STRESSES OF BORON FIBERS EXTRACTED FROM 2024 ALUMINUM: GAGE LENGTH 3.81 cm (1.5 inches)

Fiber No.	Failure Stress $kg/cm^2 \times 10^3$		Fiber No.	Failure Stress $kg/cm^2 \times 10^3$		Fiber No.	Failure Stress $kg/cm^2 \times 10^3$	
1	43.02	(611.9)	18	36.26	(515.8)	35	44.62	(634.6)
2	42.38	(602.8)	19	35.22	(500.9)	36	45.03	(640.5)
3	42.07	(598.3)	20	45.51	(647.3)	37	46.21	(657.2)
4	42.38	(602.8)	21	42.64	(606.5)	38	36.26	(515.8)
5	31.17	(443.3)	22	34.74	(494.1)	39	39.61	(563.4)
6	43.27	(615.5)	23	34.26	(487.3)	40	35.70	(507.7)
7	43.02	(611.9)	24	34.68	(493.2)	41	39.93	(567.9)
8	39.20	(557.5)	25	36.33	(516.7)	42	42.07	(598.3)
9	42.07	(598.3)	26	33.30	(473.7)	43	34.68	(493.2)
10	42.00	(597.4)	27	39.13	(556.6)	44	37.45	(532.6)
11	42.32	(601.9)	28	39.04	(555.3)	45	39.84	(566.6)
12	40.73	(579.3)	29	45.57	(648.2)	46	39.67	(564.3)
13	41.26	(586.9)	30	31.48	(447.8)	47	39.84	(566.6)
14	42.70	(607.4)	31	41.75	(593.8)	48	41.35	(588.3)
15	38.88	(553.0)	32	44.62	(634.6)	49	43.91	(624.6)
16	46.14	(656.3)	33	44.62	(634.6)	50	43.02	(611.9)
17	31.23	(444.2)	34	33.72	(479.6)			

*Numbers in parentheses are (ksi).

TABLE X

FAILURE STRESSES OF BORON FIBERS EXTRACTED FROM 2024 ALUMINUM: GAGE LENGTH 2.54 cm (1 inch)

Fiber No.	Failure Stress $kg/cm^2 \times 10^3$		Fiber No.	Failure Stress $kg/cm^2 \times 10^3$		Fiber No.	Failure Stress $kg/cm^2 \times 10^3$	
1	47.96	(682.2)	18	41.59	(591.5)	35	46.85	(666.3)
2	46.05	(655.0)	19	40.48	(575.7)	36	44.70	(635.9)
3	44.46	(632.3)	20	39.20	(557.5)	37	46.85	(666.3)
4	41.69	(592.9)	21	36.65	(521.3)	38	43.91	(624.6)
5	43.66	(621.0)	22	47.64	(677.6)	39	40.57	(577.0)
6	42.64	(606.5)	23	32.98	(469.1)	40	38.97	(554.3)
7	44.46	(632.3)	24	45.25	(643.6)	41	41.43	(589.3)
8	34.10	(485.0)	25	39.93	(567.9)	42	40.25	(572.5)
9	24.64	(350.4)	26	41.11	(584.7)	43	35.15	(500.0)
10	45.57	(648.2)	27	42.32	(601.9)	44	30.69	(436.5)
11	36.90	(524.9)	28	43.75	(622.3)	45	40.41	(574.7)
12	43.66	(621.0)	29	40.25	(572.5)	46	42.07	(598.3)
13	43.66	(621.0)	30	37.86	(538.5)	47	43.02	(611.9)
14	43.27	(615.5)	31	42.23	(600.6)	48	32.35	(460.1)
15	43.82	(623.2)	32	38.18	(543.0)	49	41.21	(586.1)
16	49.49	(703.9)	33	39.36	(559.8)	50	40.25	(572.5)
17	45.25	(643.6)	34	36.74	(522.6)			

*Numbers in parentheses are (ksi).

TABLE XI

MEASUREMENTS OF BORON FIBER DIAMETER

Fiber No.	Fiber Diameter $x10^{-3}$ cm ($x10^{-3}$ in.)[a]		Fiber No.	Fiber Diameter $x10^{-3}$ cm ($x10^{-3}$ in.)[a]	
1	13.46	(5.3)	26	13.72	(5.4)
2	13.21	(5.2)	27	13.72	(5.4)
3	13.46	(5.3)	28	13.72	(5.4)
4	13.72	(5.4)	29	13.72	(5.4)
5	13.46	(5.3)	30	13.72	(5.4)
6	13.46	(5.3)	31	13.21	(5.2)
7	13.72	(5.4)	32	13.72	(5.4)
8	13.72	(5.4)	33	13.72	(5.4)
9	13.46	(5.3)	34	13.72	(5.4)
10	13.72	(5.4)	35	13.72	(5.4)
11	13.21	(5.2)	36	13.72	(5.4)
12	13.46	(5.3)	37	13.72	(5.4)
13	13.21	(5.2)	38	13.72	(5.4)
14	12.95	(5.1)	39	13.72	(5.4)
15	12.95	(5.1)	40	13.46	(5.3)
16	13.46	(5.3)	41	13.21	(5.2)
17	13.46	(5.3)	42	13.46	(5.3)
18	13.46	(5.3)	43	13.21	(5.2)
19	13.21	(5.2)	44	13.21	(5.2)
20	13.21	(5.2)	45	13.21	(5.2)
21	13.21	(5.2)	46	13.72	(5.4)
22	13.21	(5.2)	47	13.21	(5.2)
23	13.21	(5.2)	48	13.46	(5.3)
24	13.21	(5.2)	49	13.46	(5.3)
25	13.72	(5.4)	50	13.72	(5.4)

[a]Mean 13.46 x 10^{-3} cm (5.3 x 10^{-3} in.)

*Numbers in parentheses are in inches.

TABLE XII

MEANS AND STANDARD DEVIATIONS OF FAILURE LOADS OF FIBERS EXTRACTED FROM AS-RECEIVED SPECIMENS

	Matrix Material								
	6061 Aluminum			1100 Aluminum			2024 Aluminum		
Gage Length cm	5.08 (2.0)	3.81 (1.5)	2.54 (1.0)	5.08 (2.0)	3.81 (1.5)	2.54 (1.0)	5.08 (2.0)	3.81 (1.5)	2.54 (1.0)
Mean Fiber U. T. Load kg	5.35 (11.80)	5.72 (12.62)	5.76 (12.69)	3.81 (8.39)	3.86 (8.51)	4.11 (9.06)	5.67 (12.49)	5.68 (12.53)	5.85 (12.90)
Mean Fiber U.T.S. $kg/cm^2 \times 10^3$	37.65 (535.51)	40.24 (572.34)	40.46 (575.51)	26.75 (380.50)	27.13 (385.94)	28.89 (410.88)	39.83 (566.44)	39.95 (568.25)	41.13 (585.03)
Standard Deviation kg	0.62 (1.37)	0.71 (1.57)	0.59 (1.31)	0.55 (1.21)	0.57 (1.25)	0.43 (0.95)	0.58 (1.27)	0.46 (1.01)	0.67 (1.48)
$kg/cm^2 \times 10^3$	4.37 (62.13)	5.01 (71.20)	4.18 (59.41)	3.86 (54.88)	3.99 (56.69)	3.03 (43.08)	4.05 (57.60)	3.22 (45.80)	4.72 (67.12)

*Numbers in parentheses are English units.

TABLE XIII

MEANS AND STANDARD DEVIATIONS OF FAILURE LOADS OF FIBERS EXTRACTED FROM AS-RECEIVED SPECIMENS AFTER DATA REJECTION (CHAUVENT'S CRITERION)

	Matrix Material								
	6061 Aluminum			1100 Aluminum			2024 Aluminum		
Gage Length cm	5.08 (2.0)	3.81 (1.5)	2.54 (1.0)	5.08 (2.0)	3.81 (1.5)	2.54 (1.0)	5.08 (2.0)	3.81 (1.5)	2.54 (1.0)
Mean Fiber U. T. Load kg	5.39 (11.88)	5.86 (12.91)	5.81 (12.80)	3.81 (8.39)	3.90 (8.60)	4.14 (9.12)	5.71 (12.58)	5.68 (12.53)	5.90 (13.01)
Mean Fiber U. T. S. $kg/cm^2 \times 10^3$	37.86 (538.49)	41.14 (585.17)	40.79 (580.19)	26.77 (380.29)	27.41 (389.81)	29.06 (413.38)	40.09 (570.21)	39.93 (567.95)	41.46 (589.70)
Standard Deviation									
kg	0.59 (1.29)	0.50 (1.10)	0.51 (1.13)	0.55 (1.21)	0.51 (1.12)	0.39 (0.86)	0.54 (1.19)	0.46 (1.01)	0.59 (1.29)
$kg/cm^2 \times 10^3$	4.11 (58.47)	3.51 (49.86)	3.60 (51.22)	3.86 (54.85)	3.57 (50.77)	2.74 (38.98)	3.79 (53.94)	3.22 (45.78)	4.11 (58.47)
Number of Readings Rejected	1	3	1	0	1	1	1	0	1

*Numbers in parentheses are English Units.

TABLE XIV

FREQUENCY DATA FOR FIBERS EXTRACTED FROM AN AS-RECEIVED 6061 AL-B SPECIMEN: GAGE LENGTH 5.08 cm (2 inches)

Stress Interval $kg/cm^2 \times 10^3$	Interval Midpoint, $\sigma(kg/cm^2) \times 10^3$	$\ln(\sigma)$	Frequency	Cumulative Frequency	Cumulative Relative Frequency, $G(\sigma)$	$\ln \ln[\frac{1}{1-G(\sigma)}]$
26.72 - 29.53 (380-420)	28.12 (400)	10.24 (12.90)	2	2	0.040	-3.20
29.53 - 32.34 (420-460)	30.94 (440)	10.33 (12.99)	4	6	0.120	-2.06
32.34 - 35.15 (460-500)	33.75 (480)	10.42 (13.08)	6	12	0.240	-1.29
35.15 - 37.97 (500-540)	36.56 (520)	10.50 (13.16)	7	19	0.380	-0.74
37.97 - 40.78 (540-580)	39.37 (560)	10.58 (13.24)	16	35	0.720	-0.24
40.78 - 43.59 (580-620)	42.18 (600)	10.64 (13.30)	13	48	0.960	-1.17
43.59 - 46.40 (620-660)	45.00 (640)	10.71 (13.37)	1	49	0.980	-1.36

*Numbers in parentheses are (ksi).

TABLE XV

FREQUENCY DATA FOR FIBERS EXTRACTED FROM AN AS-RECEIVED 6061 AL-B SPECIMEN: GAGE LENGTH 3.81 cm (1.5 inches)

Stress Interval $kg/cm^2 \times 10^3$	Interval Midpoint, $\sigma (kg/cm^2) \times 10^3$	$\ln(\sigma)$	Frequency	Cumulative Frequency	Cumulative Relative Frequency, $G(\sigma)$	$\ln \ln [\frac{1}{1-G(\sigma)}]$
29.53 - 32.34 (420-460)	30.94 (440)	10.33 (12.99)	1	1	0.021	-3.85
32.34 - 35.15 (460-500)	33.75 (480)	10.42 (13.08)	3	4	0.083	-2.42
35.15 - 37.97 (500-540)	36.56 (520)	10.50 (13.16)	6	10	0.208	-1.45
37.97 - 40.78 (540-580)	39.37 (560)	10.58 (13.24)	6	16	0.333	-0.90
40.78 - 43.59 (580-620)	42.18 (600)	10.64 (13.30)	19	35	0.729	0.27
43.59 - 46.40 (620-660)	45.00 (640)	10.71 (13.37)	11	46	0.958	1.15
46.40 - 49.22 (660-700)	47.81 (680)	10.77 (13.43)	1	47	0.979	1.35

*Numbers in parentheses are (ksi).

TABLE XVI

FREQUENCY DATA FOR FIBERS EXTRACTED FROM AN AS-RECEIVED 6061 AL-B SPECIMEN: GAGE LENGTH 2.54 cm (1 inch)

Stress Interval $kg/cm^2 \times 10^3$	Interval Midpoint, $\sigma(kg/cm^2) \times 10^3$	$\ln(\sigma)$	Frequency	Cumulative Frequency	Cumulative Relative Frequency, $G(\sigma)$	$\ln . \ln[\frac{1}{1-G(\sigma)}]$
32.34 - 35.15 (460-500)	33.75 (480)	10.42 (13.08)	5	5	0.100	-2.25
35.15 - 37.97 (500-540)	36.56 (520)	10.50 (13.16)	7	12	0.240	-1.29
37.97 - 40.78 (540-580)	39.37 (560)	10.58 (13.24)	6	18	0.360	-0.81
40.78 - 43.59 (580-620)	42.18 (600)	10.64 (13.30)	21	39	0.780	0.41
43.59 - 46.40 (620-660)	45.00 (640)	10.71 (13.37)	9	48	0.960	1.17
46.40 - 49.22 (660-700)	47.81 (680)	10.77 (13.43)	1	49	0.980	1.36

*Numbers in parentheses are (ksi).

TABLE XVII

FREQUENCY DATA FOR FIBERS EXTRACTED FROM AN AS-RECEIVED 1100 AL-B SPECIMEN: GAGE LENGTH 5.08 cm (2 inches)

Stress Interval $kg/cm^2 \times 10^3$	Interval Midpoint, $\sigma(kg/cm^2) \times 10^3$	$\ln(\sigma)$	Frequency	Cumulative Frequency	Cumulative Relative Frequency, $G(\sigma)$	$\ln \ln[\frac{1}{1-G(\sigma)}]$
15.47 - 18.28 (220-260)	16.87 (240)	9.73 (12.39)	1	1	0.020	-3.90
18.28 - 21.09 (260-300)	19.69 (280)	9.88 (12.54)	3	4	0.078	-2.51
21.09 - 23.90 (300-340)	22.50 (320)	10.02 (12.68)	9	13	0.255	-1.22
23.90 - 26.72 (340-380)	25.31 (360)	10.13 (12.79)	11	24	0.471	-0.45
26.72 - 29.53 (380-420)	28.12 (400)	10.24 (12.90)	14	38	0.745	0.31
29.53 - 32.34 (420-460)	30.94 (440)	10.33 (12.99)	11	49	0.961	1.18
32.34 - 35.15 (460-500)	33.75 (480)	10.42 (13.08)	1	50	0.980	1.36

*Numbers in parentheses are (ksi).

TABLE XVIII

FREQUENCY DATA FOR FIBERS EXTRACTED FROM AN AS-RECEIVED 1100 AL-B SPECIMEN: GAGE LENGTH 3.81 cm (1.5 inches)

Stress Interval $kg/cm^2 \times 10^3$	Interval Midpoint, $\sigma(kg/cm^2) \times 10^3$	$\ln(\sigma)$	Frequency	Cumulative Frequency	Cumulative Relative Frequency, $G(\sigma)$	$\ln \ln[\frac{1}{1-G(\sigma)}]$
15.47 - 18.28 (220-260)	16.87 (240)	9.73 (12.39)	1	1	0.020	-3.90
18.28 - 21.09 (260-300)	19.69 (280)	9.88 (12.54)	2	3	0.060	-2.78
21.09 - 23.90 (300-340)	22.50 (320)	10.02 (12.68)	7	10	0.200	-1.50
23.90 - 26.72 (340-380)	25.31 (360)	10.13 (12.79)	9	19	0.380	-0.74
26.72 - 29.53 (380-420)	28.12 (400)	10.24 (12.90)	15	34	0.680	0.13
29.53 - 32.34 (420-460)	30.94 (440)	10.33 (12.99)	12	46	0.920	0.93
32.34 - 35.15 (460-500)	33.75 (480)	10.42 (13.08)	3	49	0.980	1.36

*Numbers in parentheses are (ksi).

TABLE XIX

FREQUENCY DATA FOR FIBERS EXTRACTED FROM AN AS-RECEIVED 1100 AL-B SPECIMEN: GAGE LENGTH 2.54 cm (1 inch)

Stress Interval $kg/cm^2 \times 10^3$	Interval Midpoint, $\sigma(kg/cm^2) \times 10^3$	$\ln(\sigma)$	Frequency	Cumulative Frequency	Cumulative Relative Frequency, $G(\sigma)$	$\ln \ln[\frac{1}{1-G(\sigma)}]$
21.09 - 23.90 (300-340)	22.50 (320)	10.02 (12.68)	2	2	0.04	-3.20
23.90 - 26.72 (340-380)	25.31 (360)	10.13 (12.79)	9	11	0.22	-1.39
26.72 - 29.53 (380-420)	28.12 (400)	10.24 (12.90)	12	23	0.46	-0.48
29.53 - 32.34 (420-460)	30.94 (440)	10.33 (12.99)	23	46	0.92	0.93
32.34 - 35.15 (460-500)	33.75 (480)	10.42 (13.08)	3	49	0.98	1.36

*Numbers in parentheses are (ksi).

TABLE XX

FREQUENCY DATA FOR FIBERS EXTRACTED FROM AN AS-RECEIVED 2024 AL-B SPECIMEN: GAGE LENGTH 5.08 cm (2 inches)

Stress Interval $kg/cm^2 \times 10^3$	Interval Midpoint, $\sigma(kg/cm^2) \times 10^3$	$\ln(\sigma)$	Frequency	Cumulative Frequency	Cumulative Relative Frequency, $G(\sigma)$	$\ln \ln[\frac{1}{1-G(\sigma)}]$
29.53 - 32.34 (420-460)	30.94 (440)	10.33 (12.99)	1	1	0.020	-3.90
32.34 - 35.15 (460-500)	33.75 (480)	10.42 (13.08)	6	7	0.140	-1.90
35.15 - 37.97 (500-540)	36.56 (520)	10.50 (13.16)	6	13	0.260	-1.20
37.97 - 40.78 (540-580)	39.37 (560)	10.58 (13.24)	10	23	0.460	-0.48
40.78 - 43.59 (580-620)	42.18 (600)	10.64 (13.30)	19	42	0.840	0.61
43.59 - 46.40 (620-660)	45.00 (640)	10.71 (13.37)	7	49	0.980	1.36

*Numbers in parentheses are (ksi).

TABLE XXI

FREQUENCY DATA FOR FIBERS EXTRACTED FROM AN AS-RECEIVED 2024 AL-B SPECIMEN: GAGE LENGTH 3.81 cm (1.5 inches)

Stress Interval $kg/cm^2 \times 10^3$	Interval Midpoint, $\sigma(kg/cm^2) \times 10^3$	$\ln(\sigma)$	Frequency	Cumulative Frequency	Cumulative Relative Frequency, $G(\sigma)$	$\ln \ln[\frac{1}{1-G(\sigma)}]$
39.53 - 32.34 (420-460)	30.94 (440)	10.33 (12.99)	3	3	0.059	-2.80
32.34 - 35.15 (460-500)	33.75 (480)	10.42 (13.08)	6	9	0.176	-1.64
35.15 - 37.97 (500-540)	36.56 (520)	10.50 (13.16)	6	15	0.294	-1.05
37.97 - 40.78 (540-580)	39.37 (560)	10.58 (13.24)	10	25	0.490	-0.40
40.78 - 43.59 (580-620)	42.18 (600)	10.64 (13.30)	16	41	0.804	0.49
43.59 - 46.40 (620-660)	45.00 (640)	10.71 (13.37)	9	50	0.980	1.36

*Numbers in parentheses are (ksi).

TABLE XXII

FREQUENCY DATA FOR FIBERS EXTRACTED FROM AN AS-RECEIVED 2024 AL-B SPECIMEN: GAGE LENGTH 2.54 cm (1 inch)

Stress Interval $kg/cm^2 \times 10^3$	Interval Midpoint, $\sigma(kg/cm^2) \times 10^3$	$\ln(\sigma)$	Frequency	Cumulative Frequency	Cumulative Relative Frequency, $G(\sigma)$	$\ln \ln[\frac{1}{1-G(\sigma)}]$
29.53 - 32.34 (420-460)	30.94 (440)	10.33 (12.99)	1	1	0.020	-3.90
32.34 - 35.15 (460-500)	33.75 (480)	10.42 (13.08)	4	5	0.100	-2.25
35.15 - 37.97 (500-540)	36.56 (520)	10.50 (13.16)	4	9	0.180	-1.62
37.97 - 40.78 (540-580)	39.37 (560)	10.58 (13.24)	11	20	0.400	-0.67
40.78 - 43.59 (580-620)	42.18 (600)	10.64 (13.30)	11	31	0.620	-0.03
43.59 - 46.40 (620-660)	45.00 (640)	10.71 (13.37)	13	44	0.880	0.75
46.40 - 49.22 (660-700)	47.81 (680)	10.77 (13.43)	4	48	0.960	1.17
49.22 - 52.03 (700-740)	50.62 (720)	10.83 (13.49)	1	49	0.980	1.36

*Numbers in parentheses are (ksi).

TABLE XXIII

PARAMETERS OBTAINED FROM CUMULATIVE RELATIVE FREQUENCY PLOTS FOR FIBERS EXTRACTED FROM AS RECEIVED SPECIMENS AND COMPUTED VALUES OF BUNDLE EFFICIENCY, BUNDLE STRENGTH, AND MEAN FIBER STRENGTH USING THESE PARAMETERS

	Matrix Material								
	6061 Aluminum			1100 Aluminum			2024 Aluminum		
Gauge Length (cm)	5.08	3.81	2.54	5.08	3.81	2.54	5.08	3.81	2.54
ω	9.93	12.14	10.94	7.76	7.76	11.35	13.23	10.60	10.59
σ_o kg/cm^2 x 10^3	70.06 (996.48)*	66.48 (945.54)	66.77 (949.74)	57.78 (821.77)	57.56 (818.73)	46.39 (659.81)	63.22 (899.17)	68.34 (971.99)	70.22 (998.80)
$\sigma_o(\omega e)^{-1/\omega}$ kg/cm^2 x 10^3	50.27 (715.03)	49.84 (708.94)	48.97 (696.56)	39.38 (560.18)	36.75 (522.67)	34.29 (487.77)	48.08 (685.88)	49.77 (707.94)	51.13 (727.19)
$\bar{\sigma}$ (calc.) kg/cm^2 x 10^3	38.41 (546.35)	41.75 (593.77)	41.56 (591.14)	26.96 (383.51)	27.60 (392.54)	29.21 (415.44)	40.51 (576.20)	40.04 (569.45)	42.69 (607.20)
$\bar{\sigma}$ from data kg/cm^2 x 10^3	37.86 (538.49)	41.14 (585.17)	40.79 (580.19)	26.74 (380.29)	27.41 (389.81)	29.06 (413.38)	40.09 (570.21)	39.93 (567.95)	41.46 (589.70)
σ_B kg/cm^2 x 10^3	27.66 (393.37)	31.31 (445.33)	30.34 (431.53)	18.34 (260.79)	18.77 (266.93)	21.61 (307.43)	30.79 (437.91)	29.23 (415.70)	31.16 (443.26)
ϵ	0.72	0.75	0.73	0.68	0.68	0.74	0.76	0.73	0.72

$$\bar{\sigma}\ (\text{calc}) = \sigma_o\ (L/d)^{-1/\omega}\ \Gamma\left(1 + \frac{1}{\omega}\right) \qquad \sigma_B = \sigma_o\left(\frac{L}{d}\ \omega\, e\right)^{-1/\omega},\ \epsilon = \sigma_B / \bar{\sigma}$$

*Numbers in parentheses are (ksi).

TABLE XXIV

VARIATION IN DENSITY WITH THERMAL CYCLING
50 v/o B-6061 ALUMINUM SPECIMEN
(FIBER DIAMETER 10.16×10^{-3} cm)
(4×10^{-3} inch)

Specimen	Number of Cycles	Density ($gm.cm^{-3}$)
1	0	2.65
	2650	2.65
	4120	2.62
	6000	2.60
2	0	2.65
	2650	2.64
3	0	2.67
	2650	2.68
	4120	2.67

TABLE XXV

PROPERTIES OF BORON REINFORCED 1100 ALUMINUM SUBJECTED TO 6000 THERMAL CYCLES.

	As Rec.	RT-315 °C	RT-365 °C	RT-425 °C	425 °C. for 9 hrs.
σ_1 (kg/cm^2) $\times 10^3$	10.15 (144.3)*	11.79 (167.70)	11.74 (167.00)	9.90 (140.74)	11.25 (160)
	10.90 (155.0)	12.17 (173.14)	9.98 (142.00)	8.63 (122.70)	11.39 (162)
E_{11} (kg/cm^2) $\times 10^6$	2.004 (28.50)*	2.227 (31.67)	2.348 (33.4)	2.018(28.7)	1.821 (25.9)
				1.786(25.4)	1.905 (27.1)
ν_{12}	0.27	0.25	0.24	-	-
σ_2 (kg/cm^2) $\times 10^3$	569.5 (8.10)	365.6 (5.2)		256.6 (3.65)	
	489.3 (6.96)	492.2 (7.0)	-	263.7 (3.75)	-
E_{21} (kg/cm^2) $\times 10^6$	1.174 (16.7)	-	-	1.169 (16.63)	
				1.465 (20.83)	-
ν_{21}	-	-	-	0.20	-
τ_{12} (kg/cm^2) $\times 10^3$	600.4 (8.54)	534.3 (7.6)		322.0 (4.58)	
		428.2 (6.09)	553.3 (7.87)	456.3 (6.49)	-

**Numbers in parentheses are English Units.

*Contained 39 v/o reinforcement

TABLE XXVI

PROPERTIES OF BORON REINFORCED 6061 ALUMINUM ALLOY SUBJECTED TO 6000 THERMAL CYCLES.

	As Rec.	RT-315 °C	RT-365 °C	RT-425 °C.	425 °C. for 9 hrs.
σ_1 (kg/cm^2) x 10^3	14.58 (207.31) 17.30 (246.00)	14.99 (213.2)	20.25 (288.00) 12.41 (176.47) 9.91 (141.0)	11.70 (166.36) 7.93 (112.6) 2.81 (40.0) 11.18 (158.98)	11.74 (167.0) -
E_{11} (kg/cm^2) x 10^6	2.334 (33.2)	2.275 (32.36)	2.461 (35.0) 2.250 (32.0)	2.306 (32.8) 2.812 (40.0)	2.883 (41.0)
ν_{12}	0.22	-	0.24	0.29	-
σ_2 (kg/cm^2) x 10^3	1501.8 (21.36) 1314.1 (18.69)	-	1745.7 (24.83) 88.24 (12.55)	864.8 (12.3) 900.0 (12.8)	1012.4 (14.4)
E_{22} (kg/cm^2) x 10^6	1.169 (16.63) 0.963 (13.70)	-	1.476 (21.0) 1.139 (16.21)	1.174 (16.7) 1.034 (14.7)	-
ν_{21}	0.13	-	0.21	-	-
τ_{12} (kg/cm^2) x 10^3	1006.8 (14.32)	-	1183.3 (16.83) 926.7 (13.18) 563.9 (8.02)	755.8 (10.75)	-

*Numbers in parentheses are English Units.

TABLE XXVII

PROPERTIES OF BORON REINFORCED 2024 ALUMINUM ALLOY SUBJECTED TO 6000 THERMAL CYCLES.

	AS Rec.	RT-315 °C.	RT-365 °C.	RT-425 °C.	425 °C. for 9 hrs.
σ_1 (kg/cm^2) x 10^3	15.55 (221.1)	17.23 (245) 16.17 (230)	12.37 (176.00)* 16.24 (230.96)* 4.27 (60.80)** 6.10 (86.80)**	0.586 (8.33) 1.88 (26.68) 2.38 (33.9)	12.02 (171.0) 11.82 (168.1)
E_{11} (kg/cm^2) x 10^6	2.250 (32.0)	2.461 (35.0) 2.348 (33.4)	2.468 (35.1) 2.545 (36.2)	0.603 (8.52) 1.292 (18.37)	2.222 (31.6) 2.433 (34.6)
ν_{12}	0.22	-	0.33	-	0.27
σ_2 (kg/cm^2) x 10^3	774.8 (11.02) 1553.8 (22.1)	-	29.81 (4.24) 970.2 (13.8)	452.8 (6.44) 579.3 (8.24) 424.0 (6.03)	-
E_{22} (kg/cm^2) x 10^6	7.603 (22.8)	-	1.153 (16.4)	0.725 (10.31) 0.521 (7.41)	-
ν_{21}	0.15	-	-	0.10	-
τ_{12} (kg/cm^2) x 10^3	1420.2 (20.20)	-	1138.3 (16.19) 1142.5 (16.25) 1371.7 (19.51)	187.7 (2.67) 2029.8 (28.87)	-

*Surface Not Broken
**Surface Broken

***Numbers in parentheses are English Units.

TABLE XXVIII

FAILURE STRESSES OF BORON FIBERS EXTRACTED FROM THERMALLY CYCLED 6061 ALUMINUM: GAGE LENGTH 5.08 cm (2 inches)

Fiber No.	Failure Stress $kg/cm^2 \times 10^3$	Fiber No.	Failure Stress $kg/cm^2 \times 10^3$	Fiber No.	Failure Stress $kg/cm^2 \times 10^3$
1	34.35 (488.6)	18	22.79 (324.1)	35	26.29 (373.9)
2	39.77 (565.7)	19	40.73 (579.3)	36	27.67 (393.6)
3	39.04 (555.3)	20	20.56 (292.4)	37	32.60 (463.7)
4	38.87 (552.9)	21	27.18 (386.6)	38	31.55 (448.7)
5	36.81 (523.5)	22	31.96 (454.6)	39	28.20 (401.1)
6	36.43 (518.1)	23	19.85 (282.4)	40	41.27 (587.0)
7	44.76 (636.7)	24	19.92 (283.3)	41	37.45 (532.6)
8	38.34 (545.3)	25	39.84 (566.6)	42	40.79 (580.2)
9	41.36 (588.3)	26	21.83 (310.5)	43	41.75 (593.8)
10	24.22 (344.5)	27	37.54 (534.0)	44	26.61 (378.5)
11	41.36 (588.3)	28	25.66 (364.9)	45	41.05 (583.8)
12	36.65 (521.3)	29	29.09 (413.8)	46	33.46 (475.9)
13	24.06 (342.3)	30	22.15 (315.0)	47	38.34 (454.3)
14	39.84 (566.6)	31	42.38 (602.8)	48	29.48 (419.3)
15	32.50 (462.3)	32	33.56 (477.3)	49	25.59 (364.0
16	31.87 (453.3)	33	43.98 (625.5)	50	40.95 (582.5)
17	21.83 (310.5)	34	40.48 (575.7)		

*Numbers in parentheses are (ksi).

TABLE XXIX

FAILURE STRESSES OF BORON FIBERS EXTRACTED FROM THERMALLY CYCLED 6061 ALUMINUM: GAGE LENGTH 3.81 cm (1.5 inches)

Fiber No.	Failure Stress $kg/cm^2 \times 10^3$	Fiber No.	Failure Stress $kg/cm^2 \times 10^3$	Fiber No.	Failure Stress $kg/cm^2 \times 10^3$
1	19.60 (278.8)	18	30.85 (438.8)	35	34.20 (486.4)
2	43.44 (617.8)	19	36.26 (515.8)	36	40.63 (577.9)
3	41.05 (583.8)	20	41.69 (592.9)	37	44.23 (629.1)
4	38.18 (543.0)	21	43.02 (611.9)	38	38.88 (553.0)
5	41.43 (589.3)	22	43.34 (616.4)	39	20.71 (294.6)
6	24.64 (350.4)	23	37.70 (536.2)	40	39.77 (565.7)
7	33.94 (482.7)	24	34.26 (487.3)	41	21.45 (305.1)
8	37.86 (538.5)	25	39.04 (555.3)	42	40.48 (575.7)
9	34.51 (490.9)	26	34.99 (497.7)	43	40.48 (575.7)
10	30.21 (429.7)	27	40.48 (575.7)	44	35.37 (503.1)
11	38.09 (541.7)	28	41.21 (586.1)	45	43.65 (620.9)
12	34.68 (493.2)	29	36.74 (522.6)	46	24.70 (351.3)
13	27.09 (385.3)	30	27.50 (391.2)	47	35.85 (509.9)
14	34.74 (494.1)	31	40.31 (573.4)	48	27.09 (385.3)
15	31.87 (453.3)	32	37.28 (530.3)	49	38.34 (545.3)
16	38.97 (554.3)	33	43.44 (617.8)	50	38.56 (548.5)
17	39.45 (561.1)	34	26.70 (379.8)		

*Numbers in parentheses are (ksi).

TABLE XXX

FAILURE STRESSES OF BORON FIBERS EXTRACTED FROM THERMALLY CYCLED 6061 ALUMINUM: GAGE LENGTH 2.54 cm (1 inch)

Fiber No.	Failure Stress $kg/cm^2 \times 10^3$	Fiber No.	Failure Stress $kg/cm^2 \times 10^3$	Fiber No.	Failure Stress $kg/cm^2 \times 10^3$
1	40.00 (568.9)	18	41.43 (589.3)	35	33.72 (479.6)
2	37.45 (532.6)	19	33.56 (477.3)	36	43.44 (617.8)
3	42.19 (600.0)	20	41.05 (583.8)	37	29.96 (426.1)
4	38.34 (545.3)	21	30.91 (439.7)	38	37.07 (527.2)
5	37.76 (537.1)	22	43.20 (641.4)	39	37.63 (535.2)
6	31.07 (441.9)	23	27.88 (396.6)	40	41.84 (595.1)
7	39.84 (566.6)	24	43.44 (617.8)	41	42.23 (600.6)
8	20.27 (288.3)	25	40.73 (579.3)	42	28.62 (407.0)
9	30.69 (436.5)	26	41.59 (591.5)	43	20.40 (290.1)
10	38.24 (543.9)	27	36.01 (512.2)	44	44.23 (629.1)
11	38.18 (543.0)	28	28.78 (409.3)	45	43.44 (617.8)
12	41.69 (592.9)	29	24.00 (341.3)	46	42.23 (600.6)
13	34.35 (488.6)	30	25.49 (362.6)	47	41.59 (591.5)
14	39.84 (566.6)	31	34.89 (496.3)	48	42.86 (609.6)
15	38.49 (547.5)	32	38.07 (541.5)	49	28.30 (402.5)
16	36.74 (522.6)	33	41.52 (590.6)	50	40.00 (568.9)
17	40.79 (580.2)	34	42.07 (598.3)		

*Numbers in parentheses are (ksi).

TABLE XXXI

FAILURE STRESSES OF BORON FIBERS EXTRACTED FROM THERMALLY CYCLED 1100 ALUMINUM: GAGE LENGTH 5.08 cm (2 inches)

Fiber No.	Failure Stress $kg/cm^2 \times 10^3$	Fiber No.	Failure Stress $kg/cm^2 \times 10^3$	Fiber No.	Failure Stress $kg/cm^2 \times 10^3$
1	21.67 (308.2)	18	29.57 (420.6)	35	25.49 (362.6)
2	27.38 (389.4)	19	25.33 (360.3)	36	30.69 (436.5)
3	33.66 (464.6)	20	28.81 (409.8)	37	27.09 (385.3)
4	30.85 (438.8)	21	30.27 (430.6)	38	27.50 (391.1)
5	27.72 (394.3)	22	28.20 (401.1)	39	25.58 (363.9)
6	25.97 (369.4)	23	31.39 (446.5)	40	30.44 (432.9)
7	28.05 (398.9)	24	27.82 (395.7)	41	28.94 (411.6)
8	29.00 (412.5)	25	27.09 (385.3)	42	23.26 (330.9)
9	26.55 (377.6)	26	30.27 (430.6)	43	24.86 (353.6)
10	29.00 (412.5)	27	28.94 (411.6)	44	30.91 (439.7)
11	24.06 (342.2)	28	25.18 (358.1)	45	28.62 (407.0)
12	19.28 (274.2)	29	27.18 (386.6)	46	30.91 (439.7)
13	22.56 (320.9)	30	33.46 (475.9)	47	31.87 (453.3)
14	29.96 (426.1)	31	27.57 (392.1)	48	28.78 (409.3)
15	26.93 (383.0)	32	32.50 (462.3)	49	19.12 (271.9)
16	26.13 (371.7)	33	23.10 (328.6)	50	31.87 (453.3)
17	31.17 (443.3)	34	30.27 (430.6)		

*Numbers in parentheses are (ksi).

TABLE XXXII

FAILURE STRESSES OF BORON FIBERS EXTRACTED FROM THERMALLY CYCLED 1100 ALUMINUM: GAGE LENGTH 3.81 cm (1.5 inches)

Fiber No.	Failure Stress $kg/cm^2 \times 10^3$	Fiber No.	Failure Stress $kg/cm^2 \times 10^3$	Fiber No.	Failure Stress $kg/cm^2 \times 10^3$
1	27.50 (391.2)	18	27.82 (395.7)	35	29.73 (422.9)
2	29.09 (413.8)	19	30.27 (430.6)	36	26.22 (373.0)
3	37.76 (537.1)	20	33.30 (473.7)	37	30.37 (431.9)
4	32.60 (463.7)	21	26.93 (383.0)	38	30.69 (436.5)
5	32.34 (460.0)	22	27.98 (398.0)	39	29.57 (420.6)
6	28.30 (402.5)	23	28.14 (400.2)	40	30.75 (437.4)
7	32.66 (464.6)	24	32.50 (462.3)	41	30.07 (441.9)
8	28.30 (402.5)	25	29.48 (419.3)	42	32.60 (463.7)
9	16.09 (228.9)	26	31.07 (441.9)	43	30.27 (430.6)
10	28.68 (407.9)	27	29.16 (414.7)	44	29.32 (417.0)
11	28.30 (402.5)	28	29.63 (421.5)	45	32.83 (466.9)
12	31.07 (441.9)	29	32.35 (460.1)	46	30.91 (439.7)
13	34.04 (484.1)	30	28.84 (410.2)	47	29.16 (414.7)
14	23.90 (340.0)	31	30.68 (436.4)	48	25.66 (364.9)
15	23.90 (340.0)	32	28.93 (411.5)	49	25.49 (362.6)
16	30.27 (430.6)	33	29.48 (419.3)	50	29.96 (426.1)
17	31.87 (453.3)	34	27.50 (391.2)		

*Numbers in parentheses are (ksi).

TABLE XXXIII

FAILURE STRESSES OF BORON FIBERS EXTRACTED FROM THERMALLY CYCLED 1100 ALUMINUM: GAGE LENGTH 2.54 cm (1 inch)

Fiber No.	Failure Stress $kg/cm^2 \times 10^3$	Fiber No.	Failure Stress $kg/cm^2 \times 10^3$	Fiber No.	Failure Stress $kg/cm^2 \times 10^3$
1	33.08 (470.5)	18	30.69 (436.5)	35	26.70 (379.8)
2	33.08 (470.5)	19	27.88 (396.6)	36	28.30 (402.5)
3	37.54 (534.0)	20	32.29 (459.2)	37	34.99 (497.7)
4	27.88 (396.6)	21	34.99 (497.7)	38	32.19 (457.8)
5	27.88 (396.6)	22	31.07 (441.9)	39	30.69 (436.5)
6	23.26 (330.9)	23	31.87 (453.3)	40	32.76 (465.9)
7	28.30 (402.5)	24	33.87 (481.8)	41	28.84 (410.2)
8	29.26 (416.1)	25	27.57 (392.1)	42	31.01 (441.0)
9	27.03 (384.4)	26	27.88 (396.6)	43	29.48 (419.3)
10	33.30 (473.7)	27	30.37 (432.0)	44	31.23 (444.2)
11	29.48 (419.3)	28	33.14 (471.4)	45	32.35 (460.1)
12	30.91 (439.7)	29	33.14 (471.4)	46	32.66 (464.6)
13	31.96 (454.6)	30	28.52 (405.7)	47	26.70 (379.8)
14	20.80 (295.9)	31	28.52 (405.7)	48	29.96 (426.1)
15	31.39 (446.5)	32	31.33 (445.6)	49	32.29 (459.2)
16	26.55 (377.6)	33	31.07 (441.9)	50	31.23 (444.2)
17	29.73 (422.9)	34	35.06 (498.6)		

*Numbers in parentheses are (ksi).

TABLE XXXIV

FAILURE STRESSES OF BORON FIBERS EXTRACTED FROM THERMALLY CYCLED 2024 ALUMINUM: GAGE LENGTH 5.08 cm (2 inches)

Fiber No.	Failure Stress $kg/cm^2 \times 10^3$	Fiber No.	Failure Stress $kg/cm^2 \times 10^3$	Fiber No.	Failure Stress $kg/cm^2 \times 10^3$
1	13.16 (187.2)	18	18.41 (261.9)	35	14.34 (203.9)
2	16.26 (231.2)	19	9.34 (132.8)	36	14.12 (200.8)
3	12.21 (173.6)	20	11.95 (169.9)	37	15.24 (216.7)
4	8.13 (115.6)	21	7.49 (106.5)	38	11.25 (160.0)
5	18.74 (266.5)	22	9.55 (135.9)	39	8.93 (127.0)
6	11.00 (156.4)	23	12.75 (181.3)	40	7.97 (113.3)
7	15.78 (224.4)	24	14.82 (210.8)	41	8.61 (122.4)
8	10.45 (148.7)	25	17.53 (249.3)	42	18.17 (258.4)
9	12.11 (172.2)	26	7.26 (103.3)	43	11.00 (156.4)
10	11.31 (160.9)	27	15.07 (214.4)	44	17.37 (247.0)
11	9.81 (139.6)	28	7.33 (104.3)	45	16.35 (232.5)
12	11.79 (167.7)	29	14.76 (209.9)	46	15.07 (214.4)
13	18.17 (258.4)	30	8.06 (114.7)	47	9.08 (129.2)
14	18.01 (256.1)	31	11.25 (160.0)	48	17.37 (247.0)
15	11.25 (160.0)	32	7.80 (111.0)	49	14.60 (207.6)
16	15.87 (225.7)	33	15.78 (224.4)	50	9.50 (135.1)
17	16.89 (240.2)	34	14.98 (213.0)		

*Numbers in parentheses are (ksi).

TABLE XXXV

FAILURE STRESSES OF BORON FIBERS EXTRACTED FROM THERMALLY CYCLED 2024 ALUMINUM: GAGE LENGTH 3.81 cm (1.5 inches)

Fiber No.	Failure Stress $kg/cm^2 \times 10^3$	Fiber No.	Failure Stress $kg/cm^2 \times 10^3$	Fiber No.	Failure Stress $kg/cm^2 \times 10^3$
1	16.03 (228.0)	18	16.57 (235.7)	35	7.42 (105.6)
2	16.89 (240.2)	19	14.43 (205.3)	36	18.32 (260.6)
3	16.89 (240.2)	20	20.56 (292.4)	37	11.57 (164.5)
4	18.01 (256.1)	21	18.26 (259.7)	38	13.00 (184.9)
5	12.11 (172.2)	22	13.54 (192.6)	39	14.34 (204.0)
6	7.26 (103.3)	23	12.37 (175.9)	40	6.53 (92.9)
7	17.53 (249.3)	24	17.37 (247.0)	41	7.11 (101.1)
8	17.63 (250.7)	25	15.78 (224.4)	42	6.53 (92.9)
9	13.70 (194.9)	26	17.69 (251.6)	43	20.33 (289.2)
10	7.90 (112.4)	27	17.53 (249.3)	44	13.64 (194.0)
11	10.74 (152.8)	28	16.89 (240.2)	45	10.36 (147.3)
12	10.52 (149.6)	29	20.71 (294.6)	46	10.67 (151.8)
13	7.11 (101.1)	30	17.21 (244.8)	47	17.15 (243.9)
14	16.03 (228.0)	31	16.35 (232.5)	48	17.63 (250.7)
15	19.06 (271.1)	32	12.85 (182.7)	49	10.29 (146.4)
16	16.73 (237.9)	33	19.76 (281.0)	50	17.63 (250.7)
17	13.96 (198.5)	34	14.76 (209.9)		

*Numbers in parentheses are (ksi).

TABLE XXXVI

FAILURE STRESSES OF BORON FIBERS EXTRACTED FROM THERMALLY CYCLED 2024 ALUMINUM: GAGE LENGTH 2.54 cm (1 inch)

Fiber No.	Failure Stress $kg/cm^2 \times 10^3$	Fiber No.	Failure Stress $kg/cm^2 \times 10^3$	Fiber No.	Failure Stress $kg/cm^2 \times 10^3$
1	22.40 (318.6)	18	16.82 (239.3)	35	15.62 (222.1)
2	7.97 (113.3)	19	14.76 (209.9)	36	11.63 (165.4)
3	12.11 (172.2)	20	9.55 (135.9)	37	18.32 (260.6)
4	15.24 (216.7)	21	16.82 (239.3)	38	7.90 (112.4)
5	17.15 (243.9)	22	18.32 (260.6)	39	18.01 (256.1)
6	16.03 (228.0)	23	17.46 (248.4)	40	15.62 (222.1)
7	20.71 (294.6)	24	12.75 (181.3)	41	11.15 (158.6)
8	14.34 (203.9)	25	16.03 (228.0)	42	15.07 (214.4)
9	14.60 (207.6)	26	9.98 (141.9)	43	17.63 (250.7)
10	16.82 (239.3)	27	18.42 (262.0)	44	15.14 (215.3)
11	14.50 (206.2)	28	14.76 (210.0)	45	20.33 (289.2)
12	9.18 (130.5)	29	18.32 (260.6)	46	11.57 (164.5)
13	17.69 (251.6)	30	25.59 (364.0)	47	10.36 (147.3)
14	10.52 (149.6)	31	18.14 (258.4)	48	17.37 (247.0)
15	13.70 (194.9)	32	18.14 (258.4)	49	18.96 (269.7)
16	16.25 (231.1)	33	14.28 (203.1)	50	21.77 (309.6)
17	14.18 (201.7)	34	8.76 (124.6)		

*Numbers in parentheses are (ksi).

TABLE XXXVII

FREQUENCY DATA FOR FIBERS EXTRACTED FROM A THERMALLY CYCLED 6061 AL-B SPECIMEN: GAGE LENGTH 5.08 cm (2 inches)

Stress Interval $kg/cm^2 \times 10^3$	Interval Midpoint, $\sigma(kg/cm^2) \times 10^3$	$\ln(\sigma)$	Frequency	Cumulative Frequency	Cumulative Relative Frequency, $G(\sigma)$	$\ln \ln[\frac{1}{1-G(\sigma)}]$
18.28 - 21.09 (260-300)	19.69 (280)	9.88 (12.54)	3	3	0.059	-2.80
21.09 - 23.90 (300-340)	22.50 (320)	10.02 (12.68)	4	7	0.137	-1.92
23.90 - 26.72 (340-380)	25.31 (360)	10.13 (12.79)	6	13	0.255	-1.22
26.72 - 29.53 (380-420)	28.12 (400)	10.24 (12.90)	4	17	0.333	-0.90
29.53 - 32.34 (420-460)	30.94 (440)	10.33 (12.99)	3	20	0.392	-0.70
32.34 - 35.15 (460-500)	33.75 (480)	10.42 (13.08)	5	25	0.490	-0.40
35.15 - 37.97 (500-540)	36.56 (520)	10.50 (13.16)	5	30	0.588	-0.12
37.97 - 40.78 (540-580)	39.37 (560)	10.58 (13.24)	9	39	0.765	0.37
40.78 - 43.59 (580-620)	42.18 (660)	10.64 (13.30)	9	48	0.941	1.04
43.59 - 46.40 (620-660)	45.00 (640)	10.71 (13.37)	2	50	0.980	1.36

*Numbers in parentheses are (ksi).

TABLE XXXVIII

FREQUENCY DATA FOR FIBERS EXTRACTED FROM A THERMALLY CYCLED 6061 AL-B SPECIMEN: GAGE LENGTH 3.81 cm (1.5 inches)

Stress Interval $kg/cm^2 \times 10^3$	Interval Midpoint, $\sigma(kg/cm^2) \times 10^3$	$\ln(\sigma)$	Frequency	Cumulative Frequency	Cumulative Relative Frequency, $G(\sigma)$	$\ln \ln[\frac{1}{1-G(\sigma)}]$
18.28 - 21.09 (260-300)	19.69 (280)	9.88 (12.54)	2	2	0.039	-3.22
21.09 - 23.90 (300-340)	22.50 (320)	10.02 (12.68)	2	4	0.078	-2.51
23.90 - 26.72 (340-380)	25.31 (360)	10.13 (12.79)	2	6	0.118	-2.07
26.72 - 29.53 (380-420)	28.12 (400)	10.24 (12.90)	4	10	0.196	-1.52
29.53 - 32.34 (420-460)	30.94 (440)	10.33 (12.99)	3	13	0.255	-1.22
32.34 - 35.15 (460-500)	33.75 (480)	10.42 (13.08)	6	19	0.373	-0.76
35.15 - 37.97 (500-540)	36.56 (520)	10.50 (13.16)	7	26	0.510	-0.34
37.97 - 40.78 (540-580)	39.37 (560)	10.58 (13.24)	14	40	0.784	0.43
40-78 - 43.59 (580-620)	42.18 (600)	10.64 (13.30)	8	48	0.941	1.04
43.59 - 46.40 (620-660)	45.00 (640)	10.71 (13.37)	2	50	0.980	1.36

*Numbers in parentheses are (ksi).

TABLE XXXIX

FREQUENCY DATA FOR FIBERS EXTRACTED FROM A THERMALLY CYCLED 6061 AL-B SPECIMEN: GAGE LENGTH 2.54 cm (1 inch)

Stress Interval $kg/cm^2 \times 10^3$	Interval Midpoint, $\sigma(kg/cm^2) \times 10^3$	$\ln(\sigma)$	Frequency	Cumulative Frequency	Cumulative Relative Frequency, $G(\sigma)$	$\ln \ln[\frac{1}{1-G(\sigma)}]$
23.90 - 26.72 (340-380)	25.31 (360)	10.13 (12.79)	2	2	0.041	-3.17
26.72 - 29.53 (380-420)	28.12 (400)	10.24 (12.90)	4	16	0.122	-2.04
29.53 - 32.34 (420-460)	30.94 (440)	10.33 (12.99)	4	10	0.204	-1.48
32.34 - 35.15 (460-500)	33.75 (480)	10.42 (13.08)	4	14	0.286	-1.09
35.15 - 37.97 (500-540)	36.56 (520)	10.50 (13.16)	7	21	0.429	-0.58
37.97 - 40.78 (540-580)	39.37 (560)	10.58 (13.24)	9	30	0.612	-0.05
40.78 - 43.59 (580-620)	42.18 (600)	10.64 (13.30)	16	46	0.939	1.03
43.59 - 46.40 (620-660)	45.00 (640)	10.71 (13.37)	2	48	0.979	1.35

*Numbers in parentheses are (ksi).

TABLE XL

FREQUENCY DATA FOR FIBERS EXTRACTED FROM A THERMALLY CYCLED 1100 AL-B SPECIMEN: GAGE LENGTH 5.08 cm (2 inches)

Stress Interval $kg/cm^2 \times 10^3$	Interval Midpoint, $\sigma (kg/cm^2) \times 10^3$	$\ln(\sigma)$	Frequency	Cumulative Frequency	Cumulative Relative Frequency, $G(\sigma)$	$\ln \ln [\frac{1}{1-G(\sigma)}]$
21.09 - 23.90 (300-340)	22.50 (320)	10.02 (12.68)	4	4	0.082	-2.46
23.90 - 26.72 (340-380)	25.31 (360)	10.13 (12.79)	9	13	0.265	-1.18
26.72 - 29.53 (380-420)	28.12 (400)	10.24 (12.90)	18	31	0.633	0.00
29.53 - 32.34 (420-460)	30.94 (440)	10.33 (12.99)	14	45	0.918	0.92
32.34 - 35.15 (460-500)	33.75 (480)	10.42 (13.08)	3	48	0.980	1.36

*Numbers in parentheses are (ksi).

TABLE XLI

FREQUENCY DATA FOR FIBERS EXTRACTED FROM A THERMALLY CYCLED 1100 AL-B SPECIMEN: GAGE LENGTH 3.81 cm (1.5 inches)

Stress Interval $kg/cm^2 \times 10^3$	Interval Midpoint, $\sigma(kg/cm^2) \times 10^3$	$\ln(\sigma)$	Frequency	Cumulative Frequency	Cumulative Relative Frequency, $G(\sigma)$	$\ln \ln[\frac{1}{1-G(\sigma)}]$
21.09 - 23.90 (300-340)	22.50 (320)	10.02 (12.68)	2	2	0.040	-3.20
23.90 - 26.72 (340-380)	25.31 (360)	10.13 (12.79)	3	5	0.100	-2.25
26.72 - 29.53 (380-420)	28.12 (400)	10.24 (12.90)	18	23	0.460	-0.48
29.53 - 32.34 (420-460)	30.94 (440)	10.33 (12.99)	16	39	0.780	0.41
32.34 - 35.15 (460-500)	33.75 (480)	10.42 (13.08)	9	48	0.960	1.17
35.15 - 37.97 (500-540)	36.56 (520)	10.50 (13.16)	1	49	0.980	1.36

*Numbers in parentheses are (ksi).

TABLE XLII

FREQUENCY DATA FOR FIBERS EXTRACTED FROM A THERMALLY CYCLED 1100 AL-B SPECIMEN; GAGE LENGTH 2.54 cm (1 inch)

Stress Interval $kg/cm^2 \times 10^3$	Interval Midpoint, $\sigma (kg/cm^2) \times 10^3$	$\ln(\sigma)$	Frequency	Cumulative Frequency	Cumulative Relative Frequency, $G(\sigma)$	$\ln \ln [\frac{1}{1-G(\sigma)}]$
21.09 - 23.90 (300-340)	22.50 (320)	10.02 (12.68)	1	1	0.020	-3.90
23.90 - 26.72 (340-380)	25.31 (360)	10.13 (12.79)	3	4	0.080	-2.48
26.72 - 29.53 (380-420)	28.12 (400)	10.24 (12.90)	14	18	0.360	-0.81
29.53 - 32.34 (420-460)	30.94 (440)	10.33 (12.99)	18	36	0.720	0.24
32.34 - 35.15 (460-500)	33.75 (480)	10.42 (13.08)	12	48	0.960	1.17
35.15 - 37.97 (500-540)	36.56 (520)	10.50 (13.16)	1	49	0.980	1.36

*Numbers in parentheses are (ksi).

TABLE XLIII

FREQUENCY DATA FOR FIBERS EXTRACTED FROM A THERMALLY CYCLED 2024 AL-B SPECIMEN: GAGE LENGTH 5.08 cm (2 inches)

Stress Interval $kg/cm^2 \times 10^3$	Interval Midpoint, $\sigma (kg/cm^2) \times 10^3$	$\ln(\sigma)$	Frequency	Cumulative Frequency	Cumulative Relative Frequency, $G(\sigma)$	$\ln \ln [\frac{1}{1-G(\sigma)}]$
7.08 - 9.84 (100-140)	8.44 (120)	9.04 (11.70)	14	14	0.275	-1.13
9.84 - 12.66 (140-180)	11.25 (160)	9.32 (11.98)	11	25	0.490	-0.40
12.66 - 15.47 (180-220)	14.06 (200)	9.54 (12.20)	11	36	0.706	0.20
15.47 - 18.28 (220-260)	16.87 (240)	9.73 (12.39)	12	48	0.941	1.04
18.28 - 21.09 (260-300)	19.69 (280)	9.88 (12.54)	2	50	0.980	1.36

*Numbers in parentheses are (ksi).

TABLE XLIV

FREQUENCY DATA FOR FIBERS EXTRACTED FROM A THERMALLY CYCLED 2024 AL-B SPECIMEN: GAGE LENGTH 3.81 cm (1.5 inches)

Stress Interval $kg/cm^2 \times 10^3$	Interval Midpoint, $\sigma(kg/cm^2) \times 10^3$	$\ln(\sigma)$	Frequency	Cumulative Frequency	Cumulative Relative Frequency, $G(\sigma)$	$\ln \ln[\frac{1}{1-G(\sigma)}]$
4.22 - 7.03 (60-100)	5.62 (80)	8.64 (11.30)	2	2	0.039	-3.22
7.03 - 9.84 (100-140)	8.44 (120)	9.04 (11.70)	5	7	0.137	-1.92
9.84 - 12.66 (140-180)	11.25 (160)	9.32 (11.98)	8	15	0.294	-1.06
12.66 - 15.47 (180-220)	14.06 (200)	9.54 (12.21)	9	24	0.471	-0.45
15.47 - 18.28 (220-260)	16.87 (240)	9.73 (12.39)	20	44	0.863	0.69
18.28 - 21.09 (260-300)	19.69 (280)	9.88 (12.54)	6	50	0.980	1.36

*Numbers in parentheses are (ksi).

TABLE XLV

FREQUENCY DATA FOR FIBERS EXTRACTED FROM A THERMALLY CYCLED 2024 AL-B SPECIMEN: GAGE LENGTH 2.54 cm (1 inch)

Stress Interval $kg/cm^2 \times 10^3$	Interval Midpoint, $\sigma(kg/cm^2) \times 10^3$	$\ln(\sigma)$	Frequency	Cumulative Frequency	Cumulative Relative Frequency, $G(\sigma)$	$\ln \ln[\frac{1}{1-G(\sigma)}]$
7.03 - 9.84 (100-140)	8.44 (120)	9.04 (11.70)	5	5	0.098	-2.27
9.84 - 12.66 (140-180)	11.25 (160)	9.32 (11.98)	7	12	0.235	-1.32
12.66 - 15.47 (180-220)	14.06 (200)	9.54 (12.21)	12	24	0.471	-0.45
15.47 - 18.28 (220-260)	16.87 (240)	9.73 (12.39)	17	41	0.804	0.49
18.28 - 21.09 (260-300)	19.69 (280)	9.88 (12.54)	6	47	0.922	0.94
21.09 - 23.90 (300-340)	22.50 (320)	10.02 (12.68)	2	49	0.961	1.18
23.90 - 26.72 (340-380)	25.31 (360)	10.13 (12.79)	1	50	0.980	1.36

*Numbers in parentheses are (ksi).

TABLE XLVI

PARAMETERS OBTAINED FROM CUMULATIVE RELATIVE FREQUENCY PLOTS FOR FIBERS EXTRACTED FROM THERMALLY CYCLED SPECIMENS AND COMPUTED VALUES OF BUNDLE EFFICIENCY, BUNDLE STRENGTH, AND MEAN FIBER STRENGTH USING THESE PARAMETERS

	6061 Aluminum			Matrix Material 1100 Aluminum			2024 Aluminum		
Gage Length cm	5.08 (2.0)	3.81 (1.5)	2.54 (1.0)	5.08 (2.0)	3.81 (1.5)	2.54 (1.0)	5.08 (2.0)	3.81 (1.5)	2.54 (1.0)
ω	4.58	5.45	7.52	9.66	10.09	11.40	3.04	3.59	3.49
σ_o (kg/cm^2) x 10^3	128.29 (1824.72)	103.63 (1473.89)	76.69 (1090.79)	52.91 (752.51)	53.54 (761.46)	49.21 (699.89)	88.20 (1254.49)	69.55 (989.24)	71.26 (1013.60)
σ_1 (kg/cm^2) x 10^3	34.91 (496.47)	36.78 (523.08)	38.16 (542.78)	28.75 (408.92)	30.62 (435.46)	31.07 (441.96)	12.53 (178.26)	14.42 (205.06)	15.76 (224.17)
σ_1 (kg/cm^2) x 10^3 calc. from data	33.30 (473.67)	35.79 (509.02)	37.45 (532.59)	28.24 (401.60)	29.80 (423.81)	30.63 (435.59)	12.87 (183.12)	14.47	15.36
σ_3 (kg/cm^2) x 10^3	20.25 (287.95)	22.43 (319.08)	25.57 (363.66)	20.41 (290.33)	22.04 (313.53)	22.99 (327.05)	6.27 (89.13)	7.64 (108.68)	8.35 (118.81)
ϵ	0.58	0.61	0.67	0.71	0.72	0.74	0.50	0.53	0.53

Numbers in parentheses are (ksi).

TABLE XLVII

EXPERIMENTAL BUNDLE STRENGTHS OBTAINED FROM AS RECEIVED AND THERMALLY FATIGUED SPECIMENS

SPECIMEN OBTAINED FROM	FAILURE STRESS $kg/cm^2 \times 10^3$
1100 (A.R.)	15.60 (221.82)
6061 (A.R.)	16.58 (235.83)
2024 (A.R.)	21.11 (300.30)
1100 (T.C.)	18.97 (269.86)
6061 (T.C.)	15.93 (226.64)
2024 (T.C.)	7.46 (106.05)

A.R. = As-Received

T.C. = Thermally Cycled (6000 X, RT - 425°C)

*Numbers in parentheses are (ksi).

TABLE XLVIII

OBSERVED NUMBER OF BROKEN FIBERS BEFORE BUNDLE FAILURE

Bundle Type	Number of Fiber Breaks Prior to Failure
A	3
B	18
C	19

TABLE LXIX

THE LOWER STRENGTH BOUNDS OF COMPOSITES COMPUTED FROM THE EXPERIMENTAL OR THEORETICAL BUNDLE STRENGTH VALUES.

Bundles Prepared from:	Bundle Strength $kg/cm^2 \times 10^3$	Theoretical Bundle Strength $kg/cm^2 \times 10^3$	Lower Strength Bound for (0.44) Composite (0.44) $kg/cm^2 \times 10^3$	$kg/cm^2 \times 10^3$
1100 A.R.	15.60 (221.82)	17.91 (254.80)	6.85 (97.5)	8.00 (113.8)
6061 A.R.	16.58 (235.83)	28.09 (399.53)	7.52 (107.0)	12.50 (177.8)
2024 A.R.	21.11 (300.30)	26.95 (383.31)	9.33 (9.33)	11.81 (168.0)
1100 T.F.	18.97 (269.86)	19.93 (283.47)	8.31 (118.2)	8.85 (125.9)
6061 T.F.	15.93 (226.64)	19.33 (274.98)	7.00 (99.5)	8.79 (125.0)
2024 T.F.	7.46 (106.05)	6.02 (85.61)	3.28 (46.6)	2.65 (37.7)

A.R. = As-Received

T.F. = Thermally Fatigued (6000 X, RT-425°C)

*Numbers in parentheses are (ksi).

TABLE L

VALUES OF INEFFECTIVE LENGTHS, δ, CALCULATED FOR AS-RECEIVED AND THERMALLY CYCLED SPECIMENS.

SPECIMEN	MATRIX SHEAR STRENGTH $kg/cm^2 \times 10^3$	δ cm
Reinforced 1100 A.R.	555.4 (7.90)	0.320 (0.126)
Reinforced 6061 A.R.	1005.4 (14.30)	0.254 (0.100)
Reinforced 2024 A.R.	1420.2 (20.20)	0.188 (0.074)
Thermally Cycled 1100 T.F.	351.5 (5.0)	0.681 (0.268)
Thermally Cycled 6061 T.F.	689. (9.8)	0.351 (0.138)
Thermally Cycled 2024 T.F.	182.8 (2.6)	0.828 (0.326)

A.R. = As-Received

T.F. = Thermally Fatigued (6000 X, RT-425°C)

*Numbers in parentheses are (ksi) and (inches).

TABLE LI

UPPER STRENGTH BOUNDS CALCULATED FOR AS-RECEIVED AND THERMALLY CYCLED SPECIMENS, (6000X, RT-425°C)

Specimen	Upper Strength $kg/cm^2 \times 10^3$	Lower Strength Bound from Table XLIX $kg/cm^2 \times 10^3$	Actual Strengths $kg/cm^2 \times 10^3$				
1100 A.R.	12.57 (178.77)	6.85 (97.5)	10.30 (144.30)	10.90 (155.00)			
6061 A.R.	18.18 (258.54)	7.52 (107.0)	14.58 (207.32)	17.30 (246.00)			
2024 A.R.	18.98 (269.97)	9.33 (132.7)	15.55 (221.20)				
1100 T.F.	16.90 (240.34)	8.31 (118.2)	9.90 (140.74)	8.63 (122.70)			
6061 T.F.	17.21 (244.79)	7.00 (99.5)	11.70 (166.36)	7.92 (112.6)	5.61 (79.8)	10.83 (153.98)	
2024 T.F.	10.21 (145.15)	3.28 (46.6)	0.59 (8.33)	1.88 (26.68)	2.38 (33.9)		

A.R. = As-Received

T.F. = Thermally Fatigued

*Numbers in parentheses are (ksi).

TABLE LII

NUMBER OF BROKEN FIBERS EXPECTED IMMEDIATELY PRIOR TO FAILURE OF A BUNDLE OF 7.62 cm (3 inch) LONG FIBERS EXTRACTED FROM AS-RECEIVED OR THERMALLY FATIGUED SPECIMENS.

BUNDLE PREPARED FROM REINFORCED ALLOYS	NUMBER OF SINGLE BREAKS $E_1 = MNG(\sigma)$ As-Received Material		NUMBER OF SINGLE BREAKS $E_1 = MNG(\sigma)$ Thermally Cycled Material (6000X, RT-425°C)	
	Theoretical	Experimental	Theoretical	Experimental
6061	14.6292	0.022896	17.228	5.85
1100	9.1678	5.8928	11.55	6.96686
2024	11.025	0.6789	34.14	78.85

TABLE LIII

EXTRACTED NUMBER OF BROKEN FIBERS IN AS-RECEIVED BORON REINFORCED ALUMINUM ALLOYS IMMEDIATELY PRIOR TO FAILURE: GAUGE LENGTH OF SPECIMEN = 7.62 cm (3 inches).

ALLOY	NUMBER OF SINGLE FIBER BREAKS PER SPECIMEN (E_1)	NUMBER OF DOUBLE FIBER BREAKS PER SPECIMEN (E_2)	NUMBER OF TRIPLE FIBER BREAKS PER SPECIMEN(E_3)	δ, CM
6061	227.0866	44.668161	20.75026	0.226 (0.08895)
1100	173.5237	22.6576	8.147978	0.271 (0.106805)
2024	144.56934	13.97566	3.518109	0.157 (0.0617135)

*Numbers in parentheses are English Units.

TABLE LIV

ESTIMATED NUMBER OF BROKEN FIBERS IN THERMALLY CYCLED BORON REINFORCED ALUMINUM ALLOYS; GAUGE LENGTH OF SPECIMEN = 7.62 cm (3 inches).

ALLOY	NUMBER OF SINGLE FIBER BREAKS PER SPECIMEN, E_1	NUMBER OF DOUBLE FIBER BREAKS PER SPECIMEN, E_2	NUMBER OF TRIPLE FIBER BREAKS PER SPECIMEN, E_3	δ CM
6061	43.8856	0.5680	0.03050049	0.204 (0.0802463
1100	41.3003013	2.531060	0.43363554	0.403 (0.1587032)
2024	35.0170979	0.14809676	0.00421921	0.167 (0.06568)

*Numbers in parentheses are English Units.

APPENDIX I

The shear stress distribution between the machined slots of a double shear specimen fabricated from an orthotropic but homogeneous solid was obtained using a modified definite element analysis technique. The original computer program was written by E. L. Wilson, University of California. Mr. F. Hatt of the Virginia Polytechnical Institute supplied us with the sample data program.

Figure 55-57 illustrates the shear stress distribution computed for interslot distances of 0.254 cm (1.0 inch), 1.27 cm (1.5 inches), and 5.08 cm (2 inches), respectively. In each case, the load applied to each specimen was sufficient to generate a shear stress of 1406.2 kg/cm^2 (20,000 psi) calculated using the simple expression:

$$\tau = \frac{P}{2t \times d}$$

where, P is the load applied, t is the thickness of the specimen and d is the distance between the slots.

It can be seen from the figures that the actual stress distribution varies significantly along a direction connecting the slot tips. More significant, perhaps, is the realization that the mean shear stress, obtained by graphical integration, is 1561 kg/cm^2 (22.2 ksi), 1420 kg/cm^2 (20.2 ksi), and 1336 kg/cm^2 (19 ksi) for interslot distances of 0.254 cm (1.0 inch), 1.27 cm (1.5 inches), and 5.08 cm (2 inches), respectively. Apparent

differences in shear strength of about 10% may occur if the results obtained using the three specimens geometries are compared. This specimen geometry effect was considered small for the specimens reported here; therefore, it was neglected.

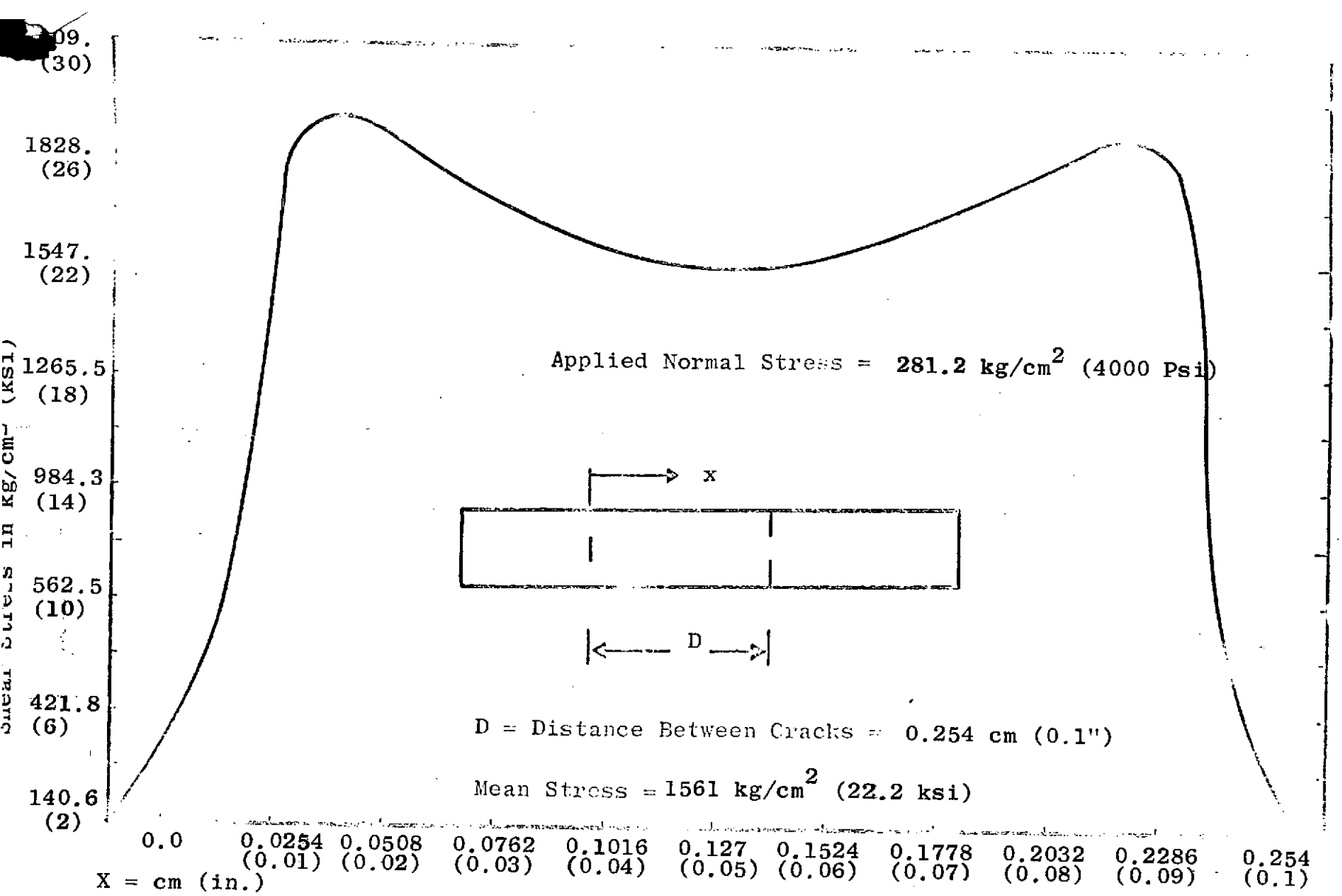

Fi[illegible] 55. Shear Stress Distribution in Double Slotted Specimen Distance Between Slots: 0.254 cm (0.1 inches)

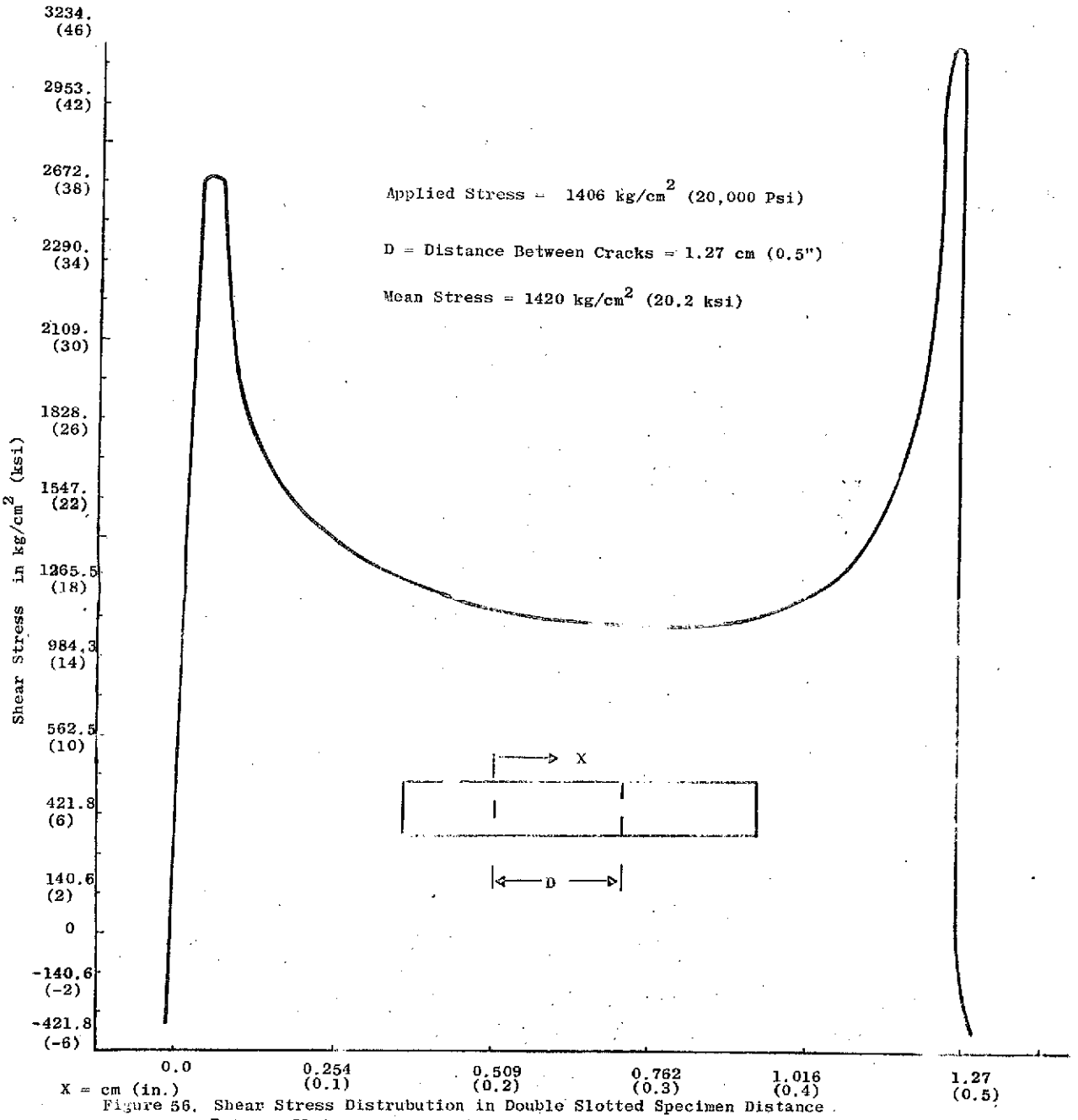

Figure 56. Shear Stress Distrubution in Double Slotted Specimen Distance Between Slots = 1.27 cm (0.5 inches)

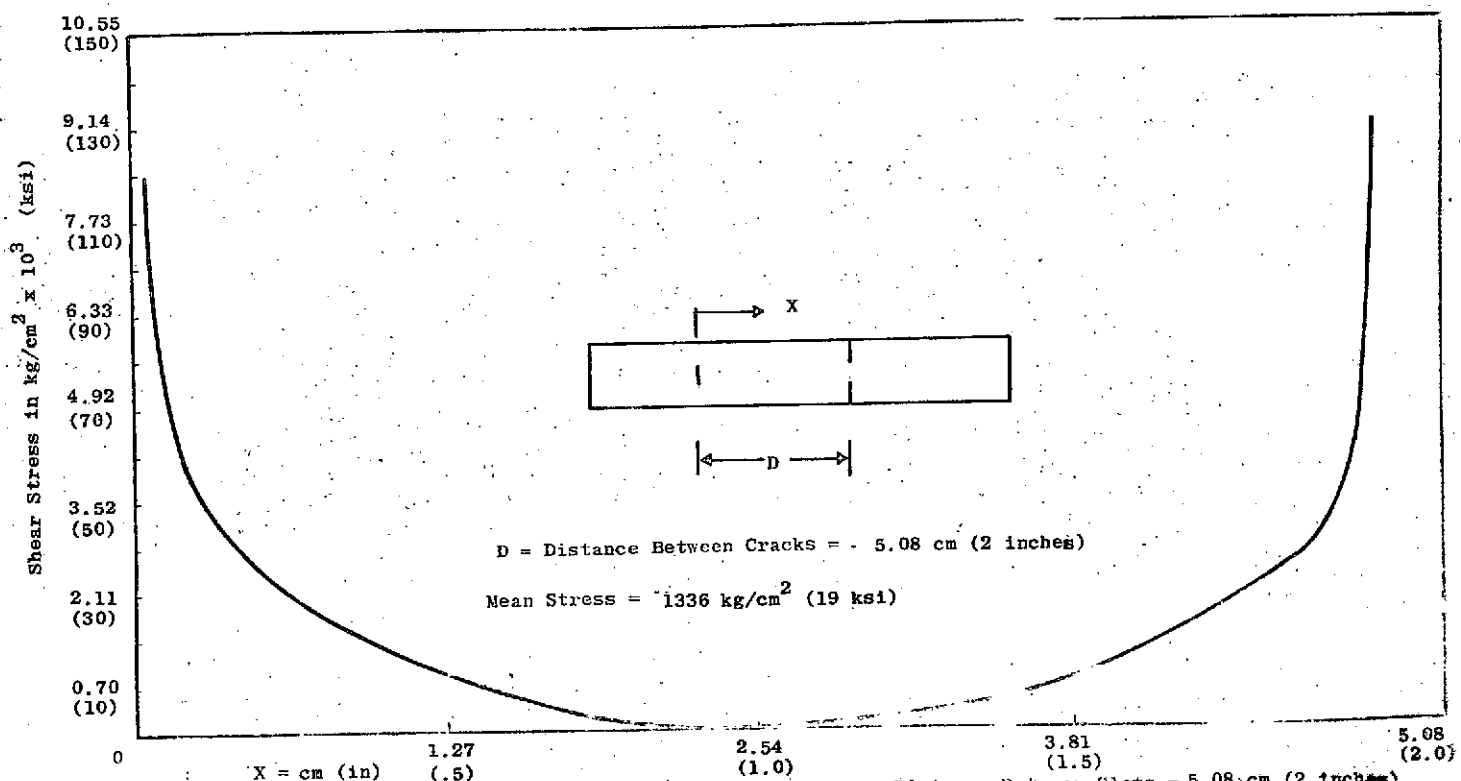

Figure 57. Shear Stress Distribution in Double Slotted Specimen-Distance Between Slots = 5.08 cm (2 inches)